THE AMERICAN JOURNAL OF PATHOLOGY

VOLUME XXXVIII MAY, 1961 NUMBER 5

SOME FEATURES OF GLOMERULAR FILTRATION AND PERMEABILITY REVEALED BY ELECTRON MICROSCOPY AFTER INTRAPERITONEAL INJECTION OF DEXTRAN IN RATS

J. A. JAMES, M.D., AND C. T. ASHWORTH, M.D.

From the Departments of Pediatrics and Pathology, The University of Texas Southwestern Medical School, Dallas, Texas

It is generally agreed that proteinuria in renal disease largely derives from a process of abnormal filtration at the glomerulus. Electron microscopic studies in human material and in animals with experimentally induced proteinuria have consistently demonstrated glomerular changes,[1,2] but the relationship of these to the abnormal filtration of protein remains obscure. In searching for an approach to the study of the fine structural aspects of glomerular filtration of large molecules, the renal excretion of dextran has been investigated in the rat. This substance is known to appear in the urine after intravenous administration to human subjects and to animals.[3] Its re-activity with the periodic acid-Schiff (PAS) procedure[4] has served as a guide to its anatomic localization within tissues, while the comparatively large molecular size of dextran gave promise of its visibility as a distinctive electron microscopic unit. The object of the present study was to attempt to define the route followed by a substance of large molecular size (dextran), during its passage through the glomerular capillary wall, and to follow the subsequent course and disposition of the particle-containing glomerular filtrate as it passed down the tubules of the kidney.

MATERIAL AND METHODS

Weanling female Sprague-Dawley rats, weighing 33 to 34 gm. at the start of the study, were used. The animals were fed a normal pellet diet. No oral fluids were

Supported by the United States Public Health Service, Grant No. H-5120.
Accepted for publication, January 10, 1961.

given. Six animals received 3 per cent dextran (Dextran Solution for Intravenous Use, Cutter Laboratories, Berkeley, California) in half-isotonic saline by intraperitoneal injection in a dose of 1 cc. per 10 gm. of body weight twice daily for 14 days. Three control animals received half-isotonic saline in the same fashion. Every 4 days the animals were weighed and overnight urine collections were made for protein determination.[5] Serum protein determinations were made on the day of sacrifice by a biuret method. Animals were killed by exsanguination under Nembutal® anesthesia. The kidneys were trimmed of adherent tissue and weighed. A 1 cu. mm. block of fresh tissue was removed and fixed in buffered osmium tetroxide for examination by electron microscopy. Kidney tissue was also fixed in 10 per cent buffered formalin for light microscopy. Sections were stained with hematoxylin and eosin and with the aqueous and alcoholic PAS techniques.[4]

Results

The experimental animals demonstrated the usual sensitivity reaction to injected dextran,[6] but otherwise remained well. Their weight gain was similar to that of the control animals. Proteinuria beyond that seen in the control animals did not appear. The concentration of serum proteins decreased to about half that observed in the control group (Table I). The kidneys of the dextran-treated animals were not enlarged, and in this respect the findings differed from those seen in rats treated with albumin solutions.[7,8]

Table I

PLASMA PROTEIN AND KIDNEY WEIGHT IN RATS RECEIVING INTRAPERITONEAL INJECTIONS OF 3 PER CENT DEXTRAN SOLUTION

Rats	Plasma proteins (gm. per 100 cc.)	Kidneys, combined wt. per 100 gm. body wt. (gm.)
Dextran-treated	1.62–2.74	1.02–1.32
Control	4.93–5.33	1.02–1.40

Light microscopic examination of the kidneys revealed slight alterations in the glomeruli and proximal convoluted tubular epithelium. Hematoxylin and eosin stains showed the glomerular capillary walls to be slightly thickened, due to swelling of the glomerular epithelium; in the latter a slightly foamy, vacuolated cytoplasm could be seen (Fig. 1). This was also prominent with PAS stains, and the fine vacuoles of the cytoplasm contained minute PAS-positive particles. The basement membrane was normally thin and delicate. Vacuoles and PAS-positive particles were also demonstrable within the cytoplasm of proximal convoluted tubular cells (Fig. 2), and occasional swollen, foamy histiocytes were observed in the interstitial tissue between proximal convoluted tubules. Minute PAS-positive particles were present in the foamy cytoplasmic areas (Fig. 3). Since alcohol-fixed tissue was not employed for the PAS stain, the amount of dextran demonstrable by light microscopy was comparatively small.[4]

Electron microscopy revealed striking alterations in glomeruli, proximal convoluted tubules, and in the interstitial tissue. The glomerular epithelial cells were slightly swollen, and contained discrete, round or oval aggregates of fine, dense particles, about 150 Å in size (Figs. 4 and 5). Although the collections of particles were clearly confined within the cytoplasm, they were not bounded by a membrane. Usually a layer or rim of dense epithelial cytoplasm was located around the individual globular aggregates, at the periphery of the cell. A few of the endothelial cells lining the glomerular capillaries were also found engorged with similarly aggregated fine particles. In many glomerular capillaries, the usual finely granular material, representative of normal plasma protein, was largely replaced by the somewhat larger, denser granules of dextran (Fig. 6). Electron micrographs of dextran solutions, which had been allowed to dry on Formvar films, showed variable-sized dense particles. Some of these were approximately 150 Å in size, resembling those found in the glomerular epithelium. This observation, with the observation of similar particles in the plasma within capillaries, and the demonstration with light microscopy of PAS-positive globular aggregates in glomerular epithelium, in proximal convoluted tubular cells, and in the foamy histiocytes of the interstitial tissue, identify the particles as dextran.

The glomerular basement membrane itself was normal in appearance. Only rarely in the lamina densa, or in the lucid zones on either side of the dense portion of the basement membrane were dextran particles observed. In all instances, the foot processes of the epithelial cells remained intact and narrow, and were not fused or swollen.

Dextran particles were found also in the cytoplasm of the proximal convoluted tubule cells (Fig. 7). Usually they occurred in sharply demarcated areas similar to those seen in the glomerular epithelium. Membranes were usually not observed around these aggregates. The particles were seen in all portions of the cells but were most numerous in the basal portions, where they were sometimes located between the basal cytoplasmic infoldings. Only rarely did the dextran particles appear to cause any great displacement or disorganization of cytoplasm in the affected tubular epithelium. Frequently, aggregates of particles were found in interstitial tissue, where they occurred adjacent to proximal convoluted tubules (Fig. 8). Their presence in the cytoplasm of large cells in this location suggested that they had been incorporated into histiocytes.

Discussion

The dextran used in this study had an average molecular weight of 75,000 ± 15,000. Not more than 10 per cent was below 25,000 and not more than 10 per cent above 200,000 (communication from Dr. E. B.

McLean, Cutter Laboratories). The size of the majority of molecules ranged from 340 to 650 Å by 14 to 19 Å. The excretion of dextran given by the intraperitoneal route has not been investigated, but following intravenous infusion there is rapid excretion of the low molecular weight fractions (less than 50,000) by the normal kidney.[9] The larger molecular fractions are removed more slowly from the circulation and appear to be slowly metabolized. Temporary vacuolation of the renal tubules, apparently due to re-absorption of dextran, has been observed by several workers.[10,11]

The most interesting observation in this study was the demonstration of abundant aggregates of dextran within the cytoplasm of the glomerular epithelial cells. The size of the particles, approximately 150 Å, indicates that dextran molecules of low molecular weight were able to pass across the glomerular capillary wall. Thus, low molecular weight dextran is present in glomerular filtrate and is taken up by the glomerular epithelial cells at some stage of transit through the capillary wall. The dextran particles are apparently then arrested and undergo accretion in the cytoplasm of these cells. Since comparatively large molecules may thus accumulate in glomerular epithelial cells, this concept might aid in understanding the nature and pathogenesis of glomerular injury in a variety of pathologic states, where antibody proteins and other abnormal proteins are deposited in the glomerular walls.[12] At least some of these deposits may actually be within the glomerular epithelium. Aggregations of ferritin[13] and silver-tagged albumin[14] have been found to occur similarly in the glomerular epithelium, particularly in animals with experimentally induced proteinuria. It was of interest that obliteration of the epithelial foot processes, apparently a characteristic of a variety of proteinuric states,[1] was not observed following infusion of dextran. This is probably due to the absence of the severe grades of epithelial swelling encountered in pathologic states with marked proteinuria.

The manner in which the glomerular filtrate or the contained dextran molecules entered the glomerular epithelial cells is speculative. In all instances, the epithelial pedicels remained dense, compact, and free from vesicles or granules. Consequently, it is difficult to envision the filtrate or particles within the filtrate as entering the epithelium through this route. Probably cellular uptake of particles by pinocytosis[15] in the glomerular epithelium occurred at some site along the cell membrane other than at the pedicels. Even here, however, pinocytotic vesicles were not numerous. For the present, though pinocytosis is the most likely explanation, the route and means of entry of particles of the glomerular filtrate into these epithelial cells remain undetermined.

The occurrence of re-absorption across the proximal convoluted tu-

bule cells is indicated by the appearance of globules of dextran in the cytoplasm of these cells. This seems quite analogous to the appearance of protein droplets (hyaline droplets) when albumin is released in quantity into the glomerular filtrate.[16] Tubular re-absorption of macromolecules seems to be based upon a mechanism that does not discriminate between the type of particles to be absorbed. This would favor some physical mechanism like pinocytosis, for which the microvilli of the proximal convoluted tubules seem to be ideally disposed.[17]

It is a matter of interest that dextran aggregates could be demonstrated in the cytoplasm of histiocytes located in the interstitial tissue. It is believed that whenever albumin is re-absorbed across the proximal tubule cells, it is readily passed on into capillaries. Although the same may be true for re-absorbed dextran, some of the dextran nevertheless becomes lodged in interstitial macrophages.

Summary

The introduction of dextran of variable molecular weights into the peritoneal cavity of rats was followed by renal excretion of some of the substance. Electron microscopy revealed extensive deposition of aggregates of dextran of comparatively small molecular size within the cytoplasm of glomerular epithelium, and slight swelling of the cells. No other significant changes were observed in the glomeruli. The findings indicate the free passage of particles approximately 150 Å in size across the capillary membrane, and that the process is accompanied by glomerular epithelial uptake and storage of such particles. This process is considered potentially significant in explaining the localization of various particles and macromolecules in disorders affecting glomeruli. The studies further indicated that some of the dextran passed into the tubules and was re-absorbed across the proximal convoluted tubular epithelium, in which collections of the particles were found. Dextran aggregates were also found lodged in histiocytes of the peritubular interstitial tissue, indicating that this route was followed in their removal from the tubular epithelium.

References

1. Farquhar, M. G.; Vernier, R. L., and Good, R. A. An electron microscope study of the glomerulus in nephrosis, glomerulonephritis and lupus erythematosus. *J. Exper. Med.*, 1957, **106**, 649–660.
2. Feldman, J. D., and Fisher, E. R. Renal lesions of aminonucleoside nephrosis as revealed by electron microscopy. *Lab. Invest.*, 1959, **8**, 371–385.
3. Ricketts, C. R.; Lorenz, L., and Maycock, W. d'A. Molecular composition of dextran solutions for intravenous use. *Nature, London*, 1950, **165**, 770–771.
4. Mowry, R. W.; Longley, J. B., and Millican, R. C. Histochemical demon-

stration of intravenously injected dextran in kidney and liver of the mouse. *J. Lab. & Clin. Med.*, 1952, **39**, 211–217.

5. SHEVKY, M. C., and STAFFORD, D. D. A clinical method for the estimation of protein in urine and other body fluids. *Arch. Int. Med.*, 1923, **32**, 222–225.
6. VOORHEES, A. B.; BAKER, H. J., and PILASKI, E. J. Reactions of albino rats to injections of dextran. *Proc. Soc. Exper. Biol. & Med.*, 1951, **76**, 254–256.
7. BAXTER, J. H., and COTZIAS, G. C. Effects of proteinuria on kidney: proteinuria, renal enlargement and renal injury consequent on protracted parenteral administration of protein solutions in rats. *J. Exper. Med.*, 1949, **89**, 643–668.
8. ASHWORTH, C. T., and JAMES, J. A. Unpublished observations.
9. GRÖNWALL, A.; HINT, H.; INGELMAN, B.; WALLENIUS, G., and WILANDER, O. Renal excretion and molecular size distribution of dextran *Scandinav. J. Clin. & Lab. Invest.*, 1952, **4**, 363–368.
10. HARTMAN, F. W. Tissue changes following the use of plasma substitutes. *A.M.A. Arch. Surg.*, 1951, **63**, 728–738.
11. GOLDENBERG, M.; CRANE, R. D., and POPPER, H. Effect of intravenous administration of dextran, a macromolecular carbohydrate in animals. *Am. J. Clin. Path.*, 1947, **17**, 939–948.
12. MELLORS, R. C.; ARIAS-STELLA, J.; SIEGEL, M., and PRESSMAN, D. Analytical Pathology. II. Histopathologic demonstration of glomerular-localizing antibodies in experimental glomerulonephritis. *Am. J. Path.*, 1955, **31**, 687–715.
13. FARQUHAR, M. G., and PALADE, G. E. Segregation of ferritin in glomerular protein absorption droplets. *J. Biophys. & Biochem. Cytol.*, 1960, **7**, 297–304.
14. VERNIER, R. L.; PAPERMASTER, B. W.; OLNESS, K.; BINET, E., and GOOD, R. A. Morphologic studies of the mechanism of proteinuria. (Abstract) *Am. J. Dis. Child.*, 1960, **100**, 476–478.
15. LEWIS, W. H. Pinocytosis. *Bull. Johns Hopkins Hosp.*, 1931, **49**, 17–27.
16. OLIVER, J.; MACDOWELL, M. C., and LEE, Y. C. Cellular mechanisms of protein metabolism in the nephron. I. The structural aspects of proteinuria; tubular absorption, droplet formation, and the disposal of proteins. *J. Exper. Med.*, 1954, **99**, 589–604.
17. RHODIN, J. Electron microscopy of the kidney. *Am. J. Med.*, 1958, **24**, 661–675.

We gratefully acknowledge the assistance of Mr. Emil Sanders and Mr. M. D. Glass in the electron microscopic work.

[*Illustrations follow*]

Legends for Figures

Fig. 1. Kidney of a rat receiving 14 daily injections of dextran solution intraperitoneally. The cytoplasm of the glomerular epithelium is finely reticulated and foamy. Occasional large, rounded, markedly vacuolated epithelial cells are seen (X). Faintly PAS-positive material was also demonstrable in these large cells and in the foamy areas of the glomerular epithelium. Hematoxylin and eosin stain. × 720.

Fig. 2. Proximal convoluted tubules. The cytoplasm contains fine vacuoles, producing a foamy appearance. PAS-positive material is visible in these vacuoles. Periodic acid-Schiff stain. × 720.

Fig. 3. A kidney showing large, foamy cells in the interstitial tissue between loops of the proximal convoluted tubules. Some PAS-positive granules and homogeneous PAS-positive material can be seen in these vacuolated cells. Periodic acid-Schiff stain. × 720.

Fig. 4. Electron micrograph of portions of a glomerulus. The glomerular epithelium (E) is swollen and contains numerous clumps of electron-dense dextran particles (D). × 5,000.

2

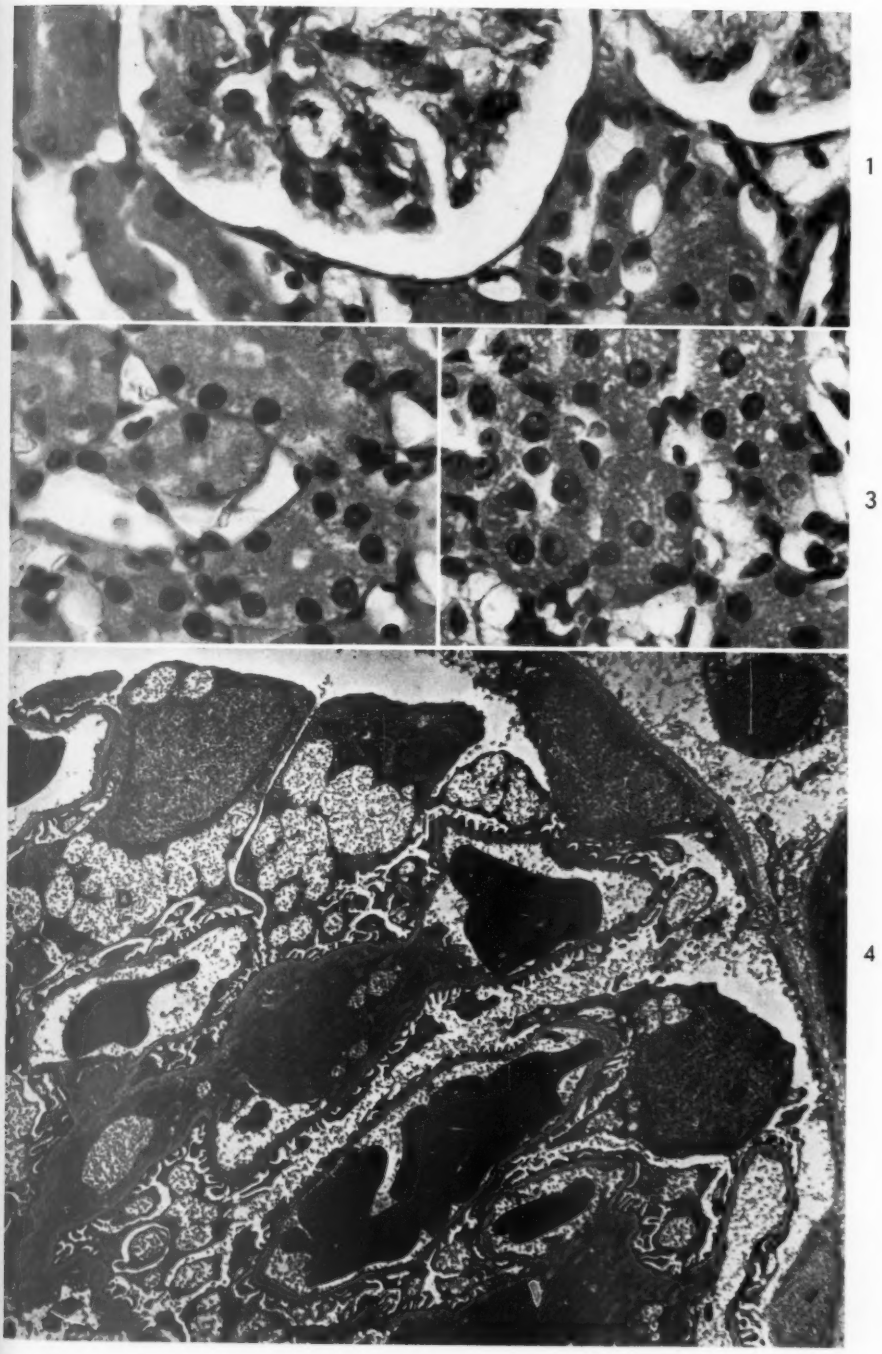

FIG. 5. Electron micrograph of a glomerulus showing dextran-containing epithelial cells (E). The epithelial pedicels (P) are discrete and are not swollen. The basement membrane (B) and capillary endothelial lining (END) are normal in appearance. × 15,000.

FIG. 6. Electron micrograph of a kidney revealing a portion of a glomerular capillary (C) and a glomerular epithelial cell (E) in which dextran particles (D) are present. In the capillary lumen, similar dextran particles are observed. These are larger and denser than the fine granules seen in normal plasma with the electron microscope. × 15,000.

FIG. 7. Electron micrograph of portions of a proximal convoluted tubule. In the cytoplasm are numerous clumps of dextran particles (D) lying in vacuoles (V). The basement membrane (B) of the tubule is normal in appearance. Mitochondria (M) are displaced by the vesicular collections of dextran. × 15,000.

FIG. 8. Electron micrograph of a kidney showing a macrophage (M) between proximal convoluted tubule loops (T). In the cytoplasm of the macrophage numerous dextran-containing vesicles (V) are observed. × 12,000.

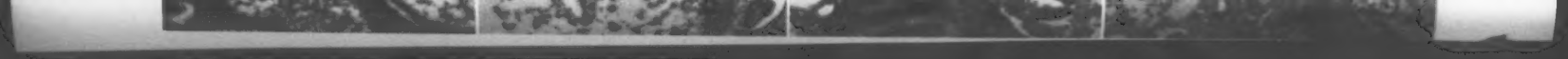

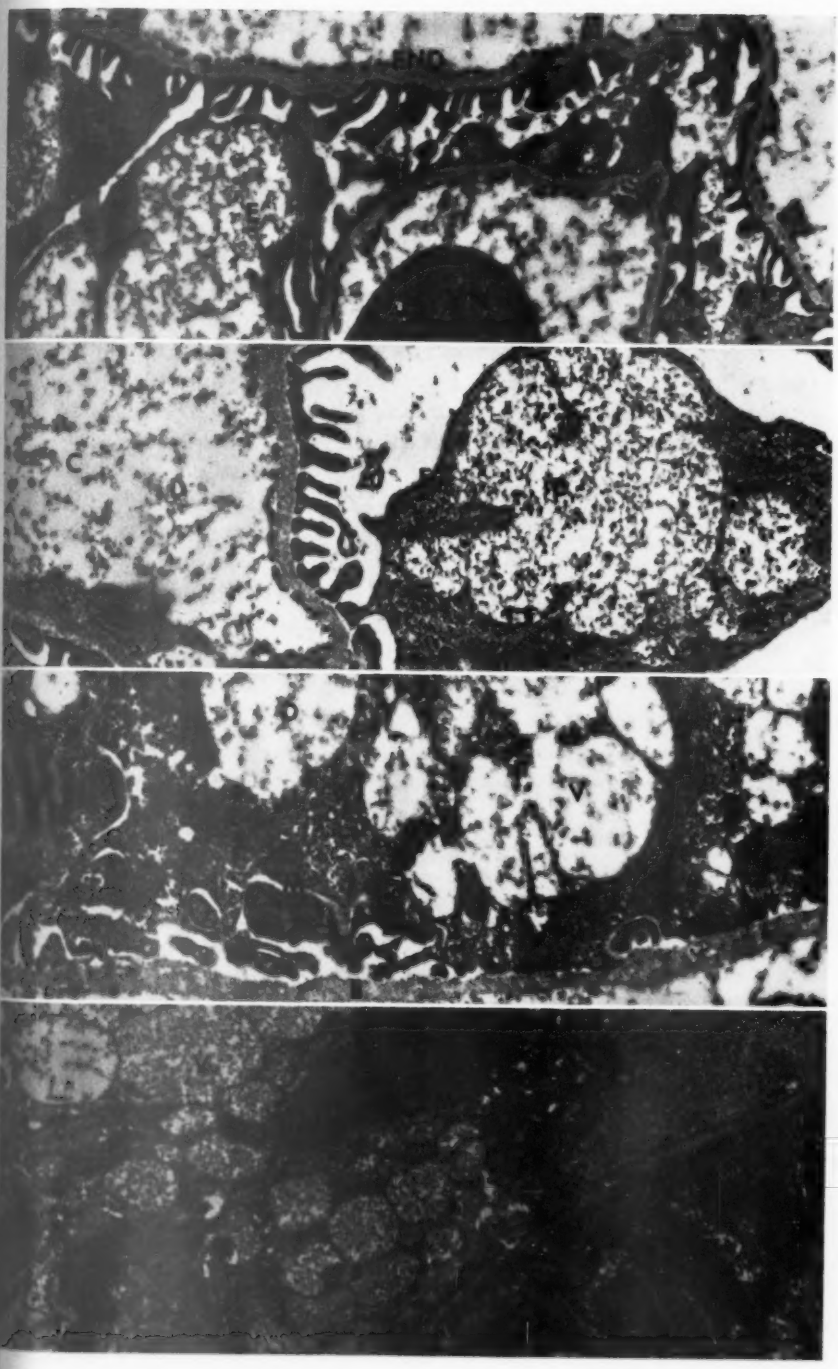

5

6

7

8

ATHEROGENESIS AND PLASMA CONSTITUENTS

ROBERT H. MOORE, M.D., AND M. DARIA HAUST, M.D.

From the Department of Pathology, Queen's University and Kingston General Hospital, Kingston, Ontario, Canada

Our previous observations indicated that the white plaque of arteriosclerosis is a prominent component of the arteriosclerotic lesion and that it represents the outcome of blood proteins deposited either on the intima as a mural thrombus or in its substance as an inflammatory exudate.[1-7] This field has been largely neglected, although McGill and colleagues [8] have more recently investigated it from another point of view. At this point it has seemed of interest to determine whether or not an atheroma had an origin similar to that of the white plaque. We have taken the term "atheroma" to refer to a local "pool" of largely extracellular lipids and tissue debris in the subendothelial connective tissue of the aortic and coronary artery intima. While this definition is generally accepted, some investigators [9] also include the fibrous component of arteriosclerotic lesions in this category. This is in accordance with the concept of Marchand.[10]

It is the purpose of this presentation to report on the morphologic features in the development of certain forms of atheroma and to evaluate their close association with unorganized remnants of some blood proteins deposited on or into the arterial wall in the course of the arteriosclerotic process.

MATERIAL AND METHODS

Material for this study consisted of 130 sections selected from 1,300 sections of arteriosclerotic lesions. These were obtained from 150 aortas and the coronary arteries of 100 hearts. The 130 sections chosen represented various stages of atheroma formation and contained lesions believed to be the precursors of atheromas.

Processing of the tissue was carried out as described elsewhere.[11] The following stains were utilized: hemalum, phloxine, saffron; pentachrome II (omitting elastica); elastica (Weigert-Hart, nuclear fast red, metanil yellow); Alcian blue, periodic acid-Schiff, hematoxylin, and orange G; phosphotungstic acid-hematein; Masson's trichrome; Fettrot and hematoxylin.

RESULTS

When the mural thrombus was small or the insudation into the intima was superficial, all of the blood protein substance was commonly "con-

This work was supported by Grants-in-aid of Research from the Bickell Foundation of Toronto, Canada, and Public Health Research Grants of Canada.

Accepted for publication, October 19, 1960.

verted" to connective tissue elements by means of avascular organization progressing from the lumen. The organization was thus complete. When the thrombus, however, was of large size, two mechanisms of organization were encountered concomitantly. In this circumstance, avascular organization progressing from the lumen co-existed with orthodox vascular organizing tissue developing from the base of the thrombus, with capillaries growing in from the media (Fig. 1). When the organization by these two processes was complete, they were seen side by side. Frequently, however, remnants of fibrin remained between the two types of organization (Fig. 2). In addition, unorganized fibrin was present in the form of coalescent bands and clumps at the base of young connective tissue plaques. This was often seen in those situations where the thrombi were deposited on older, sclerotic fibrous plaques (Fig. 3) and probably represented a failure on the part of the latter to initiate organization.

Similar in nature but different in distribution was the appearance of fibrin remnants deep in the sero-fibrinous insudate within the intimal substance. Thus, the fibrin threads and strands when unorganized in the depth of the intimal substance formed numerous small clumps (Fig. 4) or became more coalescent and aggregated to form dense bands (Fig. 5).

In early lesions, scattered macrophages appeared in both insudative and thrombotic lesions. They were closely applied to the clumps and bands of fibrin remnants, and some of them had the typical appearance of lipophages (Fig. 6). The lipophages were numerous in advanced lesions. In addition, they were also seen to accumulate at the base of entirely unorganized thrombi which in turn were covered by one or more layers of recent thrombus deposit (Fig. 7). In more advanced lesions the lipophages disintegrated, thus becoming the nidus for atheroma, while others could be seen applied closely to the inconspicuous remnants of fibrin (Fig. 8). It was clear that the intra- and extracellular lipids accumulated as the fibrin and other plasma constituents disappeared. The outcome of this process was the familiar pattern of typical atheroma containing remnants of fibrin and covered by a fibrous cap (Fig. 9). The latter represented the superficial part of the thrombus which had been organized in avascular manner from the direction of the lumen. Often, small narrow bands of unorganized fibrin were also present within the fibrous cap, and a few lipophages applied to these bands signaled the development of an atheroma at this site (Fig. 9).

That an atheroma may indeed originate within a mural thrombus, notably at its base where organization fails to develop, was indicated by the unequivocal polypoid shape of some of the lesions containing atheromas. Thus, in a section of such a lesion the base was filled with

atheromatous substance while the portion next to the lumen consisted of an avascular fibrous connective tissue. The connective tissue elements were not sharply delineated from the atheromatous substance but blended imperceptibly with it. This showed that the deeper portion of the thrombus which did not become organized underwent alterations producing typical atheromatous material. The atheroma and the avascular organizing tissue overlying it unmistakably retained the shape of the original polypoid thrombotic implant (Fig. 10). An additional hallmark of thrombotic origin was the presence of fibrin within the lesion (Figs. 10 and 11).

An eccentric plaque encountered frequently, especially in coronary arteries, was often composed of several "layers" of sclerotic tissue (Fig. 12). The genesis of each of these layers is best explained as indicative of an episode of insudation or thrombus deposition followed by organization. Between some of the fibrous layers, small or large atheromas could be seen. Careful examination revealed that these atheromas were present at the bases of broad and thick fibrous layers. The shallow, narrow fibrous layers were commonly unassociated with atheromas since they were completely organized. This was in contradistinction to the thicker and more massive protein deposits.

Discussion

Historically, four principal theories have been advanced to explain the pathogenesis of atheroma. Each of these has received support and amplification by various workers. Rokitansky[12] considered the atheroma to result from the degeneration of plasma constituents, principally fibrin, deposited on the intima of the vessel wall. This has been referred to by British workers as "encrustation."[13,14] Virchow[15] doubted that subendothelial accumulations could be the result of surface deposition and considered that the atheroma reflected degeneration following an inflammatory process within the intima. He based this concept upon the observation of a mucinous change in the intima preceding the formation of atheroma. He believed that the atheroma then served as a stimulus to connective tissue proliferation resulting in the formation of fibrous caps. Another theory and the one most widely favored has been that of Marchand.[10] He considered that there was selective imbibition of lipids into the arterial intima, with the formation of lipid pools and a resulting connective tissue proliferation. Finally, Winternitz, Thomas and LeCompte[16] postulated another theory, based on the original observations of Paterson,[17,18] who described vascularization and hemorrhage in the arteriosclerotic intima of coronary arteries. According to them an atheroma developed on the basis of a hemorrhage from intimal capillaries.

They observed that at the site of hemorrhage there was a gradual accumulation of lipoid substance and so-called "cholesterin clefts" culminating in atheroma formation.

The common feature in the theories advanced by Rokitansky, Virchow, and Winternitz and co-workers was the recognition of the role of blood proteins in atheroma formation. In previous publications [1–6] we have shown that the fibrous tissue associated with arteriosclerosis arises principally by the organization of accumulated blood proteins often rich in fibrin, deposited either on the intimal surface or in the subendothelial tissue. The observations reported here have shown that atheromatous as well as connective tissue plaques may develop from the accumulations of blood proteins. This is probably the result of degenerative changes following incomplete organization of inflammatory exudates or fibrin deposits on the endothelial surface. These observations thus incorporate elements of both Rokitansky's encrustation theory [12] and Virchow's intimal inflammation theory [15] and serve to re-emphasize the fundamental role of blood accumulations in the genesis of both the atheroma and the fibrous plaque. This work supports the findings of Clark, Graef and Chasis,[19] Duguid [14] and Crawford and Levene,[13] showing that in man, mural thrombosis represents a stage in the genesis of some atheromas. The experimental work of McLetchie [20] also supports this mechanism. In his experiments mural thrombosis of pulmonary arteries was induced by the injection of Russell's viper venom into rabbits. Failure of complete organization of the mural thrombi was associated with the accumulation of lipids. Thus, while the superficial (lumen) layers of these thrombi underwent organization, the deeper portions underwent fatty changes; the resulting lesions resembled those of human arteriosclerosis.

These observations establish the sequential relation between the accumulation of blood proteins in and on the intima and the genesis of atheroma. They, however, do not provide information on the factors which promote this sequence. Aside from the size of thrombi and the amount of insudate, there is no explanation in this or previous studies [1–6,21,22] indicating why one mass of intimal protein was completely organized while in another instance this was only partially accomplished. Furthermore, the observations provided no evidence on which to judge whether or not some disturbance in the metabolism of the body lipids may have played a role in certain stages of the progressive changes observed. In all samples of blood, lipids are demonstrable chromatographically on electrophoretic strips. The failure to demonstrate lipids readily in all protein deposits by some of the techniques used poses a problem in the interpretation of the pathogenesis of atheroma from the accumu-

lation of blood proteins. This may be a matter of the degree of lipids binding to proteins. However, it poses the question of whether or not there is some source of the accumulated lipids other than their derivation from the deposited proteins. Whatever the source of the lipids, these investigations indicate that atheromas as well as fibrous plaques may arise from mural thrombi or inflammatory exudates or both. The possibility that some atheromas may originate in a different way cannot be dismissed.

Summary

Atheroma formation has been found to be closely associated with unorganized remnants of mural thrombi on the one hand or deep sero-fibrinous intimal insudates on the other.

Atheromas appeared to develop from a few lipophages closely applied to fibrin remnants; in advancing lesions these accumulated and subsequently disintegrated. Although fibrin remnants became diminished, a few strands and bands were often found in typical atheromas.

The predilective sites for atheroma formation were found to be at the bases of mural thrombi where organization failed to occur, and within a layer of unorganized thrombus on which more recent thrombi were superimposed. In other instances this was observed between two types of organizing tissue (avascular, stemming from the lumen, and conventional vascularized tissue from the vessel wall) which failed to meet, thus leaving a layer of unorganized fibrinous material between them. Additional sites were encountered at the bases of thrombi deposited on densely sclerotic plaques and in the depth of the intima where massive sero-fibrinous insudate failed to organize.

References

1. Haust, M. D., and More, R. H. Morphologic evidence and significance of permeation in the genesis of arteriosclerosis. (Abstract) *Circulation*, 1957, 16, 496.
2. Haust, M. D.; More, R. H., and Movat, H. Z. The mechanism of fibrosis in arteriosclerosis. *Am. J. Path.*, 1959, 35, 265–273.
3. Haust, M. D.; Movat, H. Z., and More, R. H. The role of fibrin thrombi in the genesis of the common white plaque in arteriosclerosis. (Abstract) *Circulation*, 1956, 14, 483.
4. More, R. H., and Haust, M. D. Encrustation and permeation of blood proteins in the genesis of arteriosclerosis. (Abstract) *Am. J. Path.*, 1957, 33, 593.
5. More, R. H., and Haust, M. D. Thrombotic and inflammatory origin of arteriosclerosis. (Abstract) *Circulation*, 1959, 20, 974–975.
6. More, R. H.; Movat, H. Z., and Haust, M. D. Role of mural fibrin thrombi of the aorta in genesis of arteriosclerotic plaques. Report of two cases. *A.M.A. Arch. Path.*, 1957, 63, 612–620.

7. MOVAT, H. Z.; HAUST, M. D., and MORE, R. H. The morphologic elements in the early lesions of arteriosclerosis. *Am. J. Path.*, 1959, **35**, 93–101.
8. MCGILL, H. C.; STRONG, J. P.; HOLMAN, R. L.; MCMAHAN, C. A.; TEJADA, C.; RESTREPO, C.; LICHTENBERGER, E., and GALINDO, L. Epidemiology of atherosclerotic lesions. (Abstract) *Circulation*, 1959, **20**, 974.
9. MORGAN, A. D. The Pathogenesis of Coronary Occlusion. Charles C Thomas, Springfield, Ill., 1956, 175 pp.
10. MARCHAND, F. Ueber Arteriosklerose. *Verhandl. d. Kongr. f. innere Med.*, 1904, **21**, 23–59.
11. HAUST, M. D. Tetrahydrofuran (THF) for dehydration and infiltration. *Lab. Invest.*, 1958, **7**, 58–67.
12. ROKITANSKY, C. A Manual of Pathological Anatomy. Day, G. E. (transl.) The Sydenham Society, London, 1852.
13. CRAWFORD, T., and LEVENE, C. I. The incorporation of fibrin in the aortic intima. *J. Path. & Bact.*, 1952, **64**, 523–528.
14. DUGUID, J. B. Thrombosis as a factor in the pathogenesis of coronary atherosclerosis. *J. Path. & Bact.*, 1946, **58**, 207–212.
15. VIRCHOW, R. Phlogose und Thrombose im Gefässsystem. In: Gesammelte Abhandlungen zur wissenschaftlichen Medicin. Meidinger Sohn & Co., Frankfurt-am-Main, 1856, pp. 458–636.
16. WINTERNITZ, M. C.; THOMAS, R. M., and LECOMPTE, P. M. Studies in the pathology of vascular disease. *Am. Heart J.*, 1937, **14**, 399–404.
17. PATERSON, J. C. Vascularization and hemorrhage of the intima of arteriosclerotic coronary arteries. *Arch. Path.*, 1936, **22**, 313–324.
18. PATERSON, J. C. Capillary rupture with intimal hemorrhage as a causative factor in coronary thrombosis. *Arch. Path.*, 1938, **25**, 474–487.
19. CLARK, E.; GRAEF, I., and CHASIS, H. Thrombosis of the aorta and coronary arteries; with special reference to the "fibrinoid" lesions. *Arch. Path.*, 1936, **22**, 183–212.
20. MCLETCHIE, N. G. B. The pathogenesis of atheroma. *Am. J. Path.*, 1952, **28**, 413–435.
21. HAUST, M. D., and MORE, R. H. New functional aspects of smooth muscle cells. (Abstract) *Fed. Proc.*, 1958, **17**, 440.
22. HAUST, M. D.; MORE, R. H., and MOVAT, H. Z. The role of smooth muscle cells in the fibrogenesis of arteriosclerosis. *Am. J. Path.*, 1960, **37**, 377–389.

[*Illustrations follow*]

Legends for Figures

Fig. 1. Coronary artery. The eccentric thickening is made up of organizing thrombus. The organization from the lumen is avascular (homogeneous light gray in the photograph) whereas that at the base is orthodox in type with numerous capillaries and collagen fibers developing in a criss-cross fashion. Remnants of thrombotic material are seen as black clumps between the two types of organization. Pentachrome II stain (elastica omitted). × 25.

Fig. 2. Higher power view of the area between the two types of organization (avascular at the top) with clumps of thrombotic substance intervening (black in photograph, orange-yellow in section). Stain as in Figure 1. × 82.

Fig. 3. Coronary artery. A young connective tissue plaque (top, light gray) overlying an old sclerotic one (lower right corner). A considerable amount of thrombotic remnant is seen between the two plaques. The organizing tissue at the base contains capillaries, while the part of the plaque adjacent to the lumen is avascular. Hemalum, phloxine, saffron stain. × 77.

Fig. 4. Aorta. Massive repeated sero-fibrinous insudation into the intima. Fibrin threads predominate in the middle and upper third of the intima, representing a more recent insudation. Fibrin clumps and bands dominate the lower third, representing a previous insudation. Note the swollen (light gray) ground substance and distorted fragments of connective tissue fibers. The latter are absent in the upper part of the intima. Lipophages are seen in association with some fibrin clumps. Phosphotungstic acid-hematein stain. × 102.

Fig. 5. Aorta. Dense masses of fibrinous substance deep in the intima represent the remnants of an unorganized fibrinous insudation. In addition, the intimal surface is covered by mural thrombi over an extensive area. Hemalum, phloxine, saffron stain. × 77.

Fig. 6. A high power view of the intimal fibrin remnants in Figure 5. Macrophages are scattered in the area and a few lipophages are applied to the fibrin masses. Stain as in Figure 5. × 244.

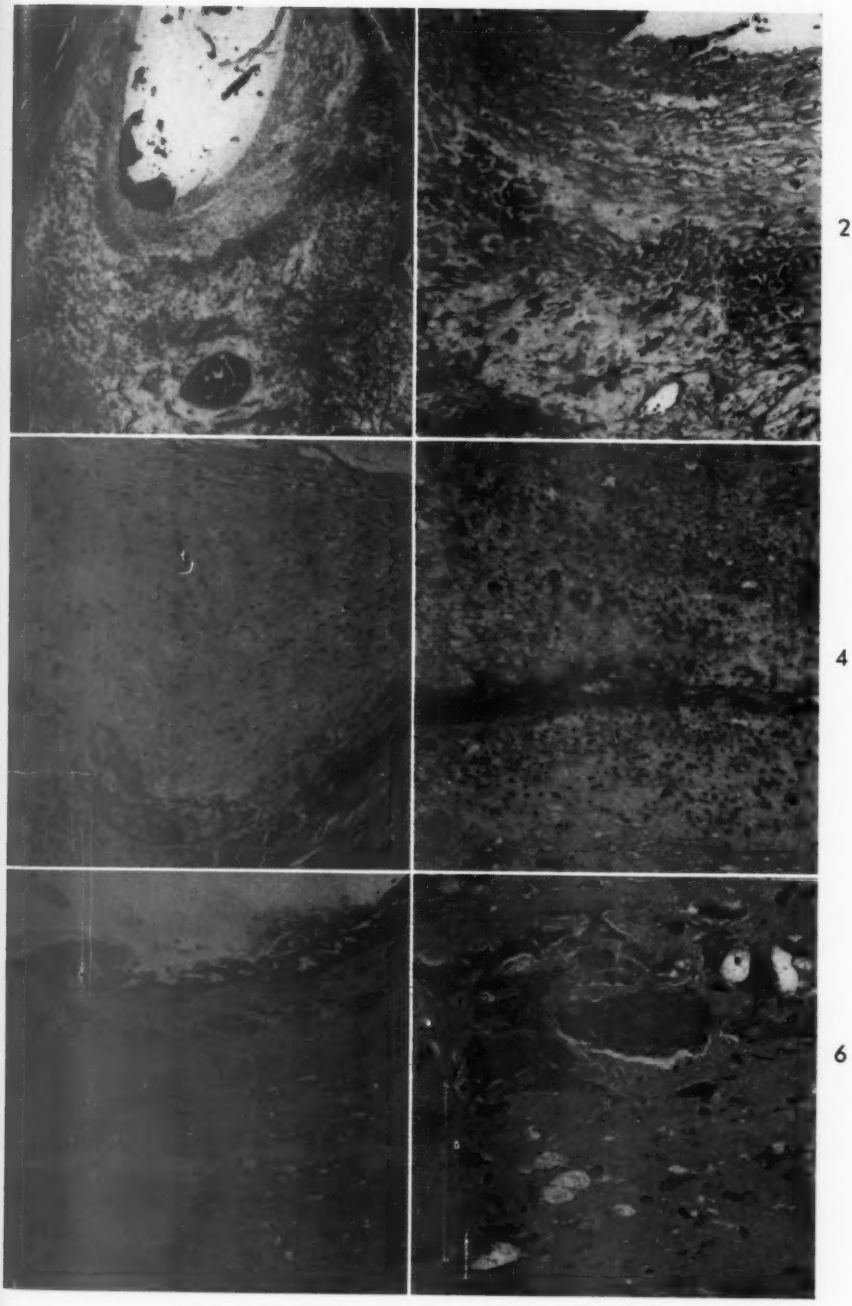

FIG. 7. Aorta. Three different layers of thrombus deposition (B, C, D) overlie the intima (A). Clusters of lipophages are seen within the oldest thrombus deposit (B) immediately overlying the intima. In some areas the accumulated lipophages have disintegrated, leaving a small pool of lipid (light) within the thrombotic coalescent mass. Phosphotungstic acid hematein stain. × 102.

FIG. 8. Aorta. The intima (A) is covered by a plaque (B) which in turn is covered by layers of thrombi. The oldest thrombus (C) blends with the substance of the plaque. Remnants of unorganized fibrin within the plaque are closely associated with lipophages. Accumulation and disintegration of the latter signals an atheromatous nidus (D). Masson's trichrome stain. × 77.

FIG. 9. Aorta. An atheroma (bottom) containing remnants of unorganized fibrin (black) is covered by a fibrous plaque containing numerous cells. A few clumps of fibrin remain in the plaque to the left. Note how intimately the connective tissue of the plaque blends with the atheroma. Hemalum, phloxine, saffron stain. × 36.

FIG. 10 Coronary artery. A large polypoid plaque almost completely occludes the lumen. Its shape unequivocally reflects its origin from a thrombus; this also holds true for the atheroma contained within its substance. A few remnants of thrombotic material are still present in the atheroma. Masson's trichrome stain. × 29.

FIG. 11. A higher power view of the fibrin remnants in the substance of the atheroma seen in Figure 10. Stain as in Figure 10. × 102.

FIG. 12. Coronary artery. An eccentric plaque is composed of several "layers" of sclerotic tissue, some being rich in elastic fibers (fine black fibers). The genesis of each of these layers is best explained as an episode of either insudation or thrombus deposition with subsequent organization. A small atheroma (whitish light gray) is present between the second and third layers from the lumen, just above the horizontal black line of elastic tissue. Weigert-Hart, nuclear fast red, metanil yellow stain. × 39.

7

9

11

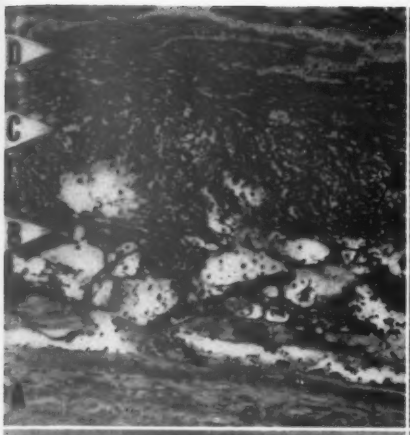

7

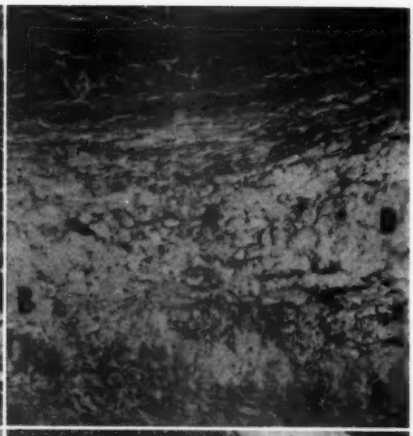

8

9

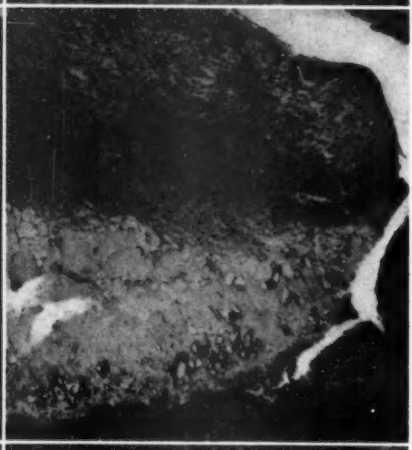

10

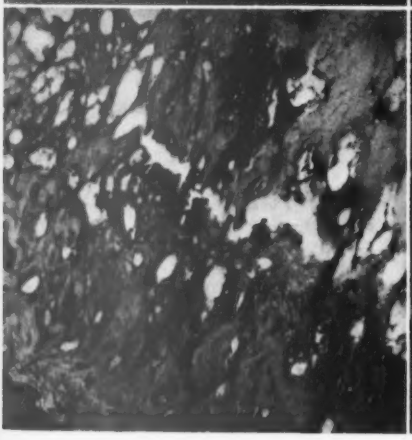

11

12

MYOCARDIAL ALTERATIONS ASSOCIATED WITH PHEOCHROMOCYTOMAS

IRWIN K. KLINE, M.D.

From the Department of Pathology, Michael Reese Hospital and Medical Center, Chicago, Ill.

Various myocardial lesions, including myocarditis, have been reported repeatedly in experimental animals subjected to infusions with large doses of *l*-norepinephrine as well as in patients treated for shock with adrenalin and with *l*-norepinephrine.[1-3] Exceedingly rare, however, are studies of the myocardium in patients with pheochromocytoma. The myocardial alterations in all these instances are strikingly similar, and it is believed that once they are recognized, they should be regarded as very characteristic of pheochromocytoma.

Our interest in this subject was aroused by the observation of an unusual type of myocarditis in a patient who, at necropsy, disclosed an unsuspected pheochromocytoma. To evaluate this type of myocarditis, the necropsy records of 6 additional cases of pheochromocytoma were reviewed. Of these, 3 also showed myocarditis of a similar nature. The 3 other patients died of unrelated conditions, and there was no evidence of myocardial involvement. Since we were unable to find detailed published studies on myocardial changes occurring in pheochromocytoma, it was thought to be of interest to report the results of this investigation. Because of the rarity of such cases, the clinical and necropsy observations are briefly discussed before the myocardial lesions are evaluated.

CASE REPORTS

Case 1. A 30-year-old white woman was admitted with a history of severe headache, sweating and hot flashes since age 17. At age 23, arterial hypertension was discovered, and 3 years later a right suprarenalectomy for pheochromocytoma was done at another hospital. Five years later the arterial blood pressure had again risen to 240/? and a laparotomy was performed in search for another pheochromocytoma; none was found. Two years later she was re-admitted for what was thought to be myocardial embarrassment caused by rheumatic heart disease. She expired unexpectedly on the 30th hospital day.

At necropsy the heart weighed 370 gm. There were a few minute verrucae at the edges of the mitral and aortic valves. The right suprarenal gland was absent and the left suprarenal was firm and markedly en-

This work was supported in part by the Wilmette Myocarditis Research Fund.
Accepted for publication, December 30, 1960.

larged, measuring 8.5 by 5 by 3.5 cm. On section, the cortex was almost obliterated by a tumor arising from and completely replacing the medulla. The tumor was grayish-brown, with multiple hemorrhagic areas and foci of necrosis. Blood cultures taken at necropsy were negative.

Microscopic examination of the myocardium showed several foci in which myocardial fibers were spread apart by loose collagenous tissue infiltrated by lymphocytes, monocytes, and a few fibroblasts and mast cells. An occasional Anitschkow cell was also evident. In other areas the fibers were spread apart by edema fluid. The myocardial fibers appeared larger than normal; there was severe cloudy swelling, and the striations were often not discernible. A number of muscle fibers showed no nuclei, and their cytoplasm frequently appeared coarsely granular. There was some increase in fibrous tissue around the blood vessels, which in turn were slightly thickened. Sections of the aortic valve revealed an acute, nonbacterial, thrombotic endocarditis with partially organized hyaline thrombi. The suprarenal neoplasm was a typical pheochromocytoma. The tumor cells resembled those seen in the suprarenal medulla, but were larger, polygonal and only occasionally assumed spindle shape. The nuclei were large and vesicular with prominent nucleoli. Here and there syncytium-like giant cells were noted. Some tumor cells were found in small masses embedded in a vascular and fibrillar stroma; others exhibited a perivascular arrangement.

Case 2. A 43-year-old white woman was admitted for removal of a breast tumor. There had been persistent hypertension for several years, and she had been treated with Serpasil.® Physical examination revealed an excited woman; blood pressure, 170/100 mm. of Hg; pulse rate, 80 per minute. At operation under Pentothal® and Cyclopropane® anesthesia, a fibro-adenoma was excised from the breast. Toward the end of the operation she became cyanotic; the blood pressure was 150/90 and the pulse rate 96 per minute. One hour later, in the recovery room, the blood pressure and pulse were unobtainable. There was an apical heart rate of 186 per minute. She was given 8 ampules of *l*-norepinephrine and intravenous digitoxin without benefit. An electrocardiogram showed a supraventricular tachycardia. She expired in a state of shock 6 hours after the operation.

At necropsy, there was marked pulmonary edema. The heart weighed 310 gm. The valvular apparatus was normal, and the myocardium showed no gross alterations. The anterior wall of the left ventricle measured 1.2 cm. in thickness. The right kidney received an anomalous polar artery arising from the aorta. Situated above and partially surrounding this artery was a soft tumor which measured 5 cm. in greatest diameter. It was lobulated and patchy bluish-gray in color with areas of red and brown. The right suprarenal gland was directly above the tumor and could be dissected away easily. Both suprarenals were normal.

Microscopically, the myocardial fibers were hypertrophied. The in-

terstitial tissue was focally edematous and contained a rich infiltration of lymphocytes with a few neutrophils and Anitschkow cells. There was perivascular fibrosis with collections of inflammatory cells. In some areas the muscle fibers were slightly spread apart by loose and cellular fibrous tissue. The muscle fibers themselves often appeared swollen and had markedly granular cytoplasm. The impression was gained that some of the muscle fibers had ruptured, allowing the extrusion of the granular cytoplasmic mass. There was considerable variation in the size of muscle fibers. A number of inflammatory cells, mainly histiocytes, were found adjacent to the severely degenerated muscle fibers. The neoplasm beneath the right suprarenal was a pheochromocytoma of extra-adrenal origin; microscopically it was similar to the one described in case 1.

Case 3. A 60-year-old white woman had rheumatoid arthritis for 25 years and received steroid treatment for 9 years. She was admitted because of severe joint and back pain. The pulse rate was 120 per minute; respirations, 20 per minute; blood pressure, 120/95. There was a gallop rhythm with a grade II or III precordial systolic murmur. A_2 equaled P_2. Rales were audible, and there were decreased breath sounds. The left ventricle appeared to be enlarged. An electrocardiogram was abnormal; it exhibited digitalis effect and possible coronary insufficiency. Treatment was given for congestive failure. The clinical impression was decompensated rheumatic heart disease. Several days later the blood pressure fell to 90/60, and ectopic auricular tachycardia became apparent. A transfusion of whole blood was begun because of a low hemoglobin level, but one hour later there was tachycardia, 150 per minute. Blood pressure was low, 80/70. Another electrocardiogram showed 3:2 A-V block. She expired suddenly shortly afterward.

At necropsy there was subluxation of both wrists and osteoarthritic degenerative changes. The heart weighed 375 gm. The aortic valve showed slight adherence between the individual cusps, and the myocardium was pale tannish-pink and smooth. Coronary arteries were patent throughout. The lungs showed edema, and several emboli were found in the branches of the left pulmonary artery. The left suprarenal gland contained a greenish-yellow tumor nodule measuring 2 cm. in greatest diameter. This was moderately firm and appeared to arise in the medulla. It was completely surrounded by cortical tissue. The remainder of the organs were the seat of chronic passive hyperemia. Dissection of the deep calf veins revealed phlebothrombosis, obviously the source of the pulmonary emboli.

Microscopically, the myocardial fibers were hypertrophied, and the nuclei were hyperchromatic. The fibers were separated by serous fluid in some areas and by loose connective tissue in others. There were collections of inflammatory cells in the interstitial tissue, mainly lymphocytes, large monocytes, Anitschkow cells, fibroblasts and a few neutrophils. A few mast cells were also present. There was an abnormal amount of interstitial fibrosis, especially noticeable in sections stained by the

van Gieson method. Isolated areas of severe degeneration of muscle fibers and even necrosis of small groups of fibers were found throughout the sections. The left suprarenal tumor was a typical pheochromocytoma.

Case 4. A 51-year-old white man was admitted with a history of fatigue, weight loss, and difficulty in swallowing of 5 months' duration. Two weeks previously, a biopsy via esophagoscopy revealed adenocarcinoma. On admission the blood pressure was 140/85; the pulse was regular, 88 per minute. Except for enlarged right posterior mandibular lymph nodes and an enlarged left supraclavicular node, the examination was negative. An esophagogastric resection and an end-to-end anastomosis were performed. He did well until the second postoperative day when shock supervened. The pressure was maintained by *l*-norepinephrine (10 to 40 drops per minute of 1,000 cc. of 5 per cent dextrose in water and 4 ampules of Levophed®). The temperature rose to 103°, and the pulse became irregular at a rate of 140 per minute. Later cyanosis and manifestations of right pleural effusion were noted. Thoracentesis was performed and 820 cc. of fluid were removed. Disruption of the anastomosis was presumed and an emergency jejunostomy was performed, but the patient expired the next day.

At necropsy the peritoneal cavity contained blood-stained fluid. The resection margins of the stomach and esophagus were joined by an end-to-end anastomosis which was intact except for a one centimeter defect in its anterior portion. This was surrounded by fibrin and a small amount of pus. The heart weighed 430 gm., and the myocardium was soft. The atriums and ventricles were slightly dilated, and the papillary muscles were flattened. Sections of the myocardium disclosed a few very poorly circumscribed areas, somewhat paler than the surrounding tissue. These were located in the posterior septum and posterior wall of the left ventricle. The valves were intact. The suprarenal glands were normal in shape; however, the right gland appeared slightly thicker than normal. On section, the medulla measured 0.4 cm. and contained a small, more or less circumscribed, grayish neoplasm. A well circumscribed tannish-white nodule measuring 2 cm. in diameter was found in the body of the pancreas.

Microscopic sections of the myocardium exhibited many foci in which muscle fibers were stained dark red and were devoid of striations or nuclei. These fibers were surrounded by edematous stroma in which a number of infiltrating histiocytes, Anitschkow cells and occasional neutrophils were noted. Often small foci of degenerating muscle fibers surrounded a few necrotic muscle bundles which were highly eosinophilic. In other sections there was an interstitial fibrosis; inflammatory cells were still manifest, but small groups of degenerated and partially necrotic muscle fibers were also observed. While these foci were relatively small, they were widely distributed in many sections.

The right suprarenal gland contained a poorly circumscribed medullary nodule which proved to be a typical pheochromocytoma. The nodule in the pancreas was an islet cell adenoma.

Results

The myocardial lesions in all 4 cases were strikingly similar; so similar, in fact, that a colleague who had examined the sections of the myocardium in 3 cases, when reviewing those in case 4, immediately asked whether the patient had received Levophed® or had a pheochromocytoma. The characteristic lesions consisted principally of two types of alterations. There were patchy areas with severe degeneration and necrosis of muscle fibers (Fig. 1) and interstitial fibrosis with chronic inflammation (Fig. 2). The affected muscle fibers were markedly swollen, granular, and deeply eosinophilic (Fig. 3). Occasionally it appeared that the sarcolemma had ruptured and the granular cytoplasmic mass had spread into the interstitial tissue. These lesions occasionally resembled those seen in diphtheria, but they were focal and never affected large areas. Small groups of fibers were densely eosinophilic, necrotic, and often appeared in the midst of swollen and degenerated fibers (Fig. 4). In addition, round cells, histiocytes and a few Anitschkow cells were observed interspersed among newly formed connective tissue fibers (Fig. 5). The latter lay parallel to the muscle fibers. Varying amounts of a serous exudate were noted (Fig. 6). Although a few neutrophils were manifest, nowhere were they prominent. The interstitial changes were more diffuse and noted with greater ease than the patchy muscle degeneration and necrosis.

All of the 4 patients with pheochromocytoma succumbed unexpectedly; it appeared probable that death was the result of acute left ventricular failure. Raab[4] stated that this might occur in patients with pheochromocytoma and was due to the insidious, long-continued injurious effect of catechols upon cardiac metabolism and structure. We certainly would have ascribed the deaths in our patients to a similar mechanism had we not found outspoken evidence of myocarditis. Two of the 4 patients had clinical evidence of myocarditis[5] shortly before death. Systolic murmur, gallop rhythm, tachycardia and the low-grade fever were the principal findings in this respect. In only one patient was a pheochromocytoma suspected clinically. While it is true that this individual also had nonbacterial, thrombotic endocarditis, the myocardial lesions were quite different from those encountered in endocarditis.[6] There were no minute infarcts, no evidence of myofibrolysis, no accumulations of neutrophils, and certainly no bacteria could be demonstrated. In the other 3 cases, no lesions were found anywhere to which the chronic inflammatory alterations in the myocardium could be ascribed.

Discussion

As early as 1905, Ziegler[7] reported degenerative changes in the myocardium in experimental animals treated with adrenalin. Pearce[8] found

severe degenerative lesions with necrosis and edema in the myocardium and, if the animals were allowed to survive a few days, more or less severe round cell infiltration and the production of connective tissue. Fleisher and Loeb[9,10] induced unmistakable myocarditis by injections of a mixture of caffeine and adrenalin. After a single injection, "chronic" myocarditis was found in 59 per cent of the animals. Franz[11] was able to produce myocardial degeneration combined with moderate inflammation by the administration of adrenalin. Maling and Highman[12] found severe fatty changes in the myocardium of dogs sacrificed one day after infusions with large doses of *l*-norepinephrine. These were still present when the animals were sacrificed 3 days later. Other features were focal necrosis, hemorrhage, and round cell infiltration of the myocardium. Szakács and Cannon[1] reported focal myocarditis and subendocardial and subepicardial hemorrhages in dogs treated with *l*-norepinephrine. Raab,[13] in reviewing the cardiac effects of adrenalin, described hypertrophy and dilatation of the heart, myocardial degeneration, and also edema, round cell infiltration, necrosis and eventually scar.

Szakács and his associates,[2,3] in recent studies, recorded various morphologic changes produced by catecholamine therapy, and presented experimental evidence in dogs, showing that *l*-norepinephrine could be a pathogenic drug. With large doses (10 to 15 μg. per minute per kg. of body weight) hemorrhages appeared in the mitral valve. After 10 hours of continuous infusion with 1 to 1.5 μg. per minute per kg., ⅔ of the dogs developed focal myocardial degeneration. Myocarditis was encountered in dogs treated with small doses over a period of several days. Hansmann and Schenken[14] stated that sparteine and adrenalin used in combination constituted one of the best means of producing experimental myocarditis.

A search of the literature also disclosed reference to myocarditis in patients treated with adrenalin, Levophed® and related substances. Franz[11] cited a 55-year-old woman who had attacks of asthma and died suddenly following gastric lavage. At necropsy the heart was hypertrophic, and there were degenerative and inflammatory lesions in the myocardium. Franz ruled out various infectious diseases as the cause of the myocarditis and concluded that it was the result of long-standing adrenalin therapy. However, he believed that adrenalin and similar drugs did not cause myocardial alterations regularly but that the development of hypersensitivity to such drugs might be responsible for myocarditis. Raab[13] noted that degenerative lesions were observed occasionally in the myocardiums of asthmatic patients treated with epinephrine for long periods of time. Szakács and Cannon[1] studied two patients with myocarditis following *l*-norepinephrine treatment. Szakács

and Mehlman[3] very recently reported myocarditis in dogs treated with *l*-norepinephrine and illustrated with photomicrographs myocarditis in 2 patients who had received this drug. As a matter of fact, they used the term "norepinephrine myocarditis." They emphasized the resemblance of the myocardial lesions to those seen in diphtheritic myocarditis.

There is evidence that the pheochromocytoma may secrete pressor substances,[15] especially epinephrine and norepinephrine. It may be expected, therefore, that patients with pheochromocytoma may occasionally also develop myocardial lesions similar to those described above. However, we were able to find only 3 references in this connection. In 1953, Dontenwill[16] reported an instance of chronic myocarditis associated with pheochromocytoma of the suprarenal. He believed, however, that the chronic myocarditis was the primary lesion causing cardiac hypertrophy and speculated that the pheochromocytoma might have constituted "an expression of a compensatory mechanism caused by the increased strain upon the suprarenal medulla." Szakács and Cannon[1] reviewed the necropsy material at the Armed Forces Institute of Pathology in 17 adults with pheochromocytoma. Myocardial lesions were present in all without exception. Acute myocarditis was found in 3 patients. Unfortunately, no detailed microscopic descriptions were given although there were photomicrographs illustrating early myocarditis in the heart of a 20-year-old patient treated with *l*-norepinephrine and perivascular myocardial inflammation in an 81-year-old patient who had received *l*-norepinephrine for 22 days. They also included an illustration of the myocardium in a 33-year-old man with pheochromocytoma, noting edema, chronic inflammatory cells and replacement fibrosis. Raab,[4] summarizing the observations of others, stated that round cell infiltration, necrosis and scar tissue may be found in the myocardium of patients with suprarenal medullary tumors. He speculated that these changes were analogous to those seen in the hearts of individuals treated with epinephrine. It is of interest that Gillman, Gilbert and Spence[17] found chronic myocarditis in over 70 per cent of albino Wistar rats who had developed suprarenal medullary tumors similar to the pheochromocytomas in man.

From this brief review it is apparent that myocardial alterations have been encountered in experimental animals and in human subjects treated with epinephrine and similar substances, and, although rarely, in patients with pheochromocytoma as well. One may question whether the myocarditis is actually caused by the secretory product of the pheochromocytoma (norepinephrine); whether it constitutes a hypersensitivity reaction; or whether it is unrelated to norepinephrine and is merely a fortuitous occurrence. In none of the experimental reports were vessel

changes such as polyarteritis recorded, nor were eosinophils observed in significant numbers in the inflammatory lesions. There is, therefore, no tangible evidence that the myocardial changes were the result of hypersensitivity. There was no evidence of hypersensitivity in the cases reported by Szakács and Cannon [1] or in our patients described herein.

Two of our patients had had administration of *l*-norepinephrine for therapeutic purposes. However, the myocardial lesions observed were obviously of longer duration than would have been the case had they resulted from the recently administered medication.

The outstanding lesions in our cases were the severe degenerative changes in groups of muscle fibers combined with focal necrosis and chronic interstitial inflammation. Even though there was no evidence of fatty degeneration, the myocardial alterations closely resembled those seen in experimental animals treated with norepinephrine and in patients with suprarenal medullary tumors. The lesions in all 4 cases were similar and quite distinctive; they differed from the myocarditis observed in infectious diseases and in hypersensitivity, but bore a close resemblance, however, to the lesions in occasional patients treated with norepinephrine. Thus, while there is no conclusive proof, it is most likely that the myocarditis in our cases was attributable to a secretory product of pheochromocytoma. The alterations, indeed, were so very characteristic that it seems reasonable to refer to them as "norepinephrine myocarditis."

Summary

Myocardial lesions have been produced experimentally with epinephrine, norepinephrine, Levophed® and adrenalin. These alterations were apparently primarily degenerative, but were followed by frank inflammation. Moreover, on rare occasions, myocarditis has been observed in patients with pheochromocytoma; this has been attributed to the norepinephrine secreted by these tumors.

Among 7 patients with pheochromocytoma whose necropsy tissues were personally inspected, myocarditis was found in 4. These 4 patients succumbed unexpectedly, and it seemed likely that the deaths were the result of acute myocardial failure brought about by myocarditis. Two patients had clinical evidence of myocarditis in the form of systolic murmur, gallop rhythm and tachycardia shortly before death. The myocardial lesions which resembled those in the experimental animal treated with norepinephrine consisted principally of severe degenerative changes in groups of muscle fibers, foci of necrosis and chronic interstitial inflammatory exudation.

References

1. Szakács, J. E., and Cannon, A. *l*-Norepinephrine myocarditis. *Am. J. Clin. Path.*, 1958, **30**, 425–434.
2. Szakács, J. E.; Dimmette, R. M., and Cowart, E. C., Jr. Pathological implication of the catechol amines, epinephrine and norepinephrine. *U.S. Armed Forces M.J.*, 1959, **10**, 908–925.
3. Szakács, J. E., and Mehlman, B. Pathologic changes induced by l-norepinephrine: quantitative aspects. *Am. J. Cardiol.*, 1960, **5**, 619–627.
4. Raab, W. Key position of catecholamines in functional and degenerative cardiovascular pathology. *Am. J. Cardiol.*, 1960, **5**, 571–578.
5. Kline, I. K., and Saphir, O. Chronic pernicious myocarditis. *Am. Heart J.*, 1960, **59**, 681–697.
6. Saphir, O. Myocarditis. In: A Text on Systemic Pathology. Saphir, O. (ed.). Grune & Stratton, New York, 1958, Vol. I, p. 32.
7. Ziegler, K. Über die Wirkung intravenöser Adrenalininjektion auf das Gefässystem und ihre Beziehung zur Arteriosklerose. *Beitr. path. Anat.*, 1905, **38**, 229–254.
8. Pearce, R. M. Experimental myocarditis: a study of the histological changes following intravenous injections of adrenalin. *J. Exper. Med.*, 1906, **8**, 400–409.
9. Fleisher, M. S., and Loeb, L. Experimental myocarditis. *Arch. Int. Med.*, 1909, **3**, 78–91.
10. Fleisher, M. S., and Loeb, L. Further investigations in experimental myocarditis. *Arch. Int. Med.*, 1910, **6**, 427–438.
11. Franz, G. Eine seltene Form von toxischer Myokardschädigung. *Virchows Arch. path. Anat.*, 1937, **298**, 743–752.
12. Maling, H. M., and Highman, B. Exaggerated ventricular arrhythmias and myocardial fatty changes after large doses of norepinephrine and epinephrine in unanesthetized dogs. *Am. J. Physiol.*, 1958, **194**, 590–596.
13. Raab, W. Pathogenic significance of adrenalin and related substances in heart muscle. *Exper. Med. & Surg.*, 1943, **1**, 188–225.
14. Hansmann, G. H., and Schenken, J. R. Acute isolated myocarditis. Report of a case with study of the development of the lesion. *Am. Heart J.*, 1938, **15**, 749–756.
15. Kvale, W. F.; Priestley, J. T., and Roth, G. M. Pheochromocytoma; clinical aspects and surgical results. *A.M.A. Arch. Surg.*, 1954, **68**, 769–778.
16. Dontenwill, W. Zur Pathogenese des Phäochromocytomas. *Ärztl. Forsch.*, 1953, **7**, 413–417.
17. Gillman, J.; Gilbert C., and Spence, I. Pheochromocytoma in the rat; pathogenesis and collateral reactions and its relation to comparable tumors in man. *Cancer*, 1953, **6**, 494–511.

The author is grateful to Dr. O. Saphir, Director of the Department of Pathology, Michael Reese Hospital, for his help and advice, and to Miss Irene Goldberger for the histologic sections.

[*Illustrations follow*]

Legends for Figures

The photographs were prepared from sections stained with hematoxylin and eosin.

Fig. 1. A number of necrotic muscle fibers are accompanied by an interstitial infiltration of lymphocytes and histiocytes. Many stromal cells are intact. × 295.

Fig. 2. Degeneration of muscle fibers is associated with an interstitial infiltration by lymphocytes and a few neutrophils. × 295.

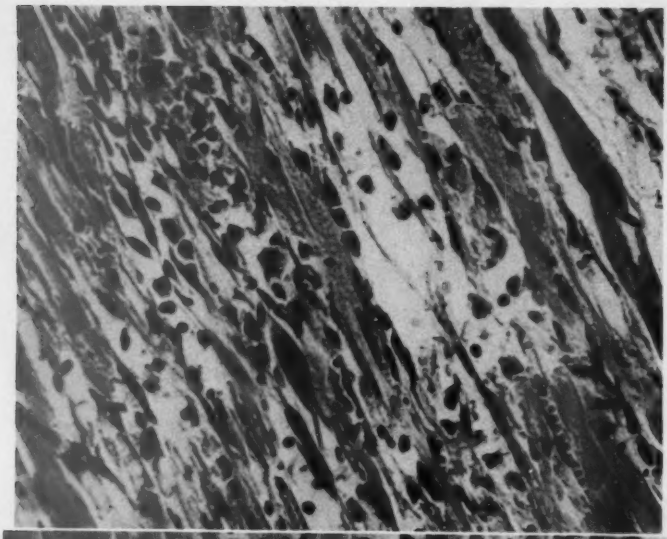

1

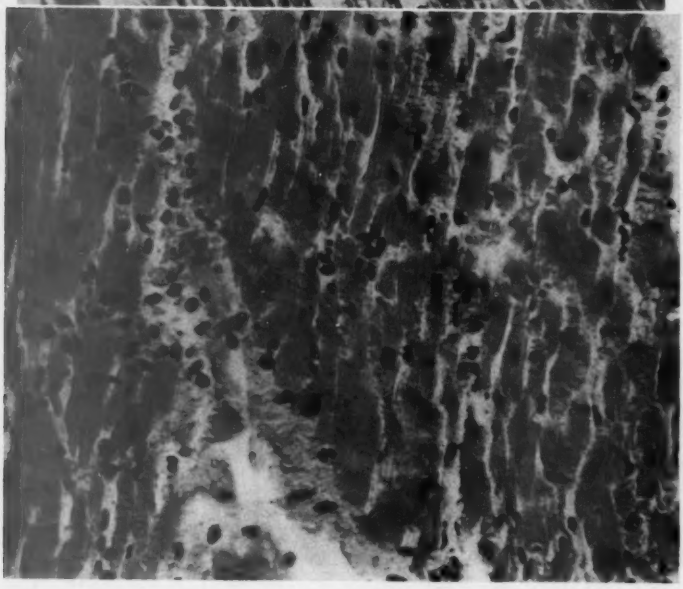

2

3

4

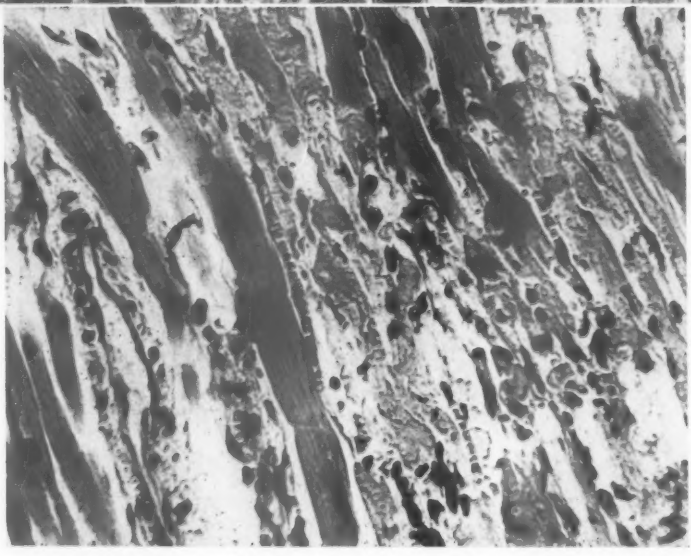

FIG. 3. There is severe degeneration of muscle fibers and a few reactive lymphocytes. × 375.

FIG. 4. Degeneration and necrosis of muscle fibers is associated with a few lymphocytes. × 295.

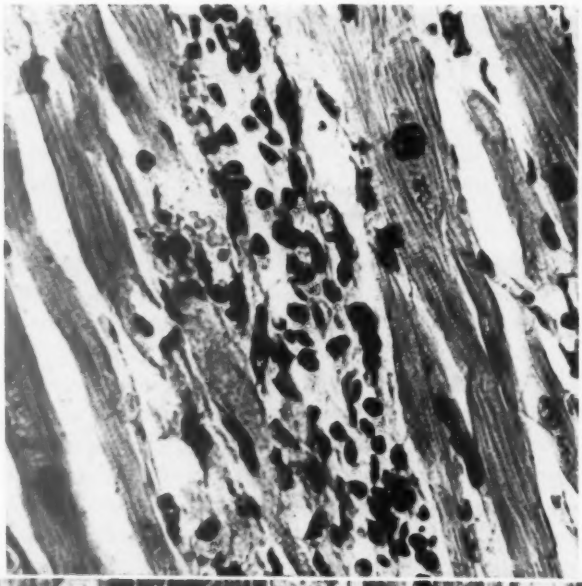

5

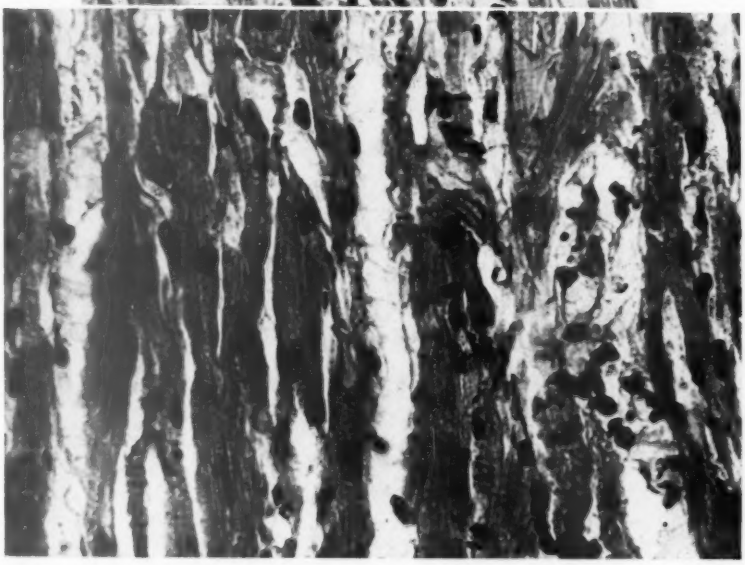

6

FIG. 5. There is marked interstitial infiltration by lymphocytes and a few neutrophils. There is also degeneration of muscle fibers. × 450.

FIG. 6. Severe degeneration of muscle fibers is recognized by inflammatory cells and a serous exudate. × 375.

THE ABSENCE OF MYOCARDITIS IN RATS INFECTED WITH RADIATED TRICHINELLA SPIRALIS

HERMAN ZAIMAN, M.D.; DAVID M. MAKIE, M.D., AND RUDOLPH G. HOWARD, M.D.

From the Department of Pathology, Albert Einstein College of Medicine, Yeshiva University, New York, N.Y.

The occurrence of myocarditis in human and experimental trichinosis is well known and has recently been reviewed by Gould.[1] Its pathogenesis, however, is not clearly established. Thus Simmonds,[2] unable to find larvae migrating through the myocardium, postulated a toxic etiology. Other authors, having reported [1,3–7] and photographed [1,8–10] migrating larvae in such lesions, consider the physical presence of the nematodes causative. The fact that myocarditis has not been reported in experimental animals before the onset of the migratory phase[5] suggests that migration has special significance in the pathogenesis of these lesions. It should be noted, however, that the number of lesions is invariably far in excess of the number of nematodes that can be demonstrated in the myocardium at a given time. While lesions lacking larvae may be due to the previous presence of nematodes in the myocardium, toxic factors have not been ruled out. Toxins could be produced by the Trichinella *per se* or by a host reaction to them. Since none of these possibilities necessarily excludes others, any combination of mechanical and toxic factors is possible.

The experiment reported here was designed to determine whether myocarditis would occur in an infestation lacking the larval migratory phase. This is made possible by the fact that exposure of Trichinella larvae to appropriate doses of roentgen radiation inhibits their reproduction. Lacking reproduction, infestation is limited to the intestine.

EXPERIMENTAL PROCEDURES

Five-week-old male albino rats of the Holtzman strain, housed in individual metal wire cages, fed Purina Lab Chow (Ralston-Purina Company, Saint Louis, Missouri) and given water *ad libitum*, were used.

Larvae were procured from 3 rats infested with *Trichinella spiralis* 2 months earlier. They were sacrificed, skinned and eviscerated. Their ground-up carcasses were digested in a solution of 1 per cent pepsin and 0.5 per cent concentrated hydrochloric acid which was continually agitated by bubbling air. Following digestion at 37° C. for 12 hours, the mixture was passed through a metal strainer (20 meshes per square inch). The larvae were washed with tap water several times by decantation. They were then divided into 3 aliquots, one of which was exposed to 12,000 r of

This work was supported by Grant #E-2612 from the National Institutes of Health.
Accepted for publication, January 11, 1961.

roentgen radiation; another received 14,000 r. The larvae in the third aliquot were not irradiated and were used for control infections.

Radiation was provided by a 250 kv. Westinghouse Duocondex machine. The irradiation factors were as follows: 250 kv., 15 ma., a half value layer of 1.5 mm. of Cu. The larvae were placed 18.5 cm. from the source of the roentgen rays and received the radiation at the rate of 785 r per minute.

For inoculation, an appropriate volume of a suspension of worms (determined previously by dilution counts) was placed in 15 ml. centrifuge tubes. Having settled, the larvae were drawn into a tapered glass pipette fitted with a rubber bulb. The pipette was introduced deep into the esophagus of the anesthetized rat and the larvae deposited into the lower esophagus by compressing the rubber bulb.

To determine the number of muscle larvae present in any rat, its carcass was digested. The volume of the water containing the total number of cleaned worms released by digestion was brought up to 500 ml., and counts were made on aliquots. The mean number of larvae found per ml. was multiplied by 500 to determine the total number of larvae present. When few larvae were found in a digest, the number and size of the aliquots searched was increased and appropriate factors used for multiplication.

Hearts were prepared for microscopic examination in the following manner. The rat was sacrificed, the skin incised and the sternum split. The heart was separated from the mediastinum at the origin of the great vessels. It was then hemisectioned along its anterior border, exposing both ventricles. These cavities were flushed with normal sodium chloride to remove blood clots. The 2 halves were placed in 10 per cent buffered formalin and fixed for 5 days. A longitudinal section of each ventricle was then taken; paraffin sections were stained with hematoxylin and eosin. Each slide, containing 2 sections, 1 of the left and 1 of the right ventricle, was examined for evidence of myocarditis.

Criteria for the diagnosis of myocarditis were established after examining many hearts from untreated rats and from rats subjected to other experimental procedures. The presence of focal collections of inflammatory cells with or without lysis of myofibers was considered evidence of myocarditis. Such lesions were present deep within the myocardium and also on the pericardial and endocardial surfaces of ventricles (Figs. 1 to 4). Valvular lesions induced by stress [11,19] and minimal perivascular infiltration were not considered significant; the latter was found in many normal rats and in our experimental controls.

Experimental Protocol

The experiment consisted of inoculating rats with normal or irradiated Trichinella, sacrificing them 10 days after infestation, and examining hematoxylin and eosin stained sections of their hearts for evidence of myocarditis. Seventy-two rats were divided into 4 groups of 18 each. Group I received no larvae but received a sham inoculum of 1 cc. of saline. Each rat in group II received 4,000 nonirradiated Trichinella larvae. In group III, each rat received 4,000 larvae irradiated with 12,000 r, and in group IV the rats each received 4,000 larvae irradiated with 14,000 r.

In order to study the virulence of the worms and the efficiency of the sterilization procedure, 40 additional animals were divided into 4 groups of 10 each. The animals in group Ia were given a sham inoculum. Each rat in group IIa was given 500 of the nonirradiated larvae. In group IIIa each received 500 of the larvae irradiated with 12,000 r; rats in group IVa were each given 500 of the larvae irradiated with 14,000 r. Thirty days later the rats were sacrificed and total worm counts made to evaluate the effect of radiation on preventing reproduction and subsequent migration.

Results

The infectivity of the nonirradiated larvae was indicated by the recovery of a mean of 160,000 muscle larvae from each of the rats inocu-

lated with 500 such worms (Table I). The fact that only 10 muscle larvae were recovered from 1 of the 20 rats receiving irradiated larvae clearly demonstrated the efficiency of the sterilization procedure.

TABLE I

LARVAE RECOVERED BY PEPTIC DIGESTION 30 DAYS FOLLOWING THE INTRODUCTION OF IRRADIATED TRICHINELLA

Group	Inoculum (No. of larvae)	Prior treatment of larvae	Average no. of worms per rat
Ia *	None		0
IIa	500	Nonirradiated	160,000
IIIa	500	Irradiated with 12,000 r	1 †
IVa	500	Irradiated with 14,000 r	0

* Each group represents 10 animals.
† This represents one animal from which 10 larvae were recovered.

Infestation of rats with Trichinella larvae led to evidence of myocarditis in the hearts of 15 animals (Table II). Of these, only one had received irradiated larvae. In contrast 14 of 18 rats receiving nonirradiated larvae showed lesions. The myocarditis consisted of both focal and

TABLE II

OCCURRENCE OF MYOCARDITIS IN RATS RECEIVING TRICHINELLA SUBJECTED TO ROENTGEN RADIATION

Group	No. of larvae (dose)	Prior treatment of larvae	No. of rats	Rats with myocarditis
I	None		18	0
II	4,000	Nonirradiated	18	14 (77.8) *
III	4,000	Irradiated with 12,000 r	18	0
IV	4,000	Irradiated with 14,000 r	18	1 (5.6)

* Values in parentheses represent per cent of total.

diffuse infiltration with inflammatory cells. Myocardial fiber destruction was evident in the advanced lesions.

The cellular infiltrate varied. Although it consisted primarily of monocytic leukocytes, occasional eosinophils and neutrophils were seen, especially in those lesions where muscle fiber necrosis had occurred. There was no preponderance of eosinophils in any of the lesions. Some of the cells exhibited the bar chromatin pattern associated with the Anitschkow myocyte; this was not common. The infiltrate often was limited to and surrounded a single muscle fiber. When fiber destruction occurred, a loose fibrillar tissue filled with inflammatory cells was frequently observed.

Discussion

The data clearly indicate that with one exception myocarditis did not occur among rats receiving 4,000 Trichinella subjected to 12,000 r or 14,000 r of irradiation. The radiation eliminated the migratory phase of the process by sterilizing the reproductive capacity of the larvae. On the other hand, the great majority of rats receiving nonirradiated larvae suffered myocardial lesions. Since myocarditis did not occur in the absence of migrating larvae, the latter may be a *sine qua non* for the former.

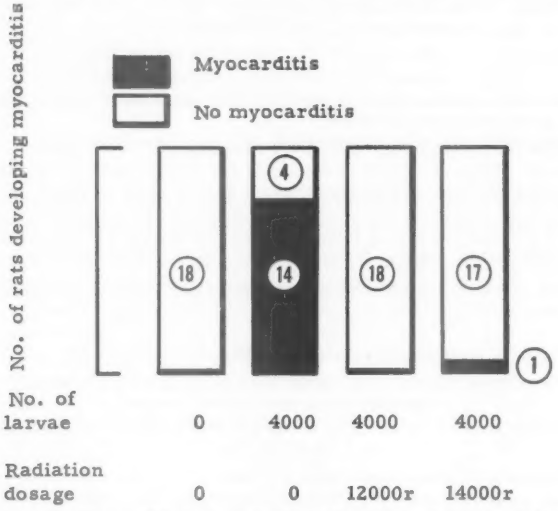

Text-figure 1. Myocarditis in 5-week-old white rats receiving irradiated *Trichinella spiralis* larvae.

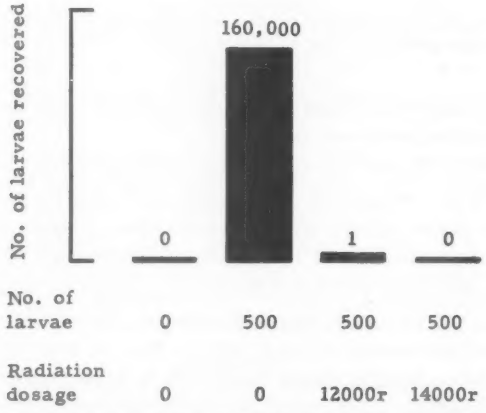

Text-figure 2. Roentgen radiation of Trichinella larvae. Average number of worms recovered one month after inoculation.

The possibility of qualitative or quantitative radiation damage to a nematode mechanism for toxin production has not, however, been excluded.

Summary

Exposure to 12,000 or 14,000 r of roentgen radiation effectively abolished the reproductive capacity of *Trichinella spiralis* larvae.

Only 1 of 36 rats, each inoculated with 4,000 radiated larvae, showed evidence of myocarditis in hematoxylin and eosin stained preparations. Fourteen of 18 rats receiving the same number of nonirradiated Trichinella exhibited myocardial lesions.

References

1. Gould, S. E. Trichinosis. Charles C Thomas, Springfield, Ill., 1945, 356 pp.
2. Simmonds, M. Ueber Myocarditis trichinosa. *Centralbl. allg. Path.*, 1919, **30**, 1–3.
3. Zenker, F. A. Ueber die Trichinenkrankheit des Menschen. *Virchows Arch. path. Anat.*, 1860, **18**, 561–572.
4. Frothingham, C. A contribution to the knowledge of the lesions caused by *Trichina spiralis* in man. *J. Med. Res.*, 1906, **15**, 483–490.
5. Dunlap, G. L., and Weller, C. V. Pathogenesis of trichinous myocarditis. *Proc. Soc. Exper. Biol. & Med.*, 1933, **30**, 1261–1262.
6. Gould, S. E. (ed.). Pathology of the Heart. Charles C Thomas, Springfield, Ill., 1960, 1138 pp.
7. Horlick, S. S., and Bicknell, R. E. Trichiniasis with widespread infestation of many tissues. *New England J. Med.*, 1929, **201**, 816–819.
8. Stryker, W. A. Parasitic Diseases of the Heart. In: Pathology of the Heart. Gould, S. E. (ed.). Charles C Thomas, Springfield, Ill., 1960, p. 831.
9. Rappaport, I. Trichinosis. In: Clinical Tropical Medicine. Gradwohl, R. B. H.; Benitez Soto, L., and Felsenfeld, O. (eds.). C. V. Mosby Co., St. Louis, 1951, p. 852.
10. Terry, L. L., and Work, J. L. Trichinosis of the myocardium; report of a case with autopsy findings. *Am. Heart J.*, 1940, **19**, 478–485.
11. Angrist, A. A. A concept of the origin of the cardiac valvular vegetation. *J. Mt. Sinai Hosp.*, 1957, **24**, 669–681.
12. Angrist, A. A.; Oka, M.; Nakao, K.; Marquiss, J., and Deane, H. The production of valvular lesions by varying stress mechanisms in the adrenalectomized rat. *Proc. New York State A. Pub. Health Labs.*, 1958, **38**, 3–5.

[*Illustrations follow*]

Legends for Figures

Photographs were prepared from sections stained with hematoxylin and eosin. In each instance a rat received 4,000 nonirradiated Trichinella larvae and was sacrificed 10 days later.

Fig. 1. Myocardium. A focal inflammatory infiltration is shown. × 230.

Fig. 2. Myocardium. There is a diffuse inflammatory infiltration. × 240.

Fig. 3. Myocardium. A single muscle fiber is infiltrated by inflammatory cells. × 600.

Fig. 4. Myocardium. A loose fibrillar tissue containing an inflammatory infiltrate replaces a muscle fiber. × 410.

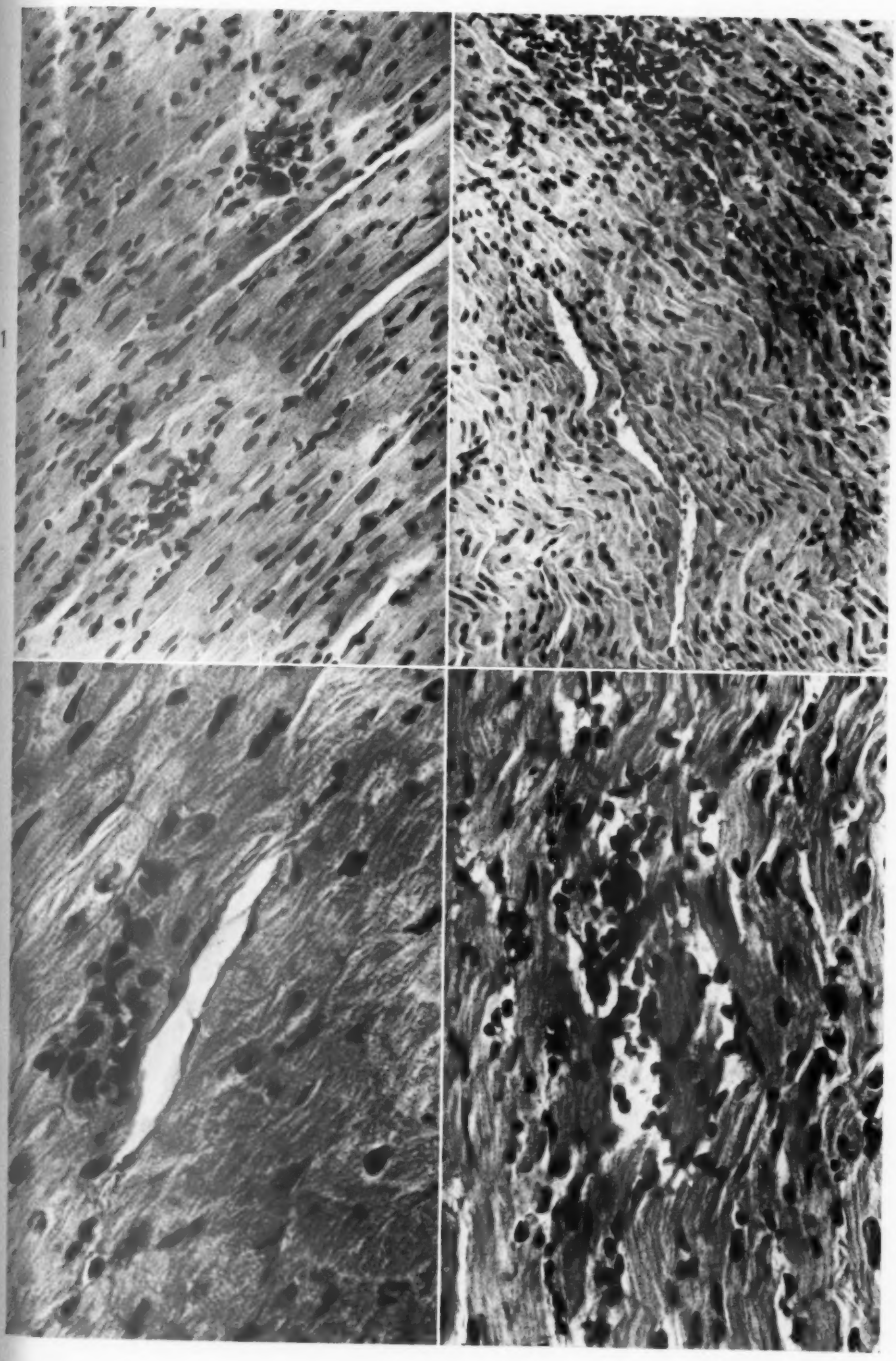

KYPHOSCOLIOSIS AND COR PULMONALE

A Study of the Pulmonary Vascular Bed

Richard L. Naeye, M.D.*

From the Department of Pathology, The University of Vermont College of Medicine, Burlington, Vt.

Certain persons with long-standing dorsal kyphoscoliosis develop pulmonary arterial hypertension and cor pulmonale. A normal pulmonary arterial wedge pressure in these cases suggests that the small pulmonary vessels are the site of an increased resistance to blood flow.[1] However, pulmonary vascular abnormalities have not been established as the basis for this high resistance.[2–9] The present study was undertaken to determine if such vascular changes occur and, if they do, what relationship they may have to other factors thought to influence the pulmonary circulation in kyphoscoliosis. These other factors include: (a) intrinsic pulmonary parenchymal disorder; (b) chronic hypoxemia; and (c) reduction in the pulmonary vascular bed by the thoracic deformity.

Intrinsic pulmonary parenchymal lesions are common in kyphoscoliosis. These may independently increase pulmonary vascular resistance. Included are chronic obstructive emphysema, bronchiectasis, pulmonary fibrosis, abscesses and atelectasis.[2–6,8,10–18] Chronic hypoxemia, often present in kyphoscoliosis, may induce both functional and anatomic changes in the pulmonary vascular bed.[1,9,19–23] Finally, the thoracic deformity itself may restrict the pulmonary vascular bed by reducing thoracic volume. Restriction of the pulmonary parenchyma is presumably associated with a reduction in the pulmonary vascular bed.[24] In adults with kyphoscoliosis the lungs are often less than one-half normal size.[1,9–12]

In the current study, each factor was considered in patients having dorsal kyphoscoliosis and chronic cor pulmonale. To evaluate the influence of the thoracic deformity, pulmonary vessels in these cases were compared with similar vessels in 3 control cases after pneumonectomy. The influence of chronic hypoxemia was assessed by comparison with vascular alterations known to be induced by chronic hypoxemia in other disorders. The influence of intrinsic lung lesions was explored by comparing the pulmonary vascular bed in kyphoscoliosis complicated by

Accepted for publication, December 19, 1960.

* Markle Scholar in Medical Science.

TABLE I

PATIENTS WITH DORSAL KYPHOSCOLIOSIS

Case number:	1	2	3	4	5	6	7	8	9	Normal
Age at death; sex	29M	49M	39F	42M	76F	49F	48M	57M	40F	
Duration of deformity (yr.)	15	49	39	41	76	Child-hood	46	55	38	
Symptoms										
Duration (yr.)	3	*	3	1	0	10	4	1½	2½	
Dyspnea	4+	4+	4+	4+	0	4+	3+	4+	4+	
Orthopnea	0	0	2+	1+	0	1+	0	1+	1+	
Signs										
Respirations per minute	40	25	38	36	30	44	*	26	30	16–22
Pul. 2nd sound, accentuation	1+	2+	1+	2+	0	0	2+	1+	3+	0
Cyanosis	3+	3+	3+	3+	0	3+	2+	3+	3+	0
Peripheral edema	3+	2+	1+	2+	0	*	*	4+	0	0
Laboratory data										
Hematocrit (%)	65.0	48.0	42.0	55.0	41.0	44.0	66.0	49.0	54.0	42–49
Arterial CO_2 cont. (vol. % at 40 mm. of Hg)	55.5	*	68.8	68.0	*	58.0	*	*	75.7	50
Arterial Hb. O_2 saturation in %	59.8	*	87.5	49.7	*	70.0	*	*	42.1	94–97
Right ventricular pressure (mm. of Hg)	58/10	*	*	*	*	53/3	*	*	*	
Vital capacity (cc.)	630	*	600	*	*	460	*	*	750	2 1/2 3400–4000

	Necropsy observations									
Heart										
Weight (gm.)	430	280	280	375	220	450	320	*	500	200–350
Dilatation of rt. atrium	1+	1+	1+	3+	0	2+	1+	3+	3+	0
Dilatation of rt. ventricle	2+	3+	1+	3+	1+	3+	2+	3+	3+	0
Rt. ventricle (thickness in mm.)	10.0	7.5	5.0	10.0	4.0	10.0	6.0	8.5	8.0	1–3
Lungs										
Vol. of lungs combined, in % of predicted	*	*	*	35%	65%	*	30%	*	35%	100%
Emphysema	1+	1+	1+	2+	2+	1+	3+	3+	3+	0
Bronchitis and bronchiolitis	0	0	0	0	0	2+	2+	2+	2+	0
Pleural adhesions	1+	2+	0	2+	0	0	0	2+	2+	0
Other pulmonary parenchymal disorders	Terminal atelectasis	Focal fibrosis, R.L.L.	0	0	Fibrosis, apex rt. lung	0	0	Bronchiectasis, L.U.L. Old atelectasis, L.L.L.	Bronchiectasis, L.U.L., abscess, L.U.L. Fibrosis	0

1+, very mild; 2+, mild; 3+, moderate; 4+, severe; *, unknown.

chronic obstructive emphysema with that in kyphoscoliosis without intrinsic parenchymal disease.

Material

Nine patients with dorsal kyphoscoliosis and chronic cor pulmonale were selected from the necropsy files at the Presbyterian and Bellevue Hospitals, New York City. There were evidences of pulmonary hypertension in all instances (Table I). Right heart catheterization in 2 of the cases demonstrated a marked elevation of right ventricular pressure which increased with exercise. At necropsy, all 9 had right ventricular myocardial hypertrophy and in 8 the right heart was dilated. None had a deformity of the great vessels sufficient to restrict blood flow through them.

All 9 patients had small lungs. In every case, the thoracic deformity was present long before skeletal growth was complete. This suggested that the skeletal deformities prevented the lungs from growing to the usual adult size. Kyphoscoliosis was usually the most important factor in reducing thoracic volume since it diminished the height of the thoracic cage. In most instances, the lateral rotation due to scoliosis was responsible for one lung being smaller than the other (Fig. 1). In the cases in which measurement was made, combined lung volumes by fluid displacement at necropsy ranged from 30 to 65 per cent of the values found in normal controls matched for body size and weight (Table I). The matched, normal controls were 17 individuals without thoracic deformity; these died with disorders unrelated to the cardiopulmonary system. The 65 per cent value was recorded in one patient who survived until old age and died of noncardiopulmonary causes (Table I). In 4 cases vital capacity measured during life was less than one third of normal.

Arterial hypoxemia and hypercapnia were noted in 5 cases in which blood gas studies were made. Eight of the 9 patients were cyanotic, some for protracted periods and others for a short time before death. A secondary polycythemia was present in 5. These phenomena may be attributed to cardiorespiratory failure, a common clinical complication of kyphoscoliosis after the third decade.[1,6] Other common clinical features of cardiorespiratory failure which the patients exhibited were dyspnea, orthopnea and peripheral edema. Several individuals were somnolent during their terminal illnesses. Clinically, this was related to hypercapnia.

Significant intrinsic pulmonary lesions were found in 3 patients at necropsy (Nos. 7, 8 and 9). Two had had repeated respiratory infections during life, with cough and purulent sputum (Nos. 8 and 9). All 3 had diffuse, chronic obstructive emphysema, and bullae were prominent. On microscopic, examination, chronic inflammatory cells could often be seen in bronchiolar walls. Respiratory bronchioles and alveolar ducts were ballooned, and alveolar spaces were dilated, Alveolar walls were narrowed and ruptured. In many cases, fibrosis involved alveolar walls and interstitial tissues. Bronchiectasis was extensive in 2 of the patients, one of whom also had a pulmonary abscess.

Intrinsic pulmonary alterations were few in the other 6 cases. Except for reduced lung size, gross alterations were insignificant. Microscopically, some alveolar spaces were distended and scattered alveolar walls were ruptured. These changes were usually localized and were never associated with bronchitis or bronchiolitis. Patches of atelectasis were found in several of the lungs. The absence of inflammation or fibrosis in

most of the atelectatic areas suggested that they were of short duration. Each of the pulmonary lesions found in these 6 cases was found in some of the matched normal controls.

Lungs from 3 patients who had had pneumonectomy were also examined in an attempt to determine the effect of the single factor, pulmonary vascular bed reduction, on the remaining pulmonary vessels. All 3 individuals had survived operation for an appreciable time without intrinsic disease in the remaining lung. None had evidence of hypoxemia. In these patients there was mild right ventricular hypertrophy and dilatation at death. This suggested that there had been at least latent pulmonary hypertension during life—that is, an abnormal pulmonary arterial pressor response when blood flow was augmented by exercise.[25] At necropsy, the remaining lung was grossly normal. Microscopically the only finding was mild overdistention of alveolar spaces.

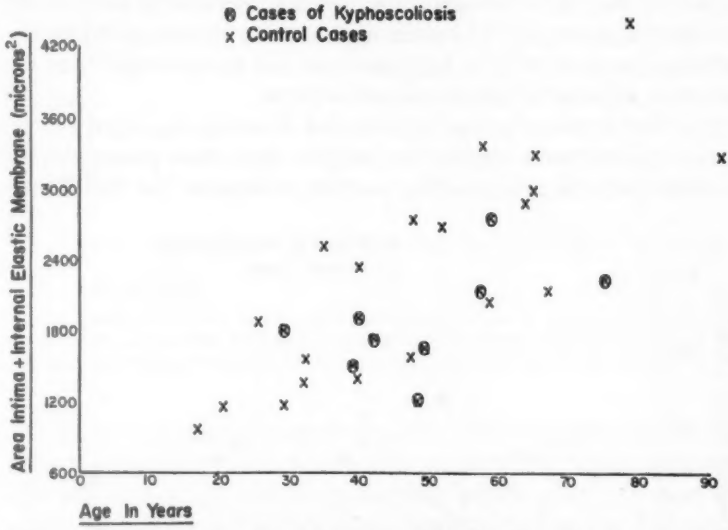

TEXT-FIGURE 1. The mean area of intima combined with internal elastic membrane is recorded for pulmonary arteries of all sizes in patients with kyphoscoliosis and in normal controls. Values for the two groups are similar. In both groups the values rise with age because of thickening of the intima.

METHODS

Blocks of tissue were taken from the lungs in each case, a balance being maintained between upper and lower lobes. Every block was serially sectioned so that vascular channels could be traced and examined for some distance. In two cases, bronchial and pulmonary arterial systems were injected with a gelatin preparation[26] in an attempt to demonstrate abnormal communications between the two circuits. Sections were stained with Verhoeff's and van Gieson's stains, a method which helped to differentiate fibrous tissue, elastic tissue and muscle.

A quantitative study of the structure of the pulmonary arterial beds was undertaken. To avoid bias, microscopic sections from control patients and those with kyphoscoliosis were mixed and examined in a random manner. Vascular measurements were made from drawings prepared at constant magnification with the aid of a camera lucida.[27] With a planimeter, the relative cross sectional areas of lumen, intima combined with internal elastic membrane, and media were determined for 15 to 30 muscular arteries and arterioles in each case. All vessels cut in cross section which were encountered were measured.

Results

Neither qualitative nor quantitative abnormalities were found in the intima or elastic membranes of pulmonary arteries in patients with kyphoscoliosis when compared with normal controls. The mean combined cross sectional area of intima and internal elastic membrane was charted for muscular arteries and arterioles in each case (Text-fig. 1). The mean values in kyphoscoliosis matched those of normal controls, indicating that these two structures had not thickened in patients with the skeletal deformity. The mean area of these structures did increase with age, however, in both kyphoscoliosis and normal controls as a result of an increase in intimal connective tissue.

For further investigation, arteries and arterioles less than 150 μ in lumen diameter were selected for analysis since these presumably had an important role in controlling vascular resistance. The fact that the

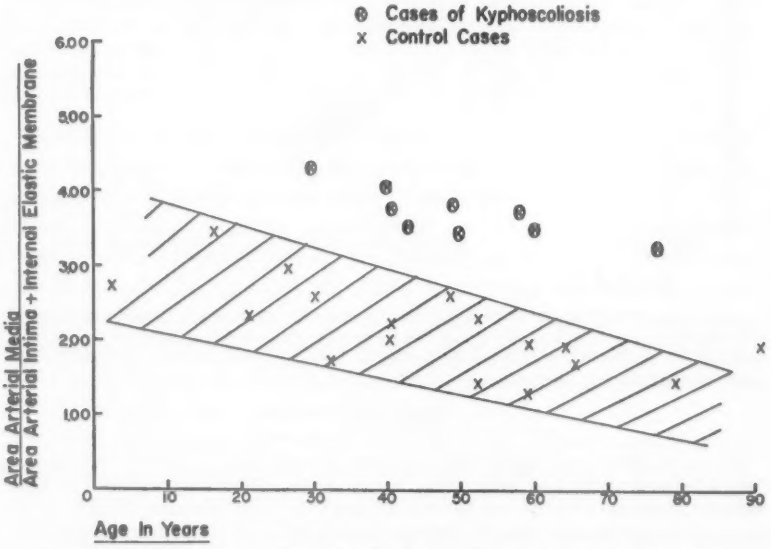

Text-figure 2. A ratio which reflects medial muscle mass is recorded for small pulmonary arteries in patients with kyphoscoliosis and in normal controls. The arteries in persons with kyphoscoliosis show a greater muscle mass than do the controls.

intimal area of pulmonary arteries was normal in our cases proved useful; it made possible the use of this value as a base line in the quantitative study of other vascular structures. The area of the media varied markedly and in a very significant manner when compared to this base line. The ratios of media to intima in cases of kyphoscoliosis and in nor-

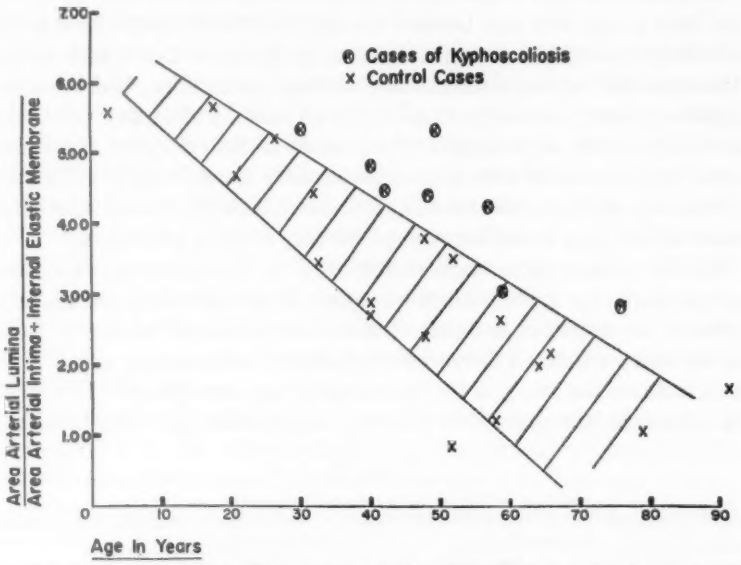

TEXT-FIGURE 3. A ratio which reflects arterial dilatation is recorded for small pulmonary arteries in patients with kyphoscoliosis and in normal controls. In all but one individual with kyphoscoliosis, the pulmonary arteries are more dilated than in control cases.

mal controls are charted in Text-figure 2. The method employed for calculating this ratio has been previously published.[23,27] The mean ratios in persons with kyphoscoliosis were considerably greater than in the control cases. This indicated that an appreciable increase had taken place in the medial muscle mass of the smaller pulmonary arteries in the kyphoscoliotic group. In some of the cases, the relative medial mass was almost twice that of the controls. One of the principal advantages of this method of measuring medial mass was that such measurements were not affected by stretching of the vessels.[27]

A similar method was employed in evaluating the degree of arterial dilatation. The same base line was used for comparison—namely, the combined area of intima and internal elastic membrane. The area of the lumen was compared with this base line, since an increasing lumen size with dilatation would be associated with an increasing ratio. The mean

ratios of lumen to intima were increased in all but one of the cases of kyphoscoliosis, indicating that terminally, at least, arteries and arterioles were dilated (Text-fig. 3). On casual examination this dilatation obscured the medial hypertrophy because the eye usually evaluates such hypertrophy by comparing medial mass with lumen size (Fig. 2).

In about one half of the cases, the arterioles were normal. They did not have a muscular coat beyond the cuff which surrounded their point of exit from the small muscular arteries. In the other cases, such a coat did extend for varying distances down toward the capillary bed. Alveolar capillaries were markedly congested in all cases. Pulmonary veins and bronchial vessels were structurally normal. In the course of examining serial sections, no abnormal communications were found between the pulmonary and bronchial vascular systems. Likewise, no abnormal communications were found between pulmonary arteries and veins.

Similar studies were made in the lungs of 3 patients who had had pneumonectomy. A comparison was made in each case between the lung removed at operation and that obtained much later at necropsy. Both of the ratios described above were calculated for muscular arteries. In each instance the ratios in the postmortem lung were greater than those calculated for the previously resected lung (Table II). This indicated

TABLE II

VASCULAR ALTERATIONS FOLLOWING PNEUMONECTOMY

	Area media: Area intima + int. elast. mem.		Area lumen: Area intima + int. elast. mem.		Interval between pneumonectomy and death	Age at death
	Before pneumonectomy	After pneumonectomy	Before pneumonectomy	After pneumonectomy		
Case A	2.15	3.43	1.85	5.98	2 yr.	58 yr.
Case B	2.06	4.35	2.24	5.64	3½ yr.	65 yr.
Case C	1.61	4.21	1.53	3.06	5 yr.	48 yr.

The mean ratio $\frac{\text{area media}}{\text{area intima + I.E.M.}}$ for pulmonary arteries is compared in 3 lungs removed by pneumonectomy with the paired lung removed at necropsy. The greater necropsy ratios indicate muscular hypertrophy. An increase in the ratio $\frac{\text{area lumen}}{\text{area intima + I.E.M.}}$ indicates arterial dilatation.

that an appreciable increase in pulmonary arterial muscle mass and in arterial dilatation took place in the years after pneumonectomy. No other vascular abnormalities were found.

DISCUSSION

Both anatomic and clinical evidence indicates that the patients with kyphoscoliosis had pulmonary arterial hypertension. The only abnor-

mality within individual pulmonary vessels which might have been related to hypertension was smooth muscle hypertrophy in the media of arteries and arterioles. Lumen narrowing by intimal fibrosis, so often responsible for pulmonary hypertension in other disorders, was absent. The genesis of the muscular hypertrophy and its possible functional significance must be evaluated in the light of other abnormalities which affect the lesser circulation in kyphoscoliosis.

The reduced size of the lungs in kyphoscoliosis imposes a severe restriction on the pulmonary vascular bed.[1,9–12] This restriction appears to be responsible for at least latent pulmonary hypertension in many cases.[1] The vascular restriction might be compared to that which follows pneumonectomy. In both groups there are individuals without hypoxemia or significant intrinsic lung disease who have an abnormal pulmonary arterial pressor response when pulmonary blood flow is augmented by exercise.[1,25] In both groups the only abnormality in individual vessels is an appreciable hypertrophy of arterial muscle. In both instances the increased muscle mass might be interpreted as a work hypertrophy, a response to normal or increased blood flow through a reduced arterial bed.

Hypoxemia, often chronic, was present in all but one of the cases of kyphoscoliosis in the current study. This was probably most directly related to alveolar hypoventilation associated with an abnormal increase in the total work of breathing.[1,9,19,20] Bergofsky, Turino and Fishman[1] have noted that pulmonary hypertension is most severe in those cases of kyphoscoliosis in which hypoxemia is present. Chronic hypoxemia of this nature is capable of increasing cardiac output and of initiating a general hypervolemia in which the pulmonary circuit participates.[21,23] In the present study, secondary polycythemia and dilatation of pulmonary arteries were evidences of the latter. The high cardiac output and hypervolemia could further increase the circulatory load on the restricted pulmonary bed in kyphoscoliosis and contribute to a work hypertrophy in arterial smooth muscle. However, all of the effects of hypertension associated with hypoxemia cannot be attributed to changes in blood flow and volume.[1,21] It is thought that hypoxemia acts either locally or by reflex means to reduce the caliber or distensibility of the small pulmonary vessels.[21] A plausible target for such an action is the smooth muscle surrounding pulmonary arteries. A consequent increase in the state of contraction of this muscle might well serve as the stimulus for its hypertrophy. This has been postulated in other cases of chronic hypoxemia.[22,23] An alternative explanation would be that the hypertrophied muscle is a consequence of the hypertension rather than part of its cause. If this hypothesis were accepted, it would be necessary

to postulate a vasomotor response to hypoxemia in some more distal segment of the lesser circulation.

Despite small lungs from childhood in most patients with kyphoscoliosis, cor pulmonale is rare before the age of 25 years.[12] The relatively late development of obstructive emphysema and other intrinsic pulmonary diseases may explain this phenomenon in some cases. Chronic obstructive emphysema was prominent in 3 individuals in the present group (Table I). These could not be distinguished from the patients with kyphoscoliosis who had no parenchymal disorders on the basis of pulmonary vascular abnormalities; vascular alterations were identical in the two groups. This similarity can probably be attributed to the factors which might contribute to hypertension in obstructive emphysema, such as hypoxemia and vascular bed reduction. Similar factors were present in the kyphoscoliotic subjects not having emphysema. It seems reasonable to assume that when obstructive emphysema is severe in kyphoscoliosis, it may contribute to pulmonary hypertension. In our cases, other pulmonary parenchymal disorders were too limited in their extent to add significantly to the development of cor pulmonale.

In conclusion, multiple factors may reduce the over-all area and the distensibility of the pulmonary bed in kyphoscoliosis. By increasing pulmonary vascular resistance they could contribute to the development of arterial hypertension. The latent hypertension observed in many younger patients is apparently due to a vascular bed reduced by the limitation of pulmonary parenchyma inherent in the thoracic deformity. Hypertension, in turn, is probably responsible for pulmonary arterial smooth muscle hypertrophy. In later life, other factors contribute to progressive cor pulmonale. Structural changes in the bones and joints of the thoracic cage increase the work of respiration, leading to the development of alveolar hypoventilation and hypoxemia. The hypoxemia may induce a narrowing of some segment of the pulmonary vascular bed and is most likely responsible for hypertrophy of periarterial smooth muscle. Furthermore, the hypoxemia may limit pulmonary vascular distensibility indirectly by increasing the pulmonary blood volume. Finally, intrinsic pulmonary diseases, such as chronic obstructive emphysema, appear to contribute to pulmonary hypertension in a number of individuals.

Summary

Nine patients with dorsal kyphoscoliosis who had evidence of cor pulmonale at death were investigated. Pulmonary arterial and arteriolar changes were similar throughout the group. These consisted of marked hypertrophy of the media and vascular dilatation. Three factors were found which may have contributed to these vascular changes and to pulmonary hypertension:

1. All cases had small lungs and a consequent reduction in the pulmonary vascular bed. The pulmonary arterial muscular hypertrophy found in kyphoscoliosis is apparently similar to that which develops in the remaining lung after pneumonectomy.

2. In all cases there was evidence of chronic hypoxemia. The muscular hypertrophy and vascular dilatation noted were similar to the pulmonary vascular changes attributed to chronic hypoxemia in other disorders.

3. Severe intrinsic pulmonary disease was present in 3 of the 9 cases. It did not appear to have a specific effect on the pulmonary vascular bed in patients with this thoracic deformity.

References

1. Bergofsky, E. H.; Turino, G. M., and Fishman, A. P. Cardiorespiratory failure in kyphoscoliosis. *Medicine*, 1959, **38**, 263–317.
2. Fischer, J. W., and Dolehide, R. A. Fatal cardiac failure in persons with thoracic deformities. *A.M.A. Arch. Int. Med.*, 1954, **93**, 687–697.
3. Reid, W. D. Spinal deformity as a cause of cardiac hypertrophy. *J.A.M.A.*, 1930, **94**, 483.
4. Lewis, C. S., Jr.; Daines, M. C.; Samuels, A. J., and Hecht, H. H. Cor pulmonale (pulmono-cardiac syndrome); a case report. *Dis. Chest*, 1952, **22**, 261–268.
5. Finley, F. G. Spinal deformity as a cause of cardiac hypertrophy and dilatation. *Canad. M.A.J.*, 1921, **11**, 719.
6. Chapman, E. M.; Dill, D. B., and Graybiel, A. The decrease in functional capacity of the lungs and heart resulting from deformities of the chest: pulmonocardiac failure. *Medicine*, 1939, **18**, 167–202.
7. Hertzog, A. J., and Manz, W. R. Right-sided heart failure (cor pulmonale) caused by chest deformity; case report. *Am. Heart J.*, 1943, **25**, 399–403.
8. Kerwin, A. J. Pulmonocardiac failure as a result of spinal deformity; report of 5 cases. *Arch. Int. Med.*, 1942, **69**, 560–572.
9. Hanley, T.; Platts, M. M.; Clifton, M., and Morris, T. L. Heart failure of the hunchback. *Quart. J. Med.*, 1958, **27**, 155–171.
10. Bachmann, M. O. Die Veränderungen der inneren Organne bei hochgradigen Skoliosen und Kyphoskoliosen. E. Nägele, Stuttgart, 1899, 172 pp.
11. Gray, F. D., Jr. Kypnoscoliosis and heart disease. *J. Chronic Dis.*, 1956, **4**, 499–507.
12. Samuelsson, S. Cor pulmonale resulting from deformities of the chest. *Acta med. scandinav.*, 1952, **142**, 399–408.
13. Klawansky, G. Pronounced mechanical stenosis of aorta from kyphoscoliosis. *Klin. Wchnschr.*, 1925, **4**, 831–832.
14. Rieder, J. Die Respirations- und Circulationsstörungen bei Kyphoscoliosis dorsalis. M. Niethe, Berlin, 1881, 32 pp.
15. Traube, L. Ein Fall von Dilatation und Hypertrophie des rechten Ventrikels bei einem mit hochgradiger Scoliose und Verbildung des Brustkorbes behaften Individuum. *Ges. Beitr. z. Path. u. Physiol.*, 1878, **3**, 354–358.
16. Cabot, R. C. Case 19432. The interesting result of severe deformity of the thorax. *New England J. Med.*, 1933, **209**, 854–855.

17. COOMBS, C. F. Fatal cardiac failure occurring in persons with angular deformity of the spine. *Brit. J. Surg.*, 1930, **18**, 326–328.

18. DALEY, R. Morphine hypersensitivity in kyphoscoliosis. *Brit. Heart J.*, 1945, **7**, 101–103.

19. SCHAUB, F.; BÜHLMANN, A., and KALIN, R. Das "Kyphoskolioseherz" und seine Pathogenese. *Cardiologia*, 1954, **25**, 147–152.

20. FISHMAN, A. P.; TURINO, G. M., and BERGOFSKY, E. H. The syndrome of alveolar hypoventilation. *Am. J. Med.*, 1957, **23**, 333–339.

21. FISHMAN, A. P.; MCCLEMENT, J.; HIMMELSTEIN, A., and COURNAND, A. Effects of acute anoxia on the circulation and respiration in patients with chronic pulmonary disease studied during the "steady state." *J. Clin. Invest.*, 1952, **31**, 770–781.

22. NAEYE, R. L., and BICKERMAN, H. A. The effects of hypoxemia on the pulmonary arterial bed of humans and rats. (Abstract) *Fed. Proc.*, 1959, **18**, 497.

23. NAEYE, R. L. Anoxia and pulmonary hypertension, a study of the pulmonary vasculature. *Arch. Path.* (In press)

24. NAEYE, R. L. Kyphoscoliosis and chronic cor pulmonale; a study of the pulmonary vascular bed. (Abstract) *Proc. New England Cardiovascular Soc.*, 1960, **18**, 19.

25. RILEY, R. L.; HIMMELSTEIN, A.; MOTLEY, H. L.; WEINER, H. M., and COURNAND, A. Studies of the pulmonary circulation at rest and during exercise in normal individuals and in patients with chronic pulmonary disease. *Am. J. Physiol.*, 1948, **152**, 372–382.

26. SCHLESINGER, M. J. New radiopaque mass for vascular injection. *Lab. Invest.*, 1957, **6**, 1–11.

27. NAEYE, R. L. Smooth muscle changes in arteries of the greater and lesser circulations during the perinatal period. *Arch. Path.*, 1961, **71**, 121–128.

I am indebted to Dr. Harry P. Smith, Presbyterian Hospital, and Dr. Marvin Kuschner, Bellevue Hospital, New York, for the necropsy material used in this investigation, and to Dr. Alfred P. Fishman for helpful criticism and for the cardiac catheterization data in two cases.

LEGENDS FOR FIGURES

FIG. 1. This posterior view of the lungs in case 5 shows the effect of the thoracic deformity on the lungs. The volume of the right lung is 95 per cent of that predicted and of the left lung 35 per cent of the predicted size. Note the absence of bullae. There is a small area of fibrosis at the apex of the right lung.

FIG. 2. Pulmonary muscular artery (A) is in a normal subject. Arteries (B) and (C) are from a patient with kyphoscoliosis and cor pulmonale. The media appears to be of about equal thickness in arteries (A) and (B). However, vessel (B) is more dilated than vessel (A) as can be determined by observing its internal elastic membrane which is less wrinkled. Artery (C) is still more dilated. The ratio $\frac{\text{area arterial media}}{\text{area intima + internal elastic membrane}}$ is much greater in arteries (B) and (C) than in artery (A). There is significant medial muscular hypertrophy in arteries (B) and (C). Verhoeff and van Gieson stains. × 150.

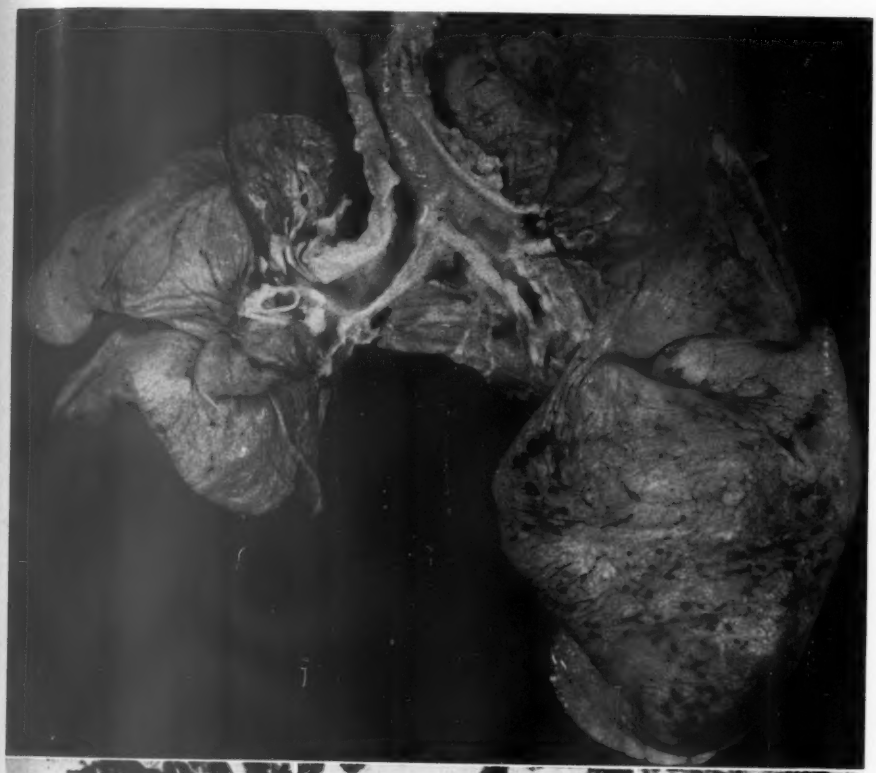

1

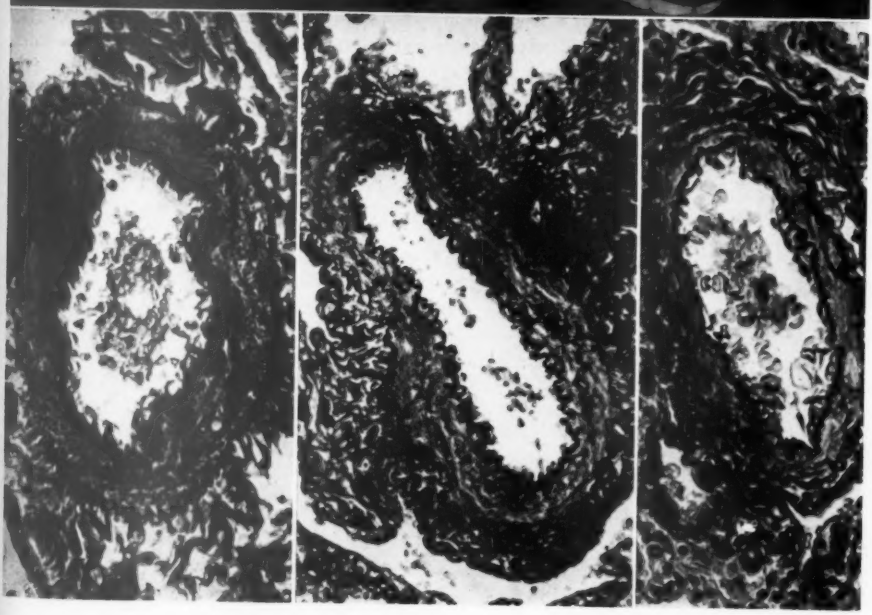

2B, 2C

CORTISONE AND ATYPICAL PULMONARY "EPITHELIAL" HYPERPLASIA

Effects of Pretreatment with Cortisone on Repair of Chemically Damaged Rabbit Lungs

Robert S. Totten, M.D., and Thomas J. Moran, M. D.

From the Department of Pathology, University of Pittsburgh School of Medicine and the Presbyterian, Womans, and Eye and Ear Hospitals, Pittsburgh, Pa.

In a study of the effects of cortisone on chemically produced bronchiolitis obliterans in rabbit lungs,[1] a striking proliferation of cells lining bronchioles and alveoli was noted. This lesion, while present in animals not receiving cortisone, was much more florid in the animals which received the drug. In that experiment, cortisone treatment was started the day before intratracheal injection of nitric acid. In another experiment[2] this change was even more pronounced in several animals which had been treated with cortisone for several weeks before the lungs were damaged by the intratracheal injection of nitric acid. Either because of a direct cortisone effect or some indirect effect such as delayed fibroblastic activity, the cellular proliferation was so atypical that the possibility of neoplasm was considered. Therefore, an experiment was designed to test the effects of pretreatment with cortisone at different time intervals on the reparative process in the chemically damaged lung. The purpose of this communication is to record the pathogenesis of the lesion produced and to discuss its possible relation to similar changes in human lungs and to experimental and human pulmonary neoplasm.

Methods

The chemical damage to the lung was produced by the intratracheal injection of 4 ml. of 1 per cent nitric acid into 24 healthy albino rabbits under light pentobarbital (Nembutal®) sodium anesthesia. They ranged in weight from 2 to 4 kg. These 24 rabbits were divided into 3 groups, all of which received daily intramuscular injections of 12.5 mg. of cortisone (Cortisone acetate; Merck, Sharpe & Dohme), 150,000 units of penicillin (penicillin G, Squibb), and 0.15 gm. of streptomycin (Distrycin,® Squibb). Group 1 (6 animals) received these drugs for 7 days before the intratracheal injection, and daily after the injections until the animals died or were sacrificed. Group 2 (6 animals) received the drugs for 14 days prior to the intratracheal injection of nitric acid and each day thereafter until the animals died or were sacrificed.

Supported by Grant H-2960 from the National Heart Institute, National Institutes of Health, United States Public Health Service.

Presented in part at the American Association for Cancer Research, Chicago, April, 1960.

Accepted for publication, December 20, 1960.

To group 3 (12 animals) were given the drugs for 30 days prior to intratracheal injection and daily thereafter until death or sacrifice of the animal.

Rabbits dying spontaneously were necropsied as soon as possible. The surviving animals were sacrificed by injection of air into marginal veins at periods ranging from 7 days to 149 days after the intratracheal injection. Blocks were taken from all lung areas showing gross abnormalities or from each lobe if no abnormalities were observed. The tissue was fixed in 4 per cent formaldehyde; hematoxylin and eosin stained sections were prepared from paraffin-embedded material. Selected sections were stained by the periodic acid-Schiff (PAS) method for mucin, by the Verhoeff stain for elastic tissue, and by Wilder's method for reticulin. Frozen sections stained with Sudan IV were also made in selected cases. The alterations were compared with those observed in animals from previous experiments,[8-7] including (a) 37 rabbits given intratracheal injections of nitric acid but no other treatment, (b) 38 rabbits which received intratracheal injections of nitric acid and intramuscular penicillin and streptomycin but no cortisone, (c) 35 animals which received intratracheal injections of nitric acid and intramuscular cortisone, penicillin and streptomycin beginning 24 hours before the intratracheal injection, (d) 9 rabbits given an intratracheal injection of 5 ml. of sterile distilled water, (e) 6 rabbits given intratracheal injections of 5 ml. of sterile 0.9 per cent solution of sodium chloride, (f) approximately 330 rabbits and guinea pigs given intratracheal injections of various other substances, and numerous apparently normal rabbits which were sacrificed by intravenous injections of air.

Results

General

The results indicate that mortality rates within 24 hours after intratracheal injection varied directly with the duration of cortisone pretreatment (Table I). The severity of lung damage and the degree of atypical alveolar proliferation in animals surviving longer than 24 hours are shown in Table II. Comparisons of lung changes in animals pre-

Table I

EARLY MORTALITY IN RELATION TO CORTISONE TREATMENT (DEATHS, 24 HOURS OR LESS)

Group	Pretreatment interval	Mortality
I	7 days	1/6
II	14 days	2/6
III	30 days	6/12

treated for different intervals and sacrificed at the same time after intratracheal injection were not possible at all time intervals because of the small number of surviving animals. However, atypical alveolar proliferation was at least as striking in the rabbits pretreated for 7 days as in those pretreated for longer intervals. For purposes of detailed gross and microscopic description, the 3 groups will be considered together.

Gross Observations

In the animals which died within 24 hours or less, the trachea and bronchi were filled with frothy pink to red fluid. Varying sized hemor-

rhages were scattered through the lung parenchyma. In some of the animals dying between 12 and 24 hours small foci of hemorrhagic necrosis were evident. In the animal which died 2 days after injection, small (0.1 to 0.4 cm.), slightly firm, yellowish tan lesions were evident on the cut

TABLE II

ANIMALS SURVIVING 24 HOURS OR LONGER

Number of days after injection of acid	Cortisone pretreatment interval (days)	Sacrificed or died	Degree of lung damage *	Atypical alveolar proliferation †
2	7	D	4+	1+
4	7	D	4+	4+
7	7	S	4+	4+
14	7	S	4+	4+
14	14	S	1+	1+
14	30	S	2+	2+
28	14	S	3+	4+
35	30	D	0	2+
37	14	D	1+	0
62	30	D	1+	2+
101	30	S	1+	1+
101	30	S	0	1+
101	30	S	0	1+
149	7	D	4+	1+
149	14	S	0	0

* Gross and microscopic estimate of the amount of bronchitis, pneumonia or edema, graded on a 0 to 4+ basis.

† Microscopic estimate of the amount and degree of proliferation of cells within alveoli, graded on a 0 to 4+ basis.

surface. In the animal surviving 7 days these were larger and more confluent. Their pale yellow color contrasted sharply with the surrounding congested parenchyma (Fig. 1). Of the 3 animals sacrificed at 14 days, one showed changes similar to those dying at 2 and 7 days and one had no gross alteration of the lungs except for some congestion. In the third animal, scattered foci of consolidation were seen, but these were more hemorrhagic and had less contrast with the surrounding parenchyma. In the animal sacrificed at 28 days, discrete and confluent firm lesions were easily palpable in both lungs. These were pale yellowish white in contrast to the grayish pink surrounding parenchyma. These striking nodular areas were not seen grossly in any of the remaining 8 animals which died or were sacrificed at intervals from 35 to 149 days. One rabbit which died in 149 days had a large lung abscess and empyema.

Histologic Observations

The histologic alterations varied considerably, depending on the length of survival of the animal. Nitric acid produced profound damage

to bronchi and bronchioles as well as focal areas of necrosis of lung parenchyma. These changes were the same as those described in previous experiments.[1] For the purpose of this paper, emphasis will be given to the histologic changes occurring in the reparative process, especially to the hyperplastic cells which presented an appearance resembling neoplasm. Generally, these cells were of two types. The first were clearly regenerated epithelial cells in terminal bronchioles. These alterations in the epithelium of the terminal bronchioles were quite striking and extensive in damaged areas, but they were not essentially different from those noted in the cortisone-treated rabbits in the previous experiment. The second type was more difficult to identify, and we were unable to determine definitely whether these represented unusual extensions of regenerating bronchiolar epithelium or were derived from alveolar lining cells. For purposes of this description they will be designated as alveolar cells, regardless of their origin, to differentiate them from the clearly recognizable bronchiolar cells.

Bronchiolar epithelial regeneration was present within 12 hours after the injection of nitric acid, but the earliest proliferation of the cells resembling alveolar lining cells was found in animals which died in 48 hours. This consisted of small collections of cuboidal cells loosely arranged in glandular spaces. These were invariably adjacent to areas of severe lung damage. In the animal examined 4 days after injection, the lesions were more prominent. Gland formation had spread to involve larger areas, and the cuboidal lining cells were distinct (Fig. 2). The most striking features were observed in animals sacrificed 7 and 14 days after the injection of acid. The polygonal lining cells were large and had prominent nuclei with coarse chromatin and nucleoli. Mitotic figures were not infrequently observed (Figs. 3 and 4). The abundant cytoplasm was finely granular, and some cells contained a few large vacuoles. Lipid (Sudan IV) was seen in some cells, but no mucin was identified by PAS stain. Desquamation of these cells was evident, and solid aggregates were seen in one of the 14-day animals. The distribution of elastic tissue, as demonstrated by the Verhoeff stain, was quite variable within the lesions, but a distinct reticulin membrane (Wilder stain) was present about most of the glandular spaces except in the areas of frank necrosis.

By 28 days gland formation was less prominent, and solid groups of cells were more frequently seen. The septal walls were thickened. Although a few fibroblasts appeared in the 14-day animals, fibrous tissue was first observed at 28 days (Fig. 5). Nucleoli were present in the alveolar cells, but mitotic figures were rarely noted. The lungs of the animals dying at 35 and 62 days showed small residual foci in which

alveolar lining cells were still easily seen, and the lumens were filled with desquamated cells (Fig. 6). Four of the remaining 6 animals examined at intervals from 37 to 149 days showed small foci of partly collapsed alveoli lined by cuboidal cells (Fig. 7). Nucleoli were inconspicuous, and mitotic figures were not observed. The other 2 rabbits did not show atypical hyperplasia of cells lining bronchioles or alveoli.

Comment

This experiment provides a method of enhancing and prolonging epithelial regeneration and hyperplasia and possibly alveolar lining cell hyperplasia by combining the use of cortisone to delay scar formation and penicillin and streptomycin to reduce infection. Whether the unusual hyperplastic reaction resembling neoplasm is produced by these factors alone, or whether cortisone has some direct stimulating effect on the growth of these cells is not established. High dosages of cortisone are known to delay scar formation and wound healing in the skin of rabbits and other animals.[8] This is also true in the lung. The animals untreated with cortisone in the previous experiment [1] showed fibroblastic activity by 3 days after acid injection, and well-developed fibrous tissue in 14 days. In this cortisone-treated group, fibroblasts were seen at 14 days, and the first definite fibrous tissue was observed in 28 days. The effect of cortisone on epithelial regeneration or proliferation has not been as thoroughly investigated as its effect on fibrous tissue. There is evidence, however, that epidermal regeneration is not significantly altered by doses of cortisone which will delay fibroblastic proliferation.[9,10]

The exact origin of the atypical cells is also of interest. This point could not be clearly established with the techniques available in the present experiment. The existence of an intact reticulin sheath about most of the spaces is evidence that alveolar walls remain at least partially intact in these areas. The shape of the cells, the presence of phagocytic activity, the tendency to desquamate in clumps, and the lack of mucin or cilia support the thesis that they are alveolar lining cells. On the other hand, these cells may be derived from bronchiolar epithelium, their unusual structure and spread being caused by the cortisone.

In order to see whether the degree of atypical alveolar proliferation observed in this experiment was present in our human necropsy specimens, lung sections from 11 patients dying with progressive systemic sclerosis (scleroderma) and 12 patients with lupus erythematosus were re-examined. Lungs from patients with these diseases were chosen since the patients in both groups often received large doses of steroids and frequently developed terminal aspiration pneumonia. In addition, interstitial fibrosis of the lungs is a frequent finding in scleroderma. In one

subject, a 63-year-old Negro woman with progressive systemic sclerosis, atypical proliferation similar to that seen in our animals was present. The patient had received large doses of prednisone for over a year prior to death and had an aspiration pneumonia as well as moderate pulmonary fibrosis. In several sections associated with the hemorrhagic aspiration pneumonia there was a striking proliferation of large polygonal cells lining alveoli; these were similar to those seen in the rabbit lungs (Figs. 8 and 9). No evidence of invasion or metastasis was noted. This observation is of interest in view of recent reports [11–15] of 8 patients with scleroderma who developed bronchiolar carcinoma. In 6 of these there were metastases. All of the cases occurred since the advent of steroid treatment, but in only one [14] was cortisone specifically mentioned. In all necropsied cases of scleroderma at this institution in the last 5 years, we have not observed any coexisting lung cancer, and the association of these two diseases has not been observed by others reviewing large series of scleroderma [16–18] or bronchiolar carcinoma. [19,20] In view of our experimental findings, it is interesting to speculate on a possible role of cortisone therapy in the development of bronchiolar carcinoma in patients with scleroderma or other diffuse fibrotic pulmonary lesions.

The effects of cortisone on experimentally produced neoplasms have been studied, but results are conflicting.[9,21,22] Gillman, Hathorn and Penn [9] have postulated that some of these conflicting results may depend upon variations in the time at which cortisone was administered or the total duration of the experiment. In their study of pulmonary tumors in mice receiving methylcholanthrene, cortisone delayed but did not reduce the incidence of neoplasms observed.

In view of the extremely atypical histologic appearance of these cells 7 to 14 days after intratracheal injection of nitric acid in cortisone-pretreated animals, the possibility of neoplasm seemed likely. However, only small, insignificant hyperplastic foci were seen in animals 35 to 149 days following injection. This may indicate either that the initial damage to these surviving animals was less than the damage to the animals sacrificed at 1 or 2 weeks or that the process does indeed regress. We believe that it is unlikely that all 8 animals examined in 35 to 149 days had escaped severe damage at the initial injection, but further long-term studies are required to establish this point. The growth potential of the hyperplastic pulmonary nodules and also undamaged lung from cortisone-treated rabbits are being tested experimentally by tissue culture and animal transplantation techniques.

Summary

Pretreatment with cortisone, penicillin and streptomycin for periods of 7, 14 and 30 days resulted in marked proliferation of cells lining

bronchioles and alveoli in rabbit lungs following the intratracheal injection of 1 per cent nitric acid. The alveolar cells, thought to be either alveolar lining cells or derived from bronchiolar epithelium, were evident within 2 days after the acid injection. The most striking changes were seen 7 to 14 days after intratracheal injection. At this time the large anaplastic cells forming glandlike spaces and solid nests appeared to be histologically neoplastic. However, the degree of proliferation apparently subsided by 35 days, and no evidence of progressive growth was seen in animals observed up to 149 days after injection.

It is not yet clear whether these changes are produced by the direct action of cortisone on the proliferating cells or whether the proliferation occurs in a favorable environment in which the cortisone reduces fibroblastic activity and the antibiotic agents reduce the inflammatory reaction.

The possible relationships of this experimental model to similar lesions observed in human lungs and to experimental and human lung cancer are discussed.

References

1. Moran, T. J., and Hellstrom, H. R. Bronchiolitis obliterans: an experimental study of the pathogenesis and the use of cortisone in modification of the lesions. *A.M.A. Arch. Path.*, 1958, **66**, 691–707.
2. Moran, T. J. Unpublished observations.
3. Moran, T. J. Experimental food-aspiration pneumonia. *A.M.A. Arch. Path.*, 1951, **52**, 350–354.
4. Moran, T. J. Milk-aspiration pneumonia in human and animal subjects. *A.M.A. Arch. Path.*, 1953, **55**, 286–301.
5. Moran, T. J. Experimental aspiration pneumonia. IV. Inflammatory and reparative changes produced by intratracheal injections of autologous gastric juice and hydrochloric acid. *A.M.A. Arch. Path.*, 1955, **60**, 122–129.
6. Moran, T. J., and Hellstrom, H. R. Experimental aspiration pneumonia. V. Acute pulmonary edema, pneumonia and bronchiolitis obliterans produced by injection of ethyl alcohol. *Am. J. Clin. Path.*, 1957, **27**, 300–308.
7. Smith, R. H., and Moran, T. J. Experimental aspiration pneumonia. III. Pneumonia produced by intratracheal injection of carbohydrate solutions. *A.M.A. Arch. Path.*, 1954, **57**, 194–200.
8. Ragan, C.; Lattes, R.; Blunt, J. W., Jr.; Vaillancourt, de G.; Jessar, R. A., and Epstein, W. The Effect of Cortisone upon Repair Processes in Dense and Loose Connective Tissue. In: The Effect of ACTH and Cortisone upon Infection and Resistance. Shwartzman, G. (ed.). Columbia University Press, New York, 1953, pp. 46–55.
9. Gillman, T.; Hathorn, M., and Penn, J. Actions of cortisone on cutaneous and pulmonary neoplasms induced in mice by cutaneous application of methylcholanthrene. *Brit. J. Cancer*, 1956, **10**, 394–400.
10. Ritchie, A. C.; Shubik, P.; Lane, M., and Leroy, E. P. The effect of cortisone on the hyperplasia produced in mouse skin by croton oil. *Cancer Res.*, 1953, **13**, 45–48.

11. BATSAKIS, J. G., and JOHNSON, H. A. Generalized scleroderma involving lungs and liver with pulmonary adenocarcinoma. *A.M.A. Arch. Path.*, 1960, **69**, 633–638.

12. CAPLAN, H. Honeycomb lungs and malignant pulmonary adenomatosis in scleroderma. *Thorax*, 1959, **14**, 89–96.

13. COLLINS, D. H.; DARKE, C. S., and DODGE, O. G. Scleroderma with honeycomb lungs and bronchiolar carcinoma. *J. Path. & Bact.*, 1958, **76**, 531–540.

14. JONSSON, S. M., and HOUSER, J. M. Scleroderma (progressive systemic sclerosis) associated with cancer of the lung; brief review and report of a case. *New England J. Med.*, 1956, **255**, 413–416.

15. ZATUCHNI, J.; CAMPBELL, W. N., and ZARAFONETIS, C. J. D. Pulmonary fibrosis and terminal bronchiolar ("alveolar cell") carcinoma in scleroderma. *Cancer*, 1953, **6**, 1147–1158.

16. LEINWAND, I.; DURYEE, A. W., and RICHTER, M. N. Scleroderma (based on a study of over 150 cases). *Ann. Int. Med.*, 1954, **41**, 1003–1041.

17. ORABONA, M. L., and ALBANO, O. Progressive systemic sclerosis (or visceral scleroderma); review of literature and report of cases. *Acta med. scandinav.*, 1957, Suppl. 333, pp. 54–79.

18. TALBOTT, J. H., and FERRANDIS, R. M. Collagen Diseases, Including Systemic Lupus Erythematosus, Polyarteritis, Dermatomyositis, Systemic Scleroderma, Thrombotic Thrombocytopenic Purpura. Grune & Stratton, New York, 1956, pp. 137–180.

19. ROELSEN, E.; LUND, T.; SØNDERGAARD, T.; MØLLER, B., and MYSCHETZKY, A. Primary alveolar carcinomatosis (carcinoma) of the lung (so-called pulmonary adenomatosis or alveolar-cell tumour); a review and report of 12 cases. *Acta med. scandinav.*, 1959, **163**, 367–384.

20. STOREY, C. F.; KNUDTSON, K. P., and LAWRENCE, B. J. Bronchiolar ("alveolar cell") carcinoma of the lung. *J. Thoracic Surg.*, 1953, **26**, 331–406.

21. SHERWIN-WEIDENREICH, R.; HERMANN, R., and ROTHSTEIN, M. J. The effect of cortisone and hair cycle on the incidence of chemically induced epidermal tumors in mice. *Cancer Res.*, 1959, **19**, 1150–1153.

22. ZACHARIAE, L., and ASBOE-HANSEN, G. Reversibility of hydrocortisone-effected regression of induced skin carcinomas in mice. *Cancer Res.*, 1958, **18**, 822–824.

Mr. Raymond Pradines, a University of Pittsburgh premedical student, provided technical assistance, and Mr. Albert Levin, University of Pittsburgh Medical Photographer, did the photography.

[*Illustrations follow*]

Legends for Figures

Photomicrographs were prepared from sections stained with hematoxylin and eosin.

Fig. 1. Cortisone pretreatment for 7 days; 7 days after intratracheal injection of nitric acid. Cut surface of formalin-fixed specimen. Discrete and confluent, pale, solid areas contrast with the adjacent congested lung.

Fig. 2. Cortisone pretreatment for 7 days; 4 days after intratracheal nitric acid. Clusters of distinct glandlike spaces are lined by cuboidal cells. A bronchiole (top, center), filled with exudate, has almost complete desquamation of lining cells. × 140.

Fig. 3. Cortisone pretreatment for 7 days; 7 days after intratracheal nitric acid. Glandlike spaces are lined by large polygonal cells with hyperchromatic nuclei. × 380.

Fig. 4. Same animal as Figure 3. Large nuclei have coarse nuclear chromatin and some have prominent nucleoli. Cytoplasm is finely granular or vacuolated. Note a mitotic figure near the center. × 600.

Fig. 5. Cortisone pretreatment for 14 days; 28 days after intratracheal nitric acid. There is separation of glandlike spaces by inflammatory exudate and cellular fibrous tissue. × 200.

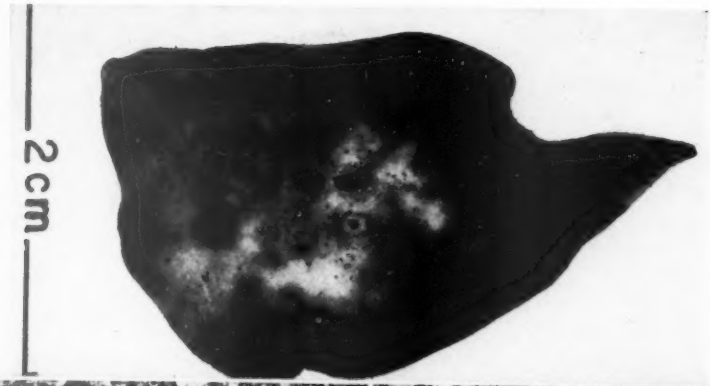

1

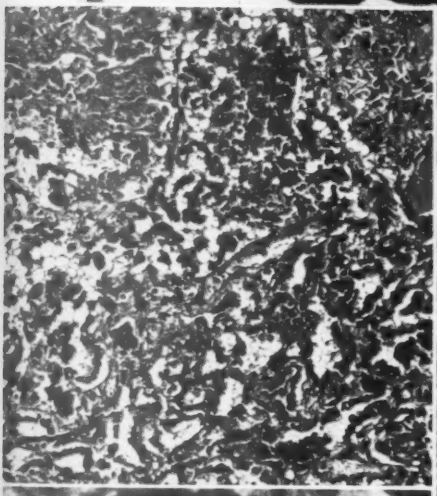

2

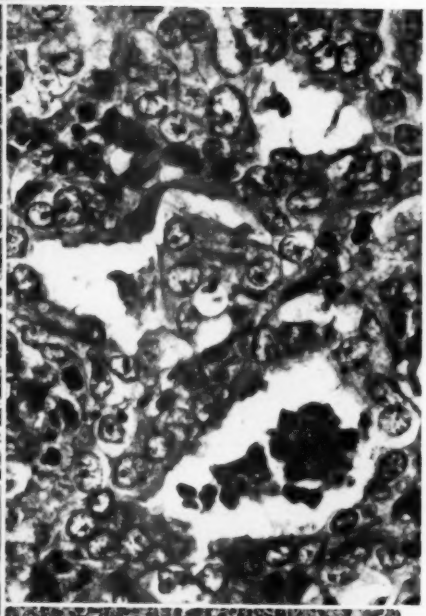

3

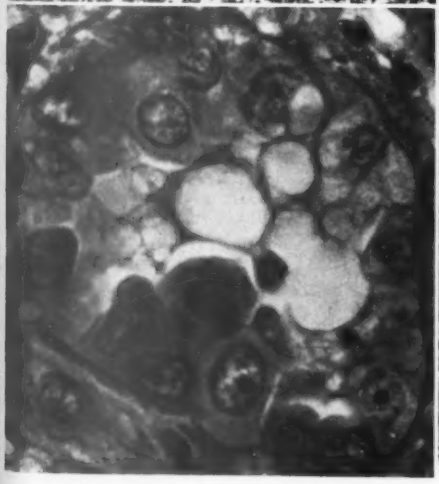

4

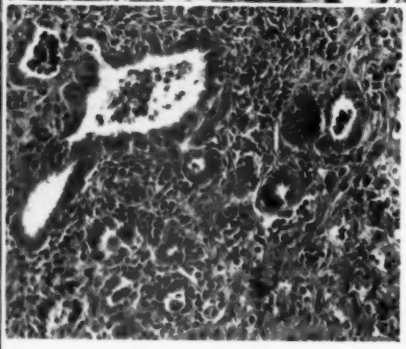

5

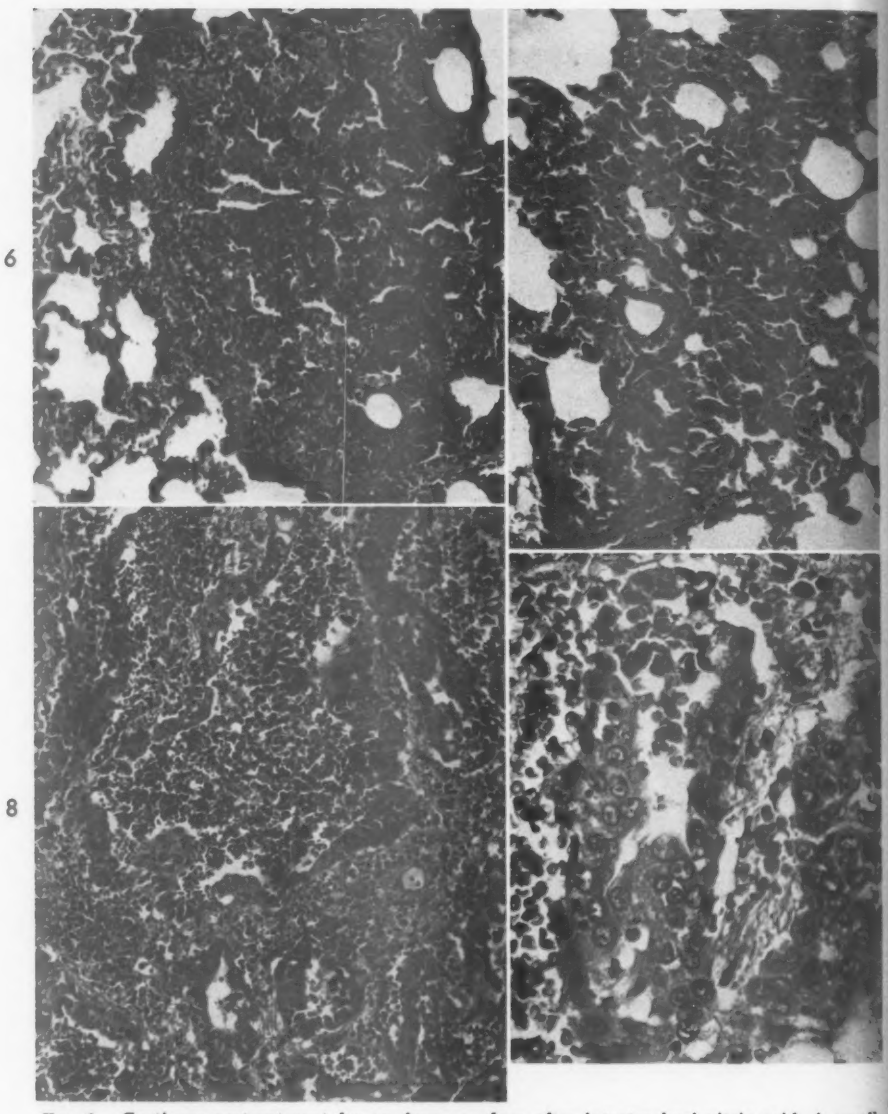

FIG. 6. Cortisone pretreatment for 30 days; 35 days after intratracheal nitric acid. A small focus of atypical proliferation exhibits groups of desquamated cells in alveoli. × 140.

FIG. 7. Cortisone pretreatment for 30 days; 101 days after intratracheal nitric acid. A focus of partly collapsed alveoli contains small cuboidal lining cells. × 140.

FIG. 8. Lung from a patient with progressive systemic sclerosis on prednisone therapy; died with aspiration pneumonia. There is striking proliferation of large cells lining bronchioles and alveoli. × 140.

FIG. 9. Same case as Figure 8. Higher power to show cell details. × 380.

THE CYTOCHEMISTRY OF ANOXIC AND ANOXIC-ISCHEMIC ENCEPHALOPATHY IN RATS

II. Alterations in Neuronal Mitochondria Identified by Diphosphopyridine and Triphosphopyridine Nucleotide Diaphorases

Norwin H. Becker, Lt. (MC), USNR

From the Medical Research Laboratory, United States Naval Submarine Base, New London, Conn.

The first part of this investigation concerned the alterations in neuronal lysosomes identified by acid phosphatase activity.[1] Significant changes in the lysosomes were noted early in the course of necrobiosis before any abnormalities could be detected in conventional hematoxylin and eosin and Nissl stains. In view of these promising observations, it was considered desirable to extend these studies to include other enzyme systems.

The development of refined histochemical techniques employing tetrazolium salts[2] has permitted the investigation of several dehydrogenases and diaphorases in the central nervous system. Observations on unfixed frozen sections[3,4] and unfixed frozen-dried[5] as well as fresh tissue[6] have been reported. Recently, the localization, both cytologic and histologic, in the normal rat brain and spinal cord, of several enzyme systems that survive cold formol-calcium fixation has been described.[7,8] The advantage of this fixative is that it preserves morphologic detail while permitting visualization of such enzyme activities as diphosphopyridine and triphosphopyridine nucleotide (DPN and TPN) diaphorases in mitochondria and basophilic substance, adenosine triphosphatase in cell membranes and acid phosphatase in lysosomes.

The purpose of this investigation is to describe alterations in neuronal sites of DPN and TPN diaphorase activity in the rat brain during postmortem autolysis and in anoxic and anoxic-ischemic encephalopathy.

Methods

Both male and female Sprague-Dawley rats (150 to 250 gm.) were used in all the experiments. They were killed by crushing the cervico-thoracic spinal cord; the cranial vault was rapidly reflected and the brain removed intact.

Postmortem Autolysis

The brains were first separated into halves by longitudinal section. One half, cut into coronal sections, was placed directly in the fixative. Before fixation the remaining half was placed in a sterile Petri dish and incubated at 37° C. for periods ranging from 5 minutes to 24 hours.

Accepted for publication, December 19, 1960.

Anoxic-Ischemic Encephalopathy

Animals were subjected to the procedure of Levine,[8] nitrogen serving as the anoxic agent. Anoxic exposure was initiated 40 to 60 minutes after ligation of the left common carotid artery under ether anesthesia. The animals were maintained in a relatively stable unconscious state for periods of 30 to 60 minutes. During this period, depressed respiratory rates of 25 to 50 per minute were observed. Following the anoxic episode, animals were allowed to survive for periods ranging from immediate sacrifice to 3 days. The brain was then divided into coronal sections, 2 or 3 mm. thick, and placed in fixative.

Anoxic Encephalopathy

Three different schedules of anoxic exposure were used. One group was exposed to a continuously flowing atmosphere of 100 per cent nitrogen for 60 to 90 seconds. Exposure was ended when apnea supervened. These animals were killed at 30 minutes, 6 and 24 hours after exposure.

In the second group, 3 such acute exposures were given 1 hour apart. The animals were killed 6 and 24 hours after the last exposure.

The third group was placed in a continuously flowing atmosphere consisting of 8 per cent oxygen and 92 per cent nitrogen containing traces of carbon dioxide. Increased bursts of nitrogen were given at hourly intervals so that oxygen levels were lowered sufficiently to produce severe agitation and respiratory distress. The rats were exposed to this environment in 4 daily periods of 4 hours each.

Control Groups

Normal rat brains were processed as controls during these experiments. In another control group, rats given 5 minutes of deep ether anesthesia or those with common carotid artery ligation without further anoxia were killed 6 and 24 hours after the respective procedures.

Histologic Technique

The blocks were allowed to fix for 18 to 24 hours in cold formol-calcium (2° to 4° C.). Frozen sections, 10 to 20 μ thick, were prepared with the use of a Sartorius sliding freezing microtome. The sections were rinsed in distilled water and stained for DPN and TPN diaphorase activity.[7] Sections were incubated for 40 minutes (DPNH) or 60 minutes (TPNH) at 37° C. in the following freshly prepared mixture:

Reduced diphosphopyridine nucleotide (DPNH) or reduced triphosphopyridine nucleotide (TPNH) (Sigma Chemical Corporation), 4 mg.; 1.2 ml. of H_2O; 0.8 ml. of 0.1 M phosphate buffer, pH 7.4; 1 ml. of Nitro BT [2,2′-di-p-nitrophenyl-5,5′-diphenyl-3,3′-(3,3′-dimethoxy-4,4′-biphenylene)-ditetrazolium chloride (Dajac Division, Borden Chemical Company)], 1 mg. per ml. The sections were then rinsed in distilled water and mounted in glycerogel. In the case of some of the injured tissue, sections were allowed to incubate for only 10 to 15 minutes. In addition to these short incubation trials, some sections were carried through 2 changes of ice-cold acetone (60 seconds each) prior to being placed in the incubation media. In all cases, substrate control sections were incubated in the absence of DPNH or TPNH.

Unfrozen blocks of tissue adjacent to those taken for frozen sections were embedded in paraffin. Sections 6 to 8 μ thick were stained with hematoxylin and eosin or thionine ("paraffin-Nissl").

Results

Normal and Control Animals

In addition to 16 normal brain halves procured in the autolysis ex-

periments, the brains of 10 normal animals were available for examination.

As previously noted,[7] there was prominent cytochemical staining of the larger neurons in the cerebral cortex, the Purkinje and granule cells of the cerebellar cortex and the neurons of the cranial and cerebellar nerve nuclei. Moderate staining was present in the remaining neurons. Within the neurons, diformazan deposits were more extensive with DPNH than with TPNH as substrate. While the localization of the TPNH diaphorase appeared to be chiefly mitochondrial, DPNH activity was present in both mitochondria and Nissl substances (Fig. 1). Some freezing and osmotic damage inherent in the techniques used undoubtedly occurred. This resulted in some variation in the distribution and size of the sites of enzyme activity.

Nevertheless, a normal base line could be established, against which pathologic alterations could be compared. All substrate control sections were negative. There were no histologic or histochemical abnormalities present in the brains of 5 animals given ether anesthesia only or in those (6 animals) obtained after unilateral common carotid artery ligation without further anoxic treatment.

Autolysis

In the sections stained for Nissl substance and with hematoxylin and eosin, no abnormalities were noted earlier than 45 minutes (6 animals). From 45 minutes to 24 hours (10 animals) increasingly severe alterations were present; these were similar to those previously noted.[1]

In sections stained for DPNH diaphorase activity, no abnormalities were observed earlier than 30 minutes. At this time neurons with swollen sites of enzyme activity (swollen mitochondria) could be seen in many zones, particularly in the cerebral cortex (Fig. 2), cerebellum and corpus striatum. A loosening and an increased pallor of the basophilic substance and an occasional loss of all neuronal activity could also be seen in these cells. Many of the abnormal mitochondria were perinuclear in location. By 8 hours most neurons were similarly altered in all parts of the brain. In addition, there was a marked reduction in the staining of the neuropil so that the blood vessels and dendritic processes which remained stained appeared more prominent (Fig. 3). At 12 hours there was considerable over-all loss of neuronal enzyme activity, and by 24 hours most of the activity had disappeared. However, even at these long periods of autolysis, a few neurons containing dense globular cytoplasmic diformazan deposits could always be detected.

Substitution of TPNH for DPNH as substrate revealed essentially similar mitochondrial swelling. The earliest changes, however, could be

seen at 20 minutes, and most of the enzyme activity was lost by 12 hours. With both substrates, the altered sites of activity could be visualized at shorter incubation times and following pre-incubation washing in acetone. In normal tissue the staining was contributed predominantly by the blue diformazan. However, after 2 hours of autolysis, a considerable amount was contributed by a red formazan. This was particularly true when TPNH was used as the substrate.

Anoxic-Ischemic Encephalopathy

Of the 61 rats subjected to the anoxic-ischemic procedure, 19 died during or after the period of anoxia. A right hemiparesis was evident in 22 of the 42 animals surviving. The distribution of the neuronal lesions was similar in extent and localization to those described by Levine[9] (Fig. 4).

Histologic lesions were noted in 11 of 17 animals allowed to survive past 24 hours and in 3 of 13 animals in the 12 to 18 hour survival group. No histologic lesions were present in 5 animals killed immediately after the anoxic period or in 7 animals killed 4 to 6 hours later.

Cytochemical studies of DPNH diaphorase activity revealed no abnormalities earlier than 12 hours. After 12 hours, in 1 of 2 animals revealing injury in sections stained for Nissl substance, scattered groups of neurons in the pyriform cortex appeared abnormal. This abnormality was again characterized by swelling of the mitochondria with increased diformazan deposition (Fig. 5). The intervening basophilic substance and neuropil became relatively unstained. Similarly abnormal neurons were noted in the cerebral cortex, corpus striatum, hippocampus and thalamus in 2 of 8 animals surviving 18 hours.

The cytochemical alterations were most marked in the 24 to 72 hour survival group. They were present in 14 of 17 rats, and were most frequent in the cerebral cortex (Fig. 6), corpus striatum and thalamus. Even at 72 hours, many neurons with swollen mitochondria were manifest. In addition, many neurons lost a good deal of their enzyme activity, and only a few swollen mitochondria remained. The surrounding neuropil showed a reduced over-all staining (Fig. 7) although many abnormally large discrete deposits of diformazan could be seen. These deposits were morphologically similar to those observed in the perikaryon. Many were as large as 3 to 5 μ in diameter. Occurring with greatest frequency on the side of the carotid ligation, occasional foci of injured neurons were present in the contralateral cerebral cortex.

The substitution of TPNH for DPNH as substrate revealed essentially similar findings although the over-all staining and morphologic detail was usually less satisfactory. However, swollen mitochondria as well as an ultimate loss of enzyme activity could be discerned. As in the

case of autolysis, much of the staining in the advanced lesions appeared to be contributed by the red formazan. The cytochemical abnormalities could be visualized at shorter incubation times and after pre-incubation washing in acetone.

Anoxic Encephalopathy

In the first groups, 9 of 14 animals survived acute exposure to 100 per cent nitrogen. Early acute cell alterations were noted only in Nissl stained sections in a few Purkinje cells of 1 in 4 animals of the 24 hour survival group. No cytochemical abnormalities were identified in these animals.

In the second group 9 of 16 animals survived repeated exposure to nitrogen. The conventionally stained paraffin sections and the cytochemical stains revealed no abnormalities.

In the third group, 7 of 11 animals survived a schedule of prolonged critical hypoxia. In 2 of 7 survivors, acute cell changes were noted in Nissl stained sections in the corpus striatum, cerebral cortex and Purkinje cells. In 4 animals, cytochemical abnormalities were noted with both DPNH and TPNH as substrates. These were characterized by swollen mitochondria which could be identified in neurons of the cerebral cortex and Purkinje cells. These abnormalities persisted in tissue incubated for short periods and in those washed in acetone prior to incubation (Fig. 8).

Discussion

The demonstration of pathologically altered mitochondria by means of the diaphorase reactions has been reviewed by Pearse.[2] An increased staining intensity of these abnormal organelles is apparently related to increased accessibility of substrate and dye following injury.

In the present investigation detectable changes in neuronal mitochondria were observed in both autolysis and necrobiosis. In both events the alterations were similar and consisted of abnormal swelling and ultimately by loss of the mitochondria with disappearance of all sites of diaphorase activity. There was usually an associated reduction of staining intensity of the basophilic substance. A loss of diaphorase activity in the neuropil suggested that the neuroglia was quite sensitive to autolytic and anoxic-ischemic damage. In the anoxic-ischemic lesions, the Purkinje cells at no time revealed any abnormalities of diaphorase activity or in conventionally stained paraffin sections. Early alterations in lysosomes, however, were observed.[1] This suggested that the early lysosomal changes might have been reversible while the mitochondrial abnormalities were associated with irreversible neuronal damage. In the

anoxic lesions, the low incidence of neuronal damage made it difficult to evaluate the sequence of enzyme changes although cytochemically altered neurons could be seen. In comparably injured anoxic tissue, alterations in lysosomes were more frequent than those in mitochondria.

Diformazan is said to be insoluble in lipid.[2] On the other hand, the possibility of artifactual deposition of this pigment in lipoidal products of neuronal degeneration must be considered.[10] However, the persistence of these cytochemical abnormalities after short incubation times and following pre-incubation washing in acetone suggests that this is not the case.

Although the mitochondrial alterations occurred relatively late in the course of both the anoxic and the anoxic-ischemic lesions, it should be emphasized that injured neurons were often seen where they were inapparent with conventional stains. Therefore, cytochemical studies of both mitochondria and lysosomes contribute promising techniques in the investigation of neuronal necrobiosis.

Summary

Alterations in neuronal mitochondria have been described in the course of postmortem autolysis and in both anoxic and anoxic-ischemic encephalopathy. The mitochondria were identified in formol-calcium fixed tissue by virtue of their diphosphopyridine and triphosphopyridine nucleotide diaphorase activity. Swelling of the mitochondria was noted during the early phases of both autolysis and necrobiosis. Loss of enzyme activity became prominent during the later phases. In some cases the earliest cytochemical lesions preceded those which could be detected by Nissl stains and by hematoxylin and eosin.

References

1. Becker, N. H., and Barron, K. D. The cytochemistry of anoxic and anoxic-ischemic encephalopathy. I. Alterations in neuronal lysosomes identified by acid phosphatase activity. *Am. J. Path.*, 1961, **38**, 161–176.
2. Pearse, A. G. E. Histochemistry, Theoretical and Applied. Little, Brown & Co., Boston, 1959, pp. 536–586.
3. Shimizu, N., and Morikawa, N. Histochemical studies of succinic dehydrogenase of the brain of mice, rats, guinea pigs and rabbits. *J. Histochem.*, 1957, **5**, 334–345.
4. Friede, R. L. Histochemical investigations on succinic dehydrogenase in the central nervous system. I. The postnatal development of rat brain. II. Atlas of the medulla oblongata of the guinea pig. *J. Neurochem.*, 1959, **4**, 101–123.
5. Wolfgram, F., and Rose, A. S. The histochemical demonstration of dehydrogenases in neuroglia. *Exper. Cell Res.*, 1959, **17**, 526–530.
6. Potanos, J.; Wolf, A., and Cowen, D. Cytochemical localization of oxidative enzymes in human nerve cells and neuroglia. *J. Neuropath. & Exper. Neurol.*, 1959, **18**, 627–635.

7. BECKER, N. H.; GOLDFISCHER, S.; SHIN, W., and NOVIKOFF, A. The localization of enzyme activities in rat brain. *J. Biophys. & Biochem. Cytol.* (In press)

8. SAMORAJSKI, T. The application of the diphosphopyridine nucleotide diaphorase methods in study of dorsal ganglia and spinal cord. *J. Neurochem.*, 1960, 5, 349–353.

9. LEVINE, S. Anoxic-ischemic encephalopathy in rats. *Am. J. Path.*, 1960, **36**, 1–17.

10. NOVIKOFF, A. B. Enzyme cytochemistry; pitfalls in the current use of tetrazolium techniques. (Abstract) *J. Histochem.*, 1959, 7, 301–302.

The technical assistance of Jonathan Sparks, HM1, USN, is acknowledged. The photographic prints were prepared by Mr. J. Walker.

[*Illustrations follow*]

Legends for Figures

In the preparation of specimens for these illustrations, incubation times were 40 minutes for DPNH and 60 minutes for TPNH.

Fig. 1. Normal neocortex. There is staining of the mitochondria (M) and diffuse staining of the basophilic substance of pyramidal cells. DPNH stain. × 800.

Fig. 2. Neocortex. Autolysis, 30 minutes. Considerable swelling and clumping of the mitochondria (M) are evident. Neurons (N) exhibit loss of enzyme activity. DPNH stain. × 700.

Fig. 3. Neocortex. Autolysis, 8 hours. Mitochondria are swollen and clumped in most of the neurons. The reduced staining of the neuropil contributes to the prominent appearance of dendritic processes (D) and blood vessels (BV). DPNH stain. × 300.

Fig. 4. Neocortex. Anoxic-ischemic lesion, 24 hours. There is shrinkage and loss of neurons with spongy degeneration of the neuropil. Thionine stain. × 100.

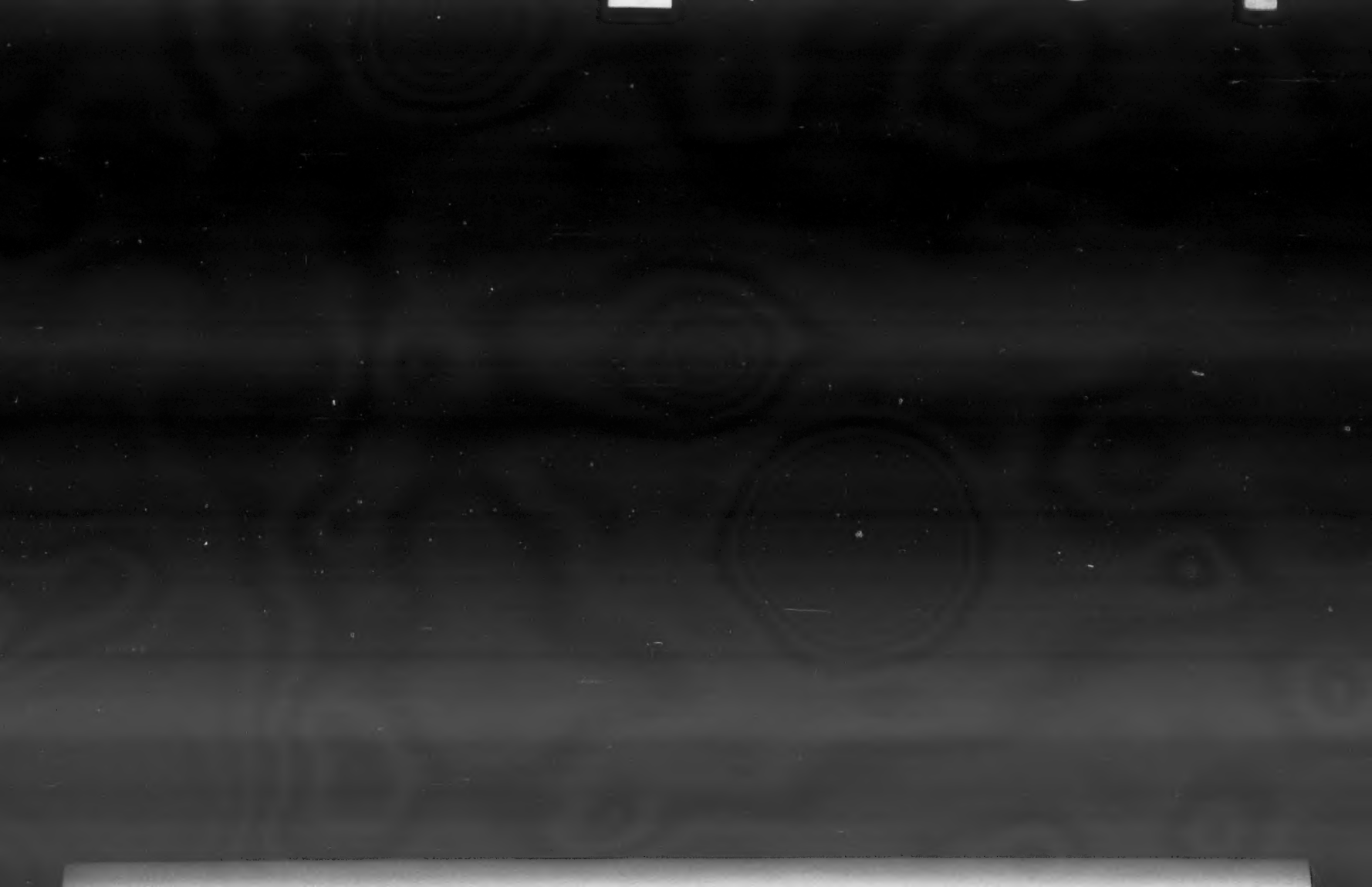

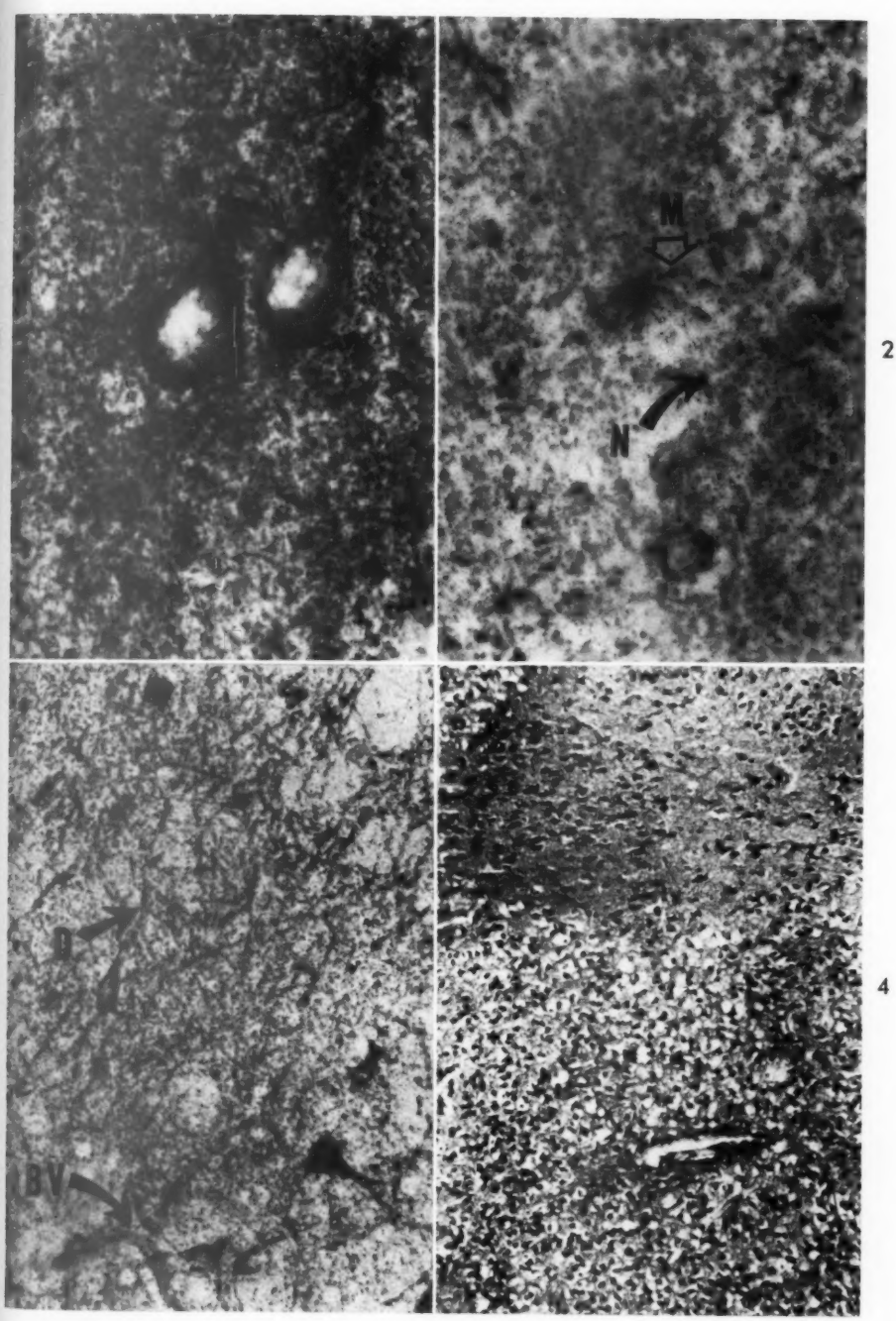
1
M
N
2
3
BV
4

FIG. 5. Pyriform cortex. Anoxic-ischemic lesion, 12 hours. Note neurons with swollen mitochondria (M). DPNH stain. × 600.

FIG. 6. Neocortex. Anoxic-ischemic lesion, 48 hours. Neuronal mitochondria are swollen. There is decreased staining of the basophilic substance and neuropil. DPNH stain. × 600.

FIG. 7. Neocortex. Anoxic-ischemic lesion, 24 hours. At low magnification the loss of staining in the neuropil is evident in this area of zonal necrosis. DPNH stain. × 100.

FIG. 8. Neocortex. Prolonged critical hypoxia, 4 days. Due to pre-incubation washing in acetone, there is some blurring of morphologic detail. Nevertheless, neurons with swollen mitochondria are easily identified. TPNH stain. × 700

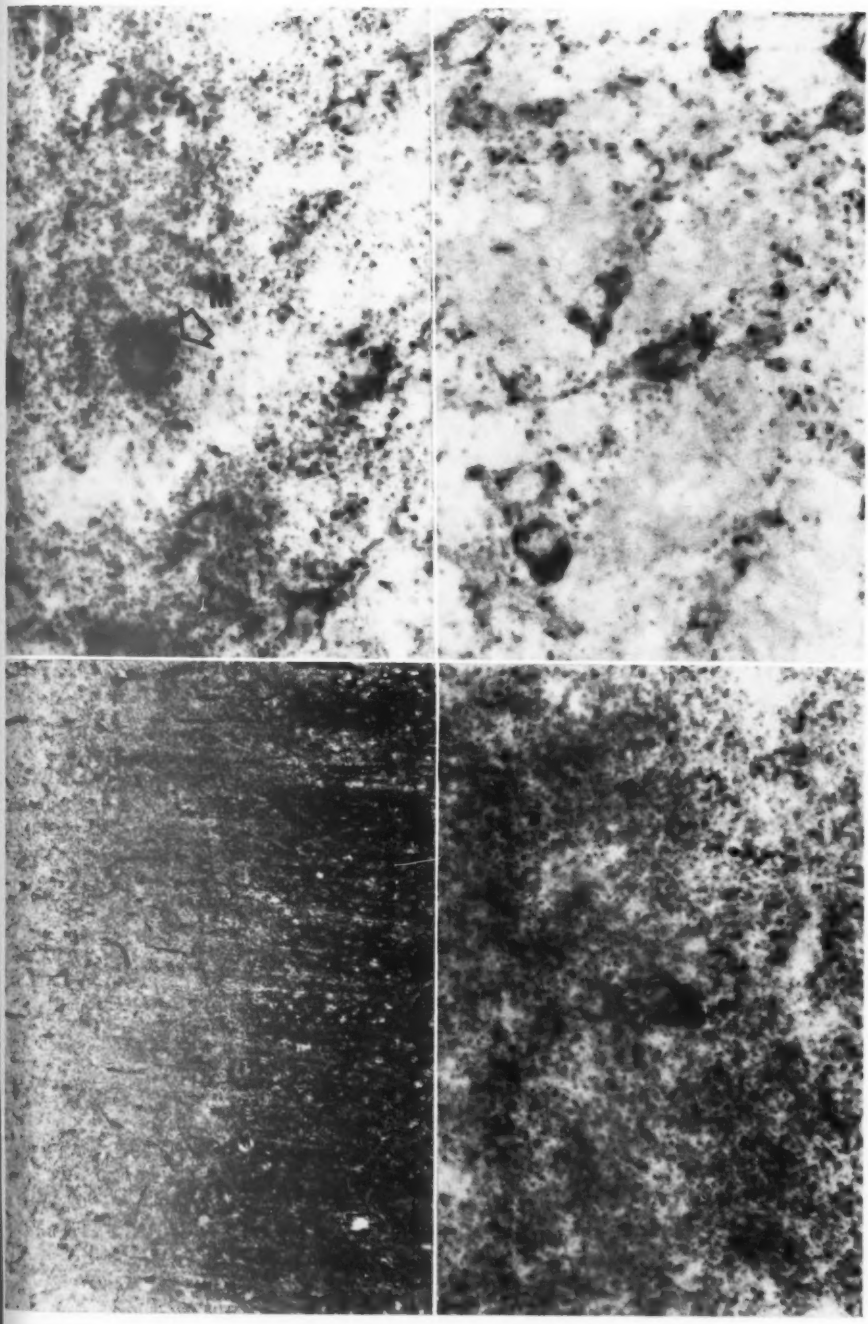

6

8

STRUCTURAL, CYTOLOGIC AND AUTORADIOGRAPHIC (H^3-THYMIDINE) CHANGES IN THE BONE MARROW FOLLOWING TOTAL BODY IRRADIATION

T. M. Fliedner, M.D.*; V. P. Bond, M. D., Ph.D., and E. P. Cronkite, M.D.

From the Medical Research Center, Brookhaven National Laboratory, Upton, L.I., N.Y.

Examination of bone marrow smears of man accidentally exposed to approximately 300 rads of mixed neutron-gamma radiation indicated significant cellular damage within hours of exposure.[1,2] Early changes in the bone marrow, before peripheral blood elements are depleted, are known from a number of studies. Structural and cellular damage, with hemorrhage into the marrow parenchyma, has been demonstrated histologically in the rat within a few hours of exposure to 800 r.[3] Despite the extensive studies of radiation damage to the marrow,[4] the pathogenesis of radiation-induced bone marrow failure is by no means completely understood. In many reports the approach to the study of radiation-induced marrow damage has been limited to descriptions of cytologic and biochemical alterations. Less attention has been focused on whether or not the unique and well defined architecture of the marrow, characterized as a highly proliferative and vascularized organ inside a rigid bony capsule, contributes by its response to radiation to its over-all radiosensitivity.

In the present investigation the bone marrow of rats was observed serially after various doses of radiation in an effort to correlate structural and cellular features during the "degenerative" and "regenerative" phases following exposure. In order to obtain additional information on the metabolic and potential proliferative capacity of individual cell types, tritiated thymidine as a specific label of deoxyribonucleic acid (DNA) synthesizing cells was injected one-half hour prior to sacrifice to allow autoradiographic studies. The effects of radiation on DNA synthesis as shown by biochemical techniques have been described,[5–8] as have been studies related to the use of tritiated thymidine as an indicator of DNA synthesis at the cellular level.[9–14] Some of the investigations described here have been presented in summary form.[15–16] Detailed studies covering the first 24 hours after exposure to 600 r have been reported separately.[17]

Supported by the United States Atomic Energy Commission.

Accepted for publication, January 5, 1961.

* Present address: Department of Medicine, Washington University School of Medicine, St. Louis, Mo.

Material and Methods

Sprague-Dawley rats, 200 to 220 gm. body weight, were divided into 3 groups for radiation exposure.

Radiation Exposure. Three groups of 24 rats each were irradiated with 550, 1,000 and 1,500 r respectively. The following factors were used: 250 Kvp; 30 ma; filtration 0.5 mm. Cu, 1 mm. Al; HVL 1.4 mm. Cu; TSD 100 cm. The animals were exposed 12 at one time in a plastic container rotated during irradiation. The dose rate measured at the center within the exposure apparatus, with animals in place, was 25 r per minute. The doses, calculated on this basis, can be converted approximately to rads by the use of the factor 0.96.[18]

H^3-Thymidine. Each animal received an intravenous injection of 100 μc. of H^3-thymidine (Schwarz Bioresearch, Inc., Mount Vernon, New York) 30 minutes before sacrifice.

Time of Sacrifice. Two rats of each group were sacrificed 1, 3, 6, 12, 18 and 24 hours after irradiation. Additional animals in the 550 r group were sacrificed on days 2, 3, 5, 7, 8 and 10. Sacrifices could be carried out only until day 8 in the 1,000 r group, when all animals had died, and until day 3 in the 1,500 r group.

Tissue Preparation. One femur and 1 tibia of each rat were removed, and the epiphyses were cut off. The metaphyseal part was fixed in 4 per cent neutral formalin *in toto* to insure unchanged conditions of the marrow architecture and vessel structure. After at least 2 days the fixed marrow cylinder was removed from the bone shaft by splitting off the bone shell. Paraffin sections were processed for stripping film autoradiography and stained with Mayer's hematoxylin. One femur and 1 tibia of each rat were used for direct marrow smears. After fixing in methyl alcohol, stripping film (Eastman Kodak AR 10) was applied. The exposure time was 30 days, and the slides were stained with Giemsa stain through the developed film.

Evaluation of the Preparations. The histologic sections were examined qualitatively, and the cell types seen were compared with cells in the marrow smear. Counts of the number of labeled cells in the erythropoietic and myelocytic series were made in direct marrow smears. Red cell (500) and white cell (400) precursors were counted in each smear and the percentage of labeled cells was recorded. A cell with more than 3 grains over the nucleus was considered to be labeled.

Results

The Normal Vascular Structure of the Femoral and Tibial Bone Marrow in the Rat

Sections cut longitudinally through the midline of the normal rat femur or tibia marrow cylinder showed a high degree of cellularity with only a little fat (Fig. 1). With respect to the vascular structures, two different components were readily distinguished: the sinusoids, characterized by very thin membranous walls with only a few flat endothelial (border-line reticulum) cells; and the arterial capillaries, characterized by thick walls relative to the diameter and with numerous endothelial cells. In the center of the marrow, part of the "central sinusoid" which goes through the marrow longitudinally was usually present. From the central sinusoid toward the periphery, numerous cross sections through sinusoids were seen. While in the peripheral part more cross sections through sinusoids ("contortal sinusoids") were present, the sinusoids

toward the center were more frequently cut longitudially ("rectal sinusoids"), and some were recognized to enter the central sinusoid at a right angle. The arterial capillaries in most instances could be followed for some length through the marrow and appeared to follow a course parallel to the central sinusoid. Some larger arterial vessels were frequently seen in cross section (Fig. 1). It has been shown that these arteries have a tortuous course through the marrow, frequently winding around the central sinusoid. [19–21] In the normal marrow, only some sinusoids appeared to be filled with blood; these were usually found in localized areas, whereas in other parts, no distended sinusoids could be demonstrated. A close examination, however, revealed that sinusoids were present but apparently closed. Thus, at any one time, only a few "sinusoidal segments" were "active," whereas a large number were "resting."

Additional details of the marrow architecture of the rat have been described earlier [19,20] and are summarized here. The marrow vascular system is supplied with blood through the nutrient artery which enters the femur proximally and the tibia distally. The artery divides into several branches shortly after entering the marrow cavity, and several branches proceed tortuously around the central sinusoid while giving rise to numerous arterial capillaries which are relatively straight and traverse the marrow in the longitudinal direction. The sinusoidal system receives blood through these capillaries, as does the bony cortex to a high extent. There is some evidence that the intersection of sinusoids and capillaries occurs at sites of "cellular sphincters" which may be responsible for the regulation of blood flow. The sinusoids of the parenchyma are directed centripetally. This was shown by studying longitudinal and cross sections which presented a 3-dimensional impression of the marrow.

The injection of India ink into the central sinusoid showed that numerous "contortal sinusoids" communicate and join as the center is approached to form larger and larger "rectal sinusoids," the last branches of which enter the central sinusoid at a right angle. By this technique it was demonstrated that the basic functional and anatomic unit is a "sinusoid segment" which can be compared with a tree, the branches of which are directed toward the marrow periphery and the trunk of which rests on the central sinusoid. The central sinusoid collects the blood from the sinusoidal segments and is drained by a vein which leaves the femur distally and the tibia close to the knee joint.

Since under normal conditions only a few sinusoidal segments are distended with blood at one time, and since the marrow as a whole cannot change its volume inside the rigid bony capsule, the hypothesis is enter-

tained that the release of mature marrow elements is based on a rhythmic alternating increase and decrease of blood flow in the sinusoidal segments. Some of the latter will be found either distended (active) or closed (resting) at any one time. The presence of a generalized sinusoidal distention would indicate a pathologic condition.

Cellularity and Vascular Damage

The time sequence of vascular changes in the bone marrow of rats exposed to 1,000 r is shown in Figures 2 and 3. One hour after total body irradiation, the marrow had a grossly normal appearance in the groups receiving 550 and 1,000 r, although in the 1,000 r group more generalized sinusoidal distention was noted. By 3 hours almost all contortal and rectal sinusoids were dilated after 1,000 r, less after 550 and more after 1,500 r. The cellularity at this time was not grossly reduced. After 6 hours the sinusoids were highly distended in all marrow areas.

With high magnification, extravasated red cells could be easily identified in the parenchyma. In many parts of the marrow the cells were "dissociated" from each other, presumably by an increase in the parenchymal fluid content. After 12 hours, the cellularity was further decreased, and destroyed sinusoids with hemorrhage were obvious with low power examination.

Twenty-four hours after the administration of 1,000 r, the marrow was markedly hypocellular, and the space was almost entirely taken by red cells, indicating a generalized hemorrhage with breakdown of sinusoidal structure. The sequence of events indicated maximal damage 3 days after 1,000 r, leaving a "lake of blood" with a few reticulum cells but no obvious structure. Red cells were recognized in equal numbers inside and outside of outlined sinusoids. Five days after 1,000 r, the blood appeared to be "contained" again in a vascular bed, and a parenchyma was simulated by large fat globules. In some areas, especially around arterial capillaries, single foci of myeloid cells, most of them heavily labeled with tritiated thymidine, were found. Taking into account the generation time of myelocytes and realizing that most of these cells were at the stage of myelocytes and metamyelocytes, one may assume that they represented an "abortive" proliferation of "left over" early myeloid precursors. The regeneration which led to a final hematologic recovery—if the animal overcame the "hematologic phase" of radiation injury—was characterized by generalized proliferation of reticulum cells throughout the marrow, with focal proliferative centers of myeloid and erythroid precursors (Fig. 3, 8 days).

An attempt was made to compare the total cellularity and the degree of hemorrhage into the parenchyma in rat marrow after 550, 1,000 and

1,500 r as a function of time. The results shown in Text-figure 1, semi-quantitative in nature, agree with those of previous, more quantitative investigations. [17,22,23] With higher doses, the rate of fall in degree of cellularity appeared to be greater. At all doses a short plateau appeared to exist after the initial high rate of fall; the plateau appeared to occur

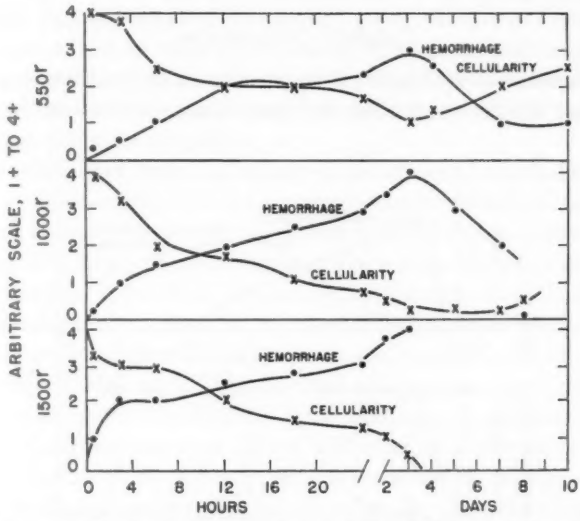

TEXT-FIGURE 1. Semi-quantitative estimates of the cellularity and degree of hemorrhage in bone marrow sections of rats exposed to total body radiation. The marrow cellularity is classified from 4+ (normal) to 0 (minimum). The degree of hemorrhage is classified from 1+ to 4+. Less than 1 indicates "hyperemia" only. One plus indicates slight but definite hemorrhage. With 2+, evidences of marked dilatation of all sinusoids and local breakdown of sinusoidal walls and leakage into the parenchyma are present. Marrows described as 3+ show generalized hemorrhage; however, the general pattern of sinusoids can be made out, indicating some degree of vascular marrow structural integrity. In marrows designated as 4+, all structures appear to be lost, and the section appears as a "lake of blood" in which the few remaining marrow cells are dispersed at random.

earlier at higher doses. While after 550 r the cellularity only reached moderately low levels with a minimum at 3 days, the cellularity was much lower after higher doses (Fig. 3, 3 days) and was minimal after 1,500 r at the time the animals died. A marked increase in the degree of cellularity was noticed following 1,000 r after 7 to 8 days, the time of onset of regeneration.

Hemorrhage into the parenchyma was obvious at all dose levels, although the time of appearance was earlier at the higher range. It was found (Text-fig. 1) that "hemorrhage" into the marrow parenchyma started with red cell diapedesis and was recognized first in the 1,500 r group at 1 hour, in the 1,000 r group at 3 to 6 hours, and in the 550 r

group at 6 to 12 hours after radiation. The maximum hemorrhage in all groups occurred at 3 days. In both the 500 and 1,000 r groups, many red cells in the parenchyma were clearly evident to at least the seventh day. The marrow had taken on a more orderly appearance, however, and the definite impression of the reconstitution of sinuses was noted by the fifth or seventh day in both the 500 and 1,000 r groups.

Cytologic Observations

The sequence of cytologic changes is shown in Text-figure 2. It was found that drastic qualitative and quantitative alterations in the cell

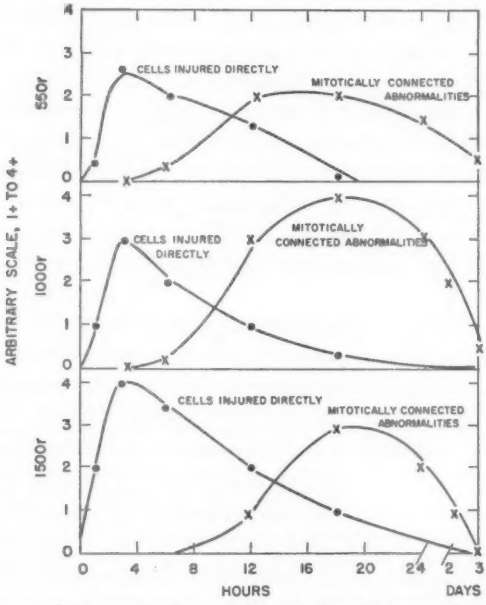

TEXT-FIGURE 2. Semi-quantitative estimates of the relative numbers of cells injured directly, and of mitotically connected cell abnormalities in the bone marrow of rats given total body radiation. The symbol 4+ indicates the largest relative number of abnormalities seen; o refers to normal marrow.

population occurred, and the precise type of cytologic abnormalities changed appreciably with time. Direct cell damage could be evaluated more accurately in sections; the mitotically induced changes on smears. However, the same general pattern of change was evident in both the sections and smears.

Two types of cell damage were recognized: (a) "cells injured directly," and (b) "mitotically connected abnormalities." Direct damage presumably indicated irrevocable changes classically described as clump-

ing of chromatin, pyknosis, karyorrhexis, karyolysis, and the presence of nuclear debris. Some cells (red cell precursors mainly) appeared intact except that the normally fine nuclear structure was replaced by clumps or aggregates of chromatin. Cells with shrunken, frequently eccentric nuclei with complete loss of structure, altered staining characteristics and often a "glassy" appearance were considered pyknotic. Some cells (usually myeloid precursors) gave evidence of "edematous" nuclei, with a loss of clear definition of the nuclear boundary and its blending with the cytoplasm. Some cells showed obvious fragmentation of the nucleus, with the small pieces, frequently "pyknotic" in appearance, dispersed in the cytoplasm.

Some evidence of direct cell injury could be seen in the earliest preparations at all dose levels, with increasing severity at higher dose levels. The peak for this direct cell injury was reached within a few hours of exposure. Evidence of these abnormalities then disappeared, within hours or at best a few days, depending on the dose level. It should be noted that the curves (Text-fig. 2) roughly indicate the relative number of obviously disturbed cells, and that the total number even with a "4+" did not exceed a few per cent of the total cells present. At 1,500 r, direct cell injury occurred very rapidly; with rapid loss of cellularity and apparently efficient removal of debris, this type of abnormality was virtually absent by 18 to 24 hours. At 1,000 r a similar pattern was seen, slightly delayed in onset and of less severity. At 550 r the time of onset was further delayed. The degree of severity was less; however, the time required for a significant decrease in the degree of abnormality appeared to be greater than at the higher doses.

Essentially all cytologic changes in the earliest hours were noted to be in the erythroid precursor cells, which disappeared almost entirely by 12 to 24 hours, depending on the dose level. Obvious changes in the myelocytic cells followed, by some 10 or more hours, changes in the erythroid cells.

Before the evidences of direct cell injury disappeared, the "mitotically connected cell abnormalities," limited mainly to the myeloid series, began to appear (Text-fig. 2). These consisted of a variety of nuclear and cellular abnormalities, presumably the result of abnormal division or of a failure of cell division, and thus appeared, of course, only when cells had time to enter or go through mitosis (Fig. 4, a to d). At earlier times the abnormalities were found in young cells (myeloblasts, myelocytes), later in metamyelocytes, band forms and mature neutrophils. The abnormalities consisted of "giant" cells, abnormal mitotic figures (chromosome stickiness, chromosome bridges, bizarre-shaped mitotic figures, broken and separated chromosomal fragments), grossly distorted nu-

clear shapes, multiple nuclear fragments including binucleated cells, additional "satellite" nuclear fragments and grossly fractionated nuclei. These forms differed from those seen with direct cell injury in that the nuclei or nuclear fragments, while obviously distorted, retained a normal chromatin structure and appeared to be metabolically active. This was confirmed by the fact that many of these cells, even those with multiple nuclear fragments, were capable of incorporating tritiated thymidine. They are thus viable monsters, rather than dying or moribund cells. These cells were present in appreciable numbers only for approximately 48 hours or less, indicating that many succumbed directly or were able to undergo mitosis only one or two times. The later appearance of giant and distorted mature forms indicated that some were capable of maturation, and possibly of division (Fig. 4, c and d). These cells were most numerous following 1,000 r, presumably because fewer cells were so affected at the lower dose and because they did not live as long (or could not undergo as many mitoses before death) at the higher dose.

Beyond the third day, normal-appearing erythroid and myeloid elements were present in the group receiving 550 r, and abnormal cells were rare to absent (Text-fig. 2). In the 1,000 r group, some but very few myeloid elements were present in proliferative foci, all cells of which seemed to be part of similar maturation compartments, from days 3 to 7 (Fig. 5e). Only rare "reticulum" and unidentified cells were present. On day 7, large, frequently labeled, unidentified cells with the general appearance of blast forms were present (Fig. 5f).

The Capability of Marrow Cells to Incorporate H^3-Thymidine at Different Times After Radiation

In bone marrow smears, the percentages of labeled myelocytes and promyelocytes were counted at different times after irradiation with 550, 1,000, and 1,500 r. Since the slopes of the curves were approximately the same for both cell groups, they were put into one category for this presentation. It should be recalled that H^3-thymidine was injected intravenously 30 minutes before sacrifice, so that the percentage of labeled cells at each point represented the percentage of cells in DNA synthesis at various times after irradiation. The results are shown in Text-figure 3. Normally about 40 to 50 per cent of immature myelocytic precursors are in DNA synthesis. After irradiation with 550, 1,000, and 1,500 r, this percentage increased slightly during the first 3 hours after irradiation. Thereafter, the percentage of cells in DNA synthesis decreased steadily after 550 r and 1,000 r, and more rapidly after 1,500 r. Eighteen hours after irradiation only a few immature myelocytes were labeled in all dose groups (Fig. 5, a to c), but these few were usually more heavily

labeled than normal and were abnormally large. In the 550 r group a large number of early, undifferentiated "blast" forms were heavily labeled, perhaps indicating the onset of regeneration at 18 and 24 hours.

The changes in the percentage of labeled immature normoblasts were studied at various times after irradiation with 550 and 1,000 r. Since

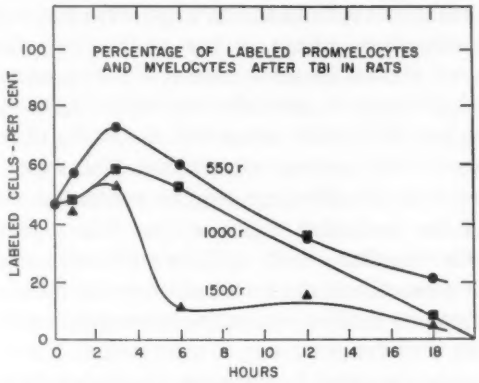

TEXT-FIGURE 3. Time sequence of changes in the percentage of labeled myeloid precursors in rats exposed to total body radiation.

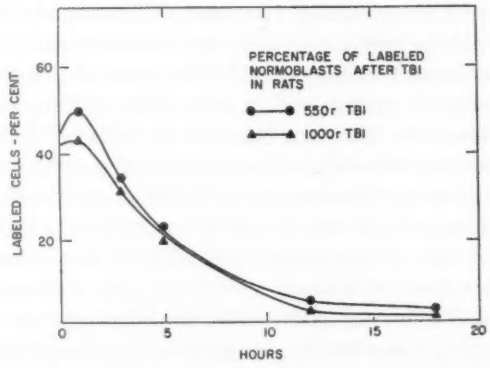

TEXT-FIGURE 4. Time sequence of changes in the percentage of labeled erythroid precursors in rats exposed to total body radiation.

the slope of the change as a function of time was the same for all groups of normoblasts capable of cell division, they were compiled in this study as "immature normoblasts" (Text-fig. 4). One hour after irradiation, the percentage of labeled cells was questionably increased. Three hours after irradiation, the percentage started to decrease and reached a minimum 12 hours after irradiation. Thereafter it remained at a low level until the end of the observation period.

Discussion

Structural changes in rat bone marrow following irradiation were early and striking, with pathologic sinusoidal dilatation apparent as early as one hour. By 6 hours in all dose levels and as early as 1 hour after 1,500 r, generalized sinusoidal dilatation was marked, and red cells within the parenchyma (definite hemorrhage) were observed easily. The dilatation preceding hemorrhage, at least at the lower dose levels, did not appear to be a gradual increase; rather, it first appeared in localized areas not conforming to a particular anatomic region of the femur. Hemorrhage appeared in some areas with markedly distended vessels before dilatation in other regions was obvious. This segmental development of dilatation and hemorrhage may be associated with the physiologic state of the particular region at the time of exposure, since differences in the vascular activity in different marrow regions are seen normally.[3,24] Noteworthy is the fact that when the later thrombopenic hemorrhage is present in other organs, the bone marrow is free of hemorrhage in regions with definite zones of regeneration.

The mechanisms involved in the early hemorrhage are not known; however, it is clear that it is not on the basis of the thrombopenia, which plays a key role in the later (eighth to 15th day, depending on dose) hemorrhage seen in essentially all organs. It is possible that early and direct damage to the fragile sinusoidal wall or to the mechanisms controlling sinusoidal blood flow may play an essential role. Besides direct action on the vascular system and its controlling mechanisms, a passive component is possible. This acts through the factor of rather rapid cell loss in the parenchyma without the marrow being able to adjust to the new size by shrinkage because of containment within the rigid bony capsule. The blood stream may distend the vascular bed until it is broken down mechanically. The parenchyma, with its few remaining intact cells, is thus flooded with blood which is in part no longer accessible to the general circulation (indicated by the later appearance of macrophages containing hemosiderin). It may be true also that openings exist normally in the structure of the sinusoidal walls which under normal conditions permit the release of mature elements into the circulation in "active" or distended sinusoidal segments. The fewer cells released after radiation injury, the more the pressure of circulating cells to enter the parenchyma, rather than the reverse as under normal conditions. This "inverse sinusoidal pressure" may be one reason why no immature cells are found in the circulating blood after total body irradiation, even if the otherwise closed circulation is completely disrupted. If this is true, red cell extravasation after irradiation of the marrow represents "cell replacement" rather than "hemorrhage."

The same pattern of cytologic change in the marrow appears to occur at all dose levels studied, and is accelerated with increasing dose. The earliest cytologic alteration is direct cell destruction, observed mostly in the erythroid precursor series. Essentially all of these cells disappear in the first 12 hours by this mechanism, and only a few erythroid forms with mitotically linked damage are seen. Some of the myeloid elements undergo direct damage and death. However, the damage appears to be of a different type, which occurs later and is more subtle than that in the erythroid elements. The most striking features in the myeloid series are the mitotically connected abnormalities—giant cells, abnormal mitosis and bizarre nuclear configurations. The giant cells result in part presumably from continued DNA synthesis, and thus there is polyploidy in cells that are unable to enter mitosis. The remaining abnormalities result from cells that have entered but have been unable to complete the cell division process normally. Cells resulting from this process ("giant neutrophils") appear in the blood after 48 and 72 hours. Similar observations have been made in human subjects after accidental exposure to radiation.[2]

At no time is there evident damage to a large percentage of cells. Thus at 3 and 6 hours at even very high doses, many cells, though having a vague appearance of not being quite normal, do not show evidence of definite cytologic injury. Yet the total cellularity decreases markedly, and with 1,000 r or more the marrow is essentially completely depleted of normal erythroid and myeloid elements after 3 to 4 days. Thus, the cytologic abnormalities seen in a small fraction of cells must either represent a very ephemeral stage in the process of disintegration, with only a few being seen at any given time (as with mitotic figures normally), or many cells must disintegrate directly as the result of more subtle cytologic damage. In any event, removal of debris (transformed into fat?) must be very rapid. While some debris is visible, particularly after 6 and 12 hours, at no time is the amount seen apparently consistent with the degree of progressive cell breakdown. This is consistent with the experience that the nuclei of oxyphilic normoblasts are rarely seen being released and catabolized in the marrow.

The interrelationship between structural and cytologic change is not clear. Both progress simultaneously and may be mutually contributory to the total disruption of architecture and destruction that is seen. The disruption of normal architecture results in a transient loss of matrix that may be necessary for regeneration. The matrix becomes reconstituted after the vascular bed returns to normal. It was found that the animal *glis glis,* irradiated during hibernation,[25] did not develop any evidence of marrow hemorrhage within 3 weeks after irradiation so long as it was kept in hibernation. However, the marrow was slowly depleted

of early hematopoietic precursors during this time. When the hibernating irradiated animals were brought to room temperature after more than 3 weeks, the complete picture of early marrow hemorrhage developed within the next 24 hours. This was identical with the lesion described in this paper and would indicate a dependence of the process of structural marrow damage on metabolic activity.

The epithelium of the large intestine, following doses that result in complete denudation within approximately 3 days, is able to regenerate rapidly so that the intestine is again histologically normal within 5 to 6 days.[26] In the animals receiving the 1,000 r dose with complete marrow destruction, beginning but definite evidence of regeneration was not seen until the seventh day. It thus seems that the marrow, even at such high doses, is capable of early regeneration but that the disruption of architecture with disturbance of the matrix may not allow regeneration to proceed. Regeneration is preceded by reconstitution of the normally closed sinusoidal system, and the first nests of regenerating cells are seen along vessels, the reconstituted sinuses, and along the endosteum. It thus appears that if it were possible to prevent the initial sinusoidal breakdown, regeneration of the marrow might commence before depletion of peripheral blood elements, and that survival might be possible at otherwise lethal dose levels.

The possible mechanisms involved in the changes in the percentage of labeled cells and of grain counts have been discussed previously [16,17] and will only be summarized. The percentage of cells labeled is approximately equal to the number of cells in the DNA synthesis phase, divided by the sum of cells in DNA synthesis, those in the postmitotic and premitotic rest periods, and those in mitosis. The early and marked reduction in the percentage of labeled cells at all dose levels reflects the decreased proliferative capacity of the marrow. The early rise in percentage of labeled cells could be the result of selective loss of cells not in DNA synthesis or of a prolongation of DNA synthesis time. The present data do not allow differentiation between these possibilities. The later fall could be the result of an effect on the process of DNA synthesis or a lack of cells capable of entering DNA synthesis and lost in the postmitotic rest period. The increased percentage of labeled cells at 18 and 24 hours after 550 and 1,000 r is due for the most part to labeled "giant" neutrophils which undergo a mitotic phase without division and then re-enter the DNA synthesis phase.

Summary

Structural and cellular alterations in the bone marrow of rats were correlated during the "degenerative" and "regenerative" phases follow-

ing exposure to 550, 1,000 and 1,500 r of x-radiation. To obtain additional information on the metabolic and potential proliferative capacity of the individual maturation compartments, tritiated thymidine as a specific label of DNA synthesizing cells was injected 30 minutes prior to sacrifice. The thymidine label was detected with stripping film autoradiography.

It was clearly demonstrated that the vascular bed of the marrow was destroyed. Maximum damage at 3 days after irradiation led to severe marrow hemorrhage long before the platelet count began to fall. The time of onset of the early nonthrombopenic marrow hemorrhage was dose-dependent and was evident as early as 1 hour after 1,500 r. The cellularity in the marrow decreased as the extravasation of red cells increased. After 1,000 r, abortive myelocytic regeneration was observed on days 5 and 6, whereas final recovery was found to start after 7 to 8 days with a generalized proliferative stimulation of marrow reticulum. After 550 r, the "degenerative" and "regenerative" phases overlapped and were difficult to separate. After 1,500 r all animals died on day 3; however, cells capable of DNA synthesis, as indicated by thymidine uptake, remained.

It is not possible to state to what degree the early radiation damage to the vascular integrity contributed to the severe over-all damage to and the disappearance of the marrow cells observed. However, it seems clear that the early marrow hemorrhage was one additional component to be taken into account in explaining the high sensitivity of the marrow to radiation injury and its delayed recovery as compared to the intestinal mucosa.

References

1. Brucer, M. (comp.). The Acute Radiation Syndrome: a Medical Report on the Y-12 Accident June 16, 1958. (ORINS-25), Oak Ridge Institute of Nuclear Studies, Oak Ridge, Tenn., 1959, 179 pp.
2. Fliedner, T. M.; Cronkite, E. P.; Bond, V. P., and Andrews, G. Mitotic activity and cytology of human bone marrow after accidental exposure to ionizing radiation. Proceedings of the 7th European Society of Haematology, London, 1959. (In preparation)
3. Fliedner, T.; Sandkühler, S., and Stodtmeister, R. Die Knochenmarkstruktur bei Ratten nach Bestrahlung mit schnellen Elektronen. *Ztschr. Zellforsch.*, 1955, **43**, 195–205.
4. Bloom, W. (ed.). Histopathology of Irradiation from External and Internal Sources. McGraw-Hill Book Co., Inc., New York, 1948, 808 pp.
5. Smellie, R. M. S.; Humphrey, G. F.; Kay, E. R. M., and Davidson, J. N. Incorporation of radioactive phosphorus into nucleic acids of different rabbit tissues. *Biochem. J.*, 1955, **60**, 177–185.
6. Mandel, P.; Gros, C. M.; Rodesch, J.; Jaudel, C., and Chambon, P. Effect of Various Doses of X-Rays—Whole Body and Local Irradiation—on the

Nucleic Acids of the Bone Marrow. In: Advances in Radiobiology; Proceedings of the 5th International Conference on Radiobiology, Stockholm, 15–19 August, 1956. De Hevesy, G. C.; Forssberg, A. G., and Abbatt, J. D. (eds.). Oliver & Boyd, Edinburgh, 1957, pp. 59–64.

7. Butler, J. A. V. Changes Induced in Nucleic Acids by Ionizing Radiations and Chemicals. In: Proceedings of the International Congress of Radiation Research, 1st, Burlington, Vermont, August 11–15, 1958. Smith, D. E. (ed.). Academic Press, Inc., New York, 1959, pp. 403–416. (*Radiation Res.*, 1959, Suppl. 1.)
8. Kelly, L. S. Effect of Radiation on DNA Synthesis in Mammalian Cells. In: Progress in Biophysics and Biophysical Chemistry. Butler, J. A. V., and Katz, B. (eds.). Pergamon Press, New York, 1957, Vol. 8, pp. 143–163.
9. Cronkite, E. P.; Fliedner, T. M.; Rubini, J. R.; Bond, V. P., and Hughes, W. L. Dynamics of proliferating cell systems of man studied with tritiated thymidine. (Abstract) *J. Clin. Invest.*, 1958, **37**, 887.
10. Lajtha, L. G.; Oliver, R., and Ellis, F. Incorporation of ^{32}P and adenine ^{14}C into DNA by human bone marrow cells *in vitro*. *Brit. J. Cancer*, 1954, **8**, 376–379.
11. Friedkin, M.; Tilson, D., and Roberts, de W. Studies of deoxyribonucleic acid biosynthesis in embryonic tissue with thymidine-C^{14}. *J. Biol. Chem.*, 1956, **220**, 627–637.
12. Taylor, J. H.; Woods, P. S., and Hughes, W. L. The organization and duplication of chromosomes as revealed by autoradiographic studies using tritium-labeled thymidine. *Proc. Nat. Acad. Sc.*, 1959, **43**, 122–128.
13. Cronkite, E. P.; Fliedner, T. M.; Bond, V. P.; Rubini, J. R.; Brecher, G., and Quastler, H. Dynamics of hemopoietic proliferation in man and mice studied by H^3-thymidine incorporation into DNA. *Ann. New York Acad. Sc.*, 1959, **77**, 803–820.
14. Bond, V. P.; Fliedner, T. M.; Cronkite, E. P.; Rubini, J. R.; Brecher, G., and Schork, P. K. Proliferative potentials of bone marrow and blood cells studied by *in vitro* uptake of H^3-thymidine. *Acta haemat.*, 1959, **21**, 1–15.
15. Fliedner, T. M.; Cronkite, E. P., and Bond, V. P. Autoradiographic and cytologic studies using H^3-thymidine on the proliferative capacity of bone marrow in total-body irradiated mammals. (Abstract) *Radiation Res.*, 1958, **9**, 114.
16. Fliedner, T. M.; Bond, V. P., and Cronkite, E. P. The Effect of Total Body Irradiation on H^3-Thymidine Incorporation into DNA of Rat Bone Marrow Cells. In: Proceedings of the 9th International Conference of Radiology, Munich, 1959. G. Thieme, Stuttgart. (To be published)
17. Tsuya, A.; Bond, V. P.; Fliedner, T. M., and Feinendegen, L. E. Cellularity and DNA synthesis in bone marrow following total and partial body irradiation. *Radiation Res.* (In press)
18. Report of the International Commission on Radiological Units and Measurements, 1956. National Bureau of Standards, U.S. Government Printing Office, Washington, D.C.
19. Fliedner, T.; Sandkühler, S., and Stodtmeister, R. Untersuchungen über Gefässarchitektonik des Knochenmarkes der Ratte. *Ztschr. Zellforsch.*, 1956, **45**, 328–338.
20. Fliedner, T. M. Relations between the architecture of the marrow circulation and function. (Abstract) *Fed. Proc.*, 1958, **17**, 47.
21. Cronkite, E. P.; Fliedner, T. M.; Bond, V. P., and Robertson, J. S. Anatomic and Physiologic Facts and Hypotheses about Hemopoietic Pro-

liferating Systems. In: Conference on Fundamental Problems and Techniques for the Study of the Kinetics of Cellular Proliferation, Salt Lake City, 1959. STOHLMAN, F., JR. (ed.). Grune & Stratton, New York, 1959, pp. 1–14.

22. STODTMEISTER, R.; SANDKÜHLER, S., and FLIEDNER, T. Über die Pathogenese akuter Knochenmarkatrophie bei Ratten nach Ganzkörperbestrahlung mit schnellen Elektronen. *Folia haemat.*, 1956, **74**, 303–345.

23. BECKER, J., and FLIEDNER, T. M. Premesse della rigenerazione del midollo osseo dopo radiazione ionizzante su tutto il corpo. *Minerva med.*, 1958, **49**, 714–717.

24. DOAN, C. A. Bone Marrow. Normal and Pathologic Physiology with Special Reference to Diseases Involving the Cells of the Blood. In: Handbook of Hematology. DOWNEY, H. (ed.). Paul B. Hoeber, Inc., New York, 1938, Vol. 3, pp. 1839–1961.

25. HECKMANN, U., and KUNKEL, H. A. Hämatologische Untersuchungen am Hiberninerten Siebenschlafer nach Ganzkörperbestrahlung. In: Proceedings of the 9th International Conference on Radiology, Munich, 1959. G. Thieme, Stuttgart. (To be published)

26. QUASTLER, H.; SHERMAN, F. G.; BRECHER, G., and CRONKITE, E. P. Cell Renewal, Maturation and Decay in the Gastrointestinal Epithelia of Normal and Irradiated Animals. In: Second United Nations International Conference on the Peaceful Uses of Atomic Energy. Biological Effects of Radiation, 1958, **22**, 202–205.

[*Illustrations follow*]

Legends for Figures

Photomicrographs were prepared from sections stained with Giemsa stain.

Fig. 1. Normal architecture of the marrow. The vascular structure permits recognition of arterial vessels, the larger branches of which, "tortuous arteries" (a), can wind around the central sinusoid. The smaller capillaries, arterial capillaries (b), go through the marrow longitudinally, supplying the sinusoidal system with blood. The contortal sinusoids (c) send their blood through collecting rectal sinusoids (d) to the central sinusoid (e) which courses longitudinally through the marrow shaft and is in direct communication with the femoral veins. × 200.

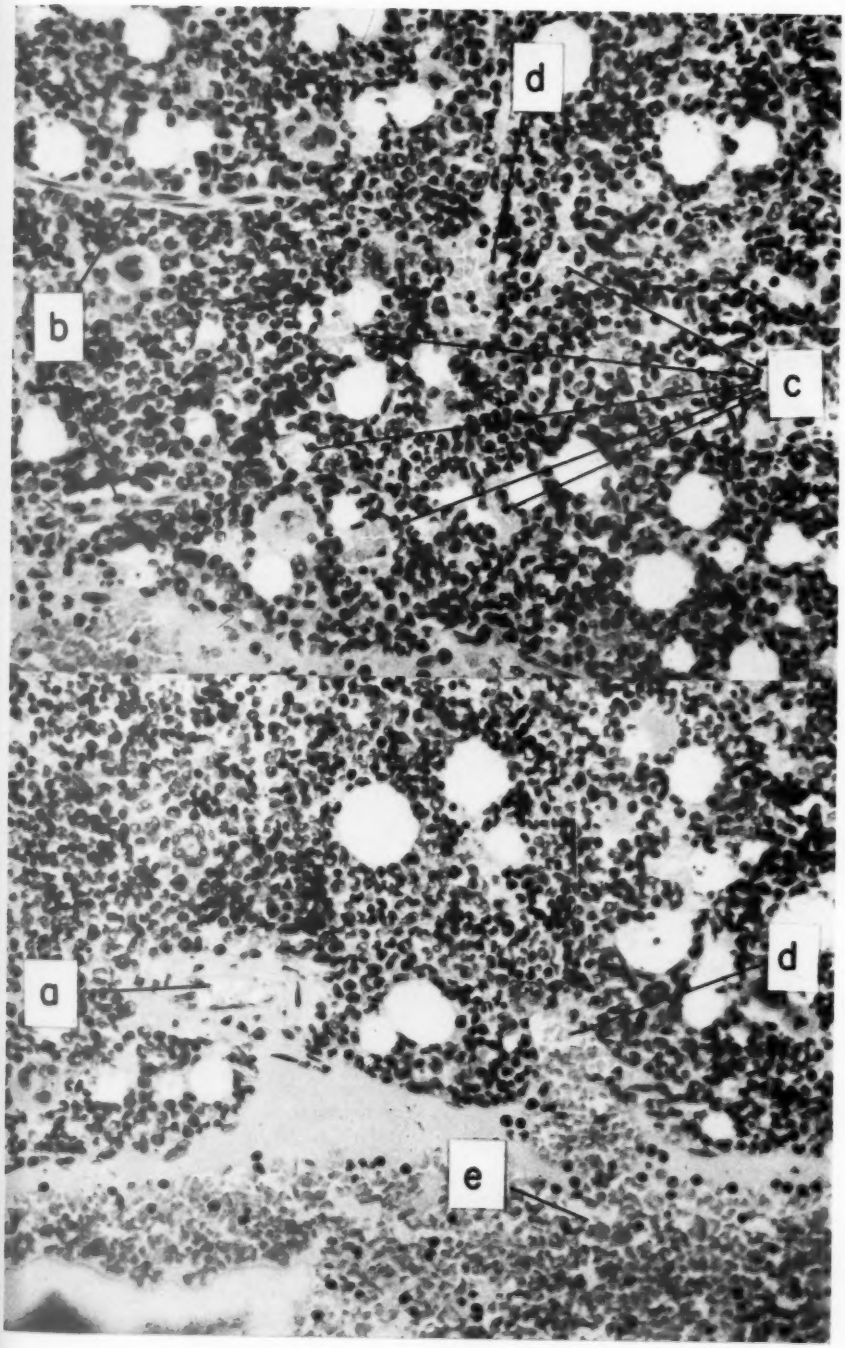
d
b
c
a
d
e

FIG. 2. Pathogenesis of radiation-induced marrow damage after 1,000 r x-irradiation. Slight but generalized sinusoidal distention after 1 hour leads to progressive sinusoidal widening after 3 and 6 hours. After 6 hours the first red cell extravasation seen with high oil magnification indicates the beginning of vascular breakdown. After 12 hours the sinusoidal distention increases and frank breakdown of sinusoids with extravasation of blood becomes obvious. × 320.

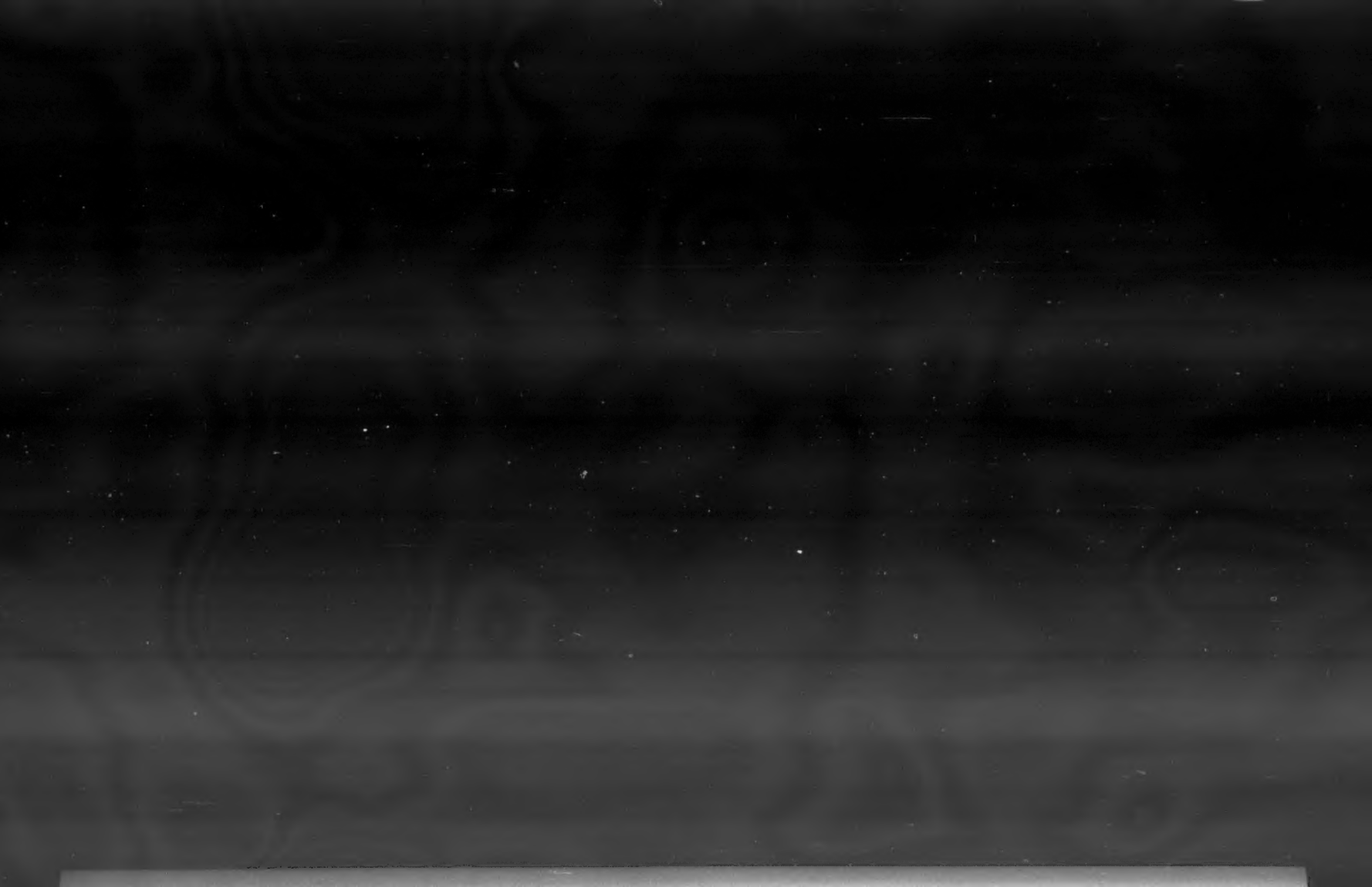

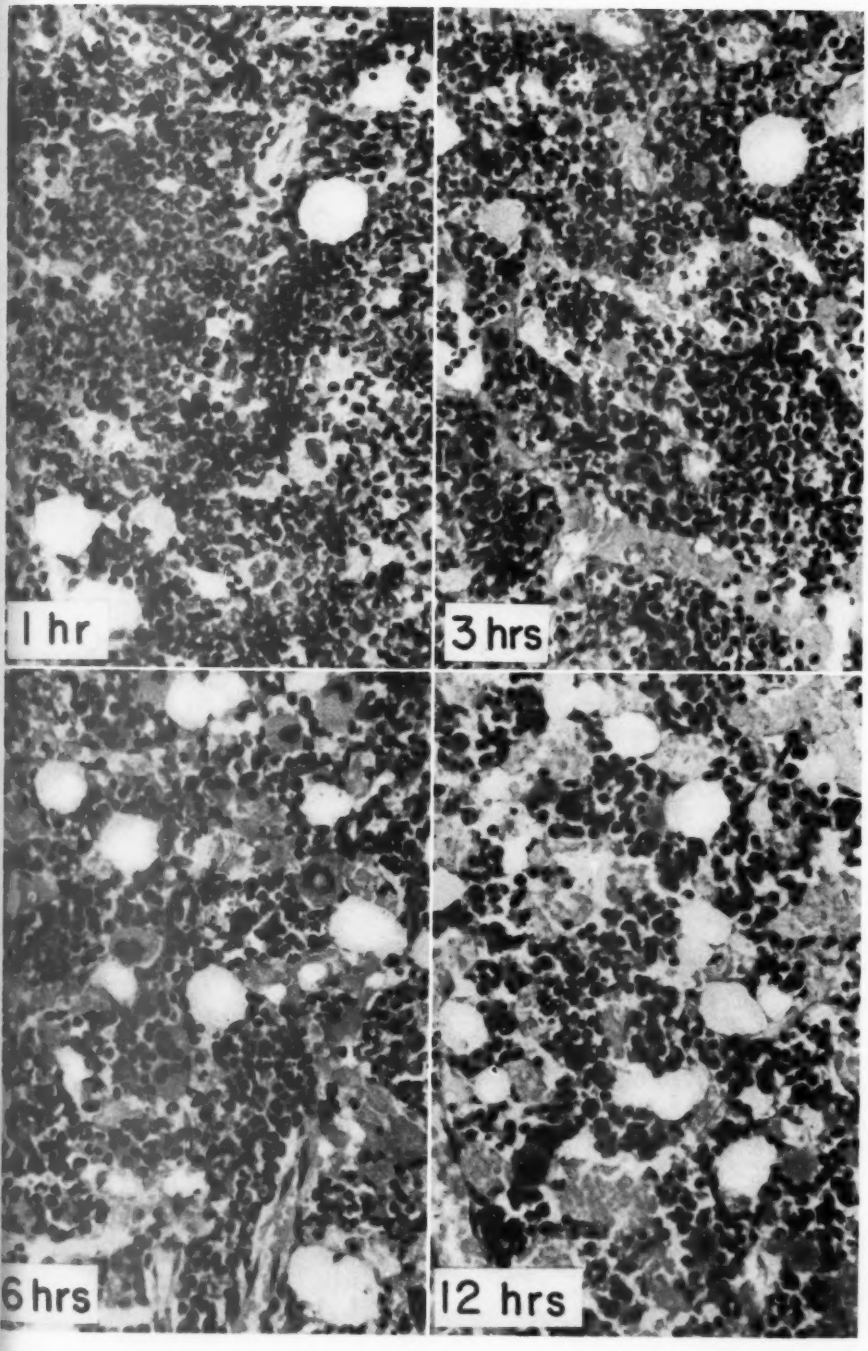

2

FIG. 3. Pathogenesis and regeneration of radiation-induced marrow injury after 1,000 r x-irradiation. The vascular integrity is highly affected at 1 day, at which time a generalized hemorrhage is observed. After 3 days, no vascular architecture can be recognized. The parenchyma is depleted, and mainly reticulum cells remain. At 5 days, sinusoidal walls are outlined again in a fatty, atrophic marrow. Around capillaries, labeled hematopoietic foci are noted. These are considered to be due to the proliferation of a few remaining undamaged precursors. At 8 days, the onset of final recovery is initiated by a generalized reticulum cell hyperplasia, but at this time the vascular outlines are again visible. × 320.

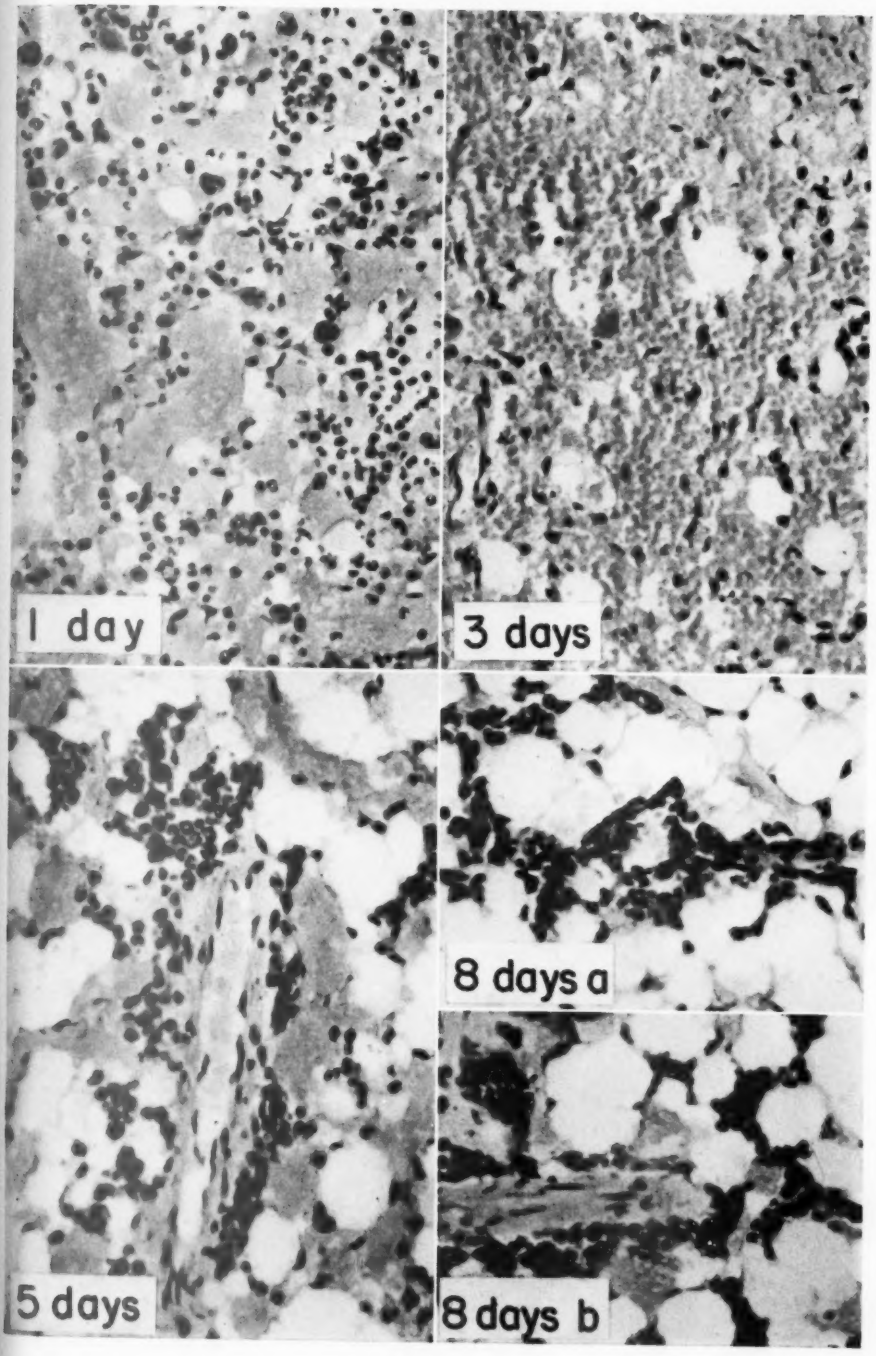

3

FIG. 4. Bone marrow of rats after 1,000 r x-irradiation. (a) Three hours, with evidence of nuclear fragmentation, karyorrhexis, pyknosis (see circles) and cellular "dissociation" (edema?); (b) 6 hours, onset of red cell extravasation; (c) 12 hours, parenchymal hemorrhage, cell damage, nuclear fragmentation in a cell inside a sinusoid (see circles); (d) 18 hours, formation of micronuclei after abnormal mitosis (circle); mitosis, binucleated cell and H^3-thymidine-labeled cell; generalized hemorrhage. × 800.

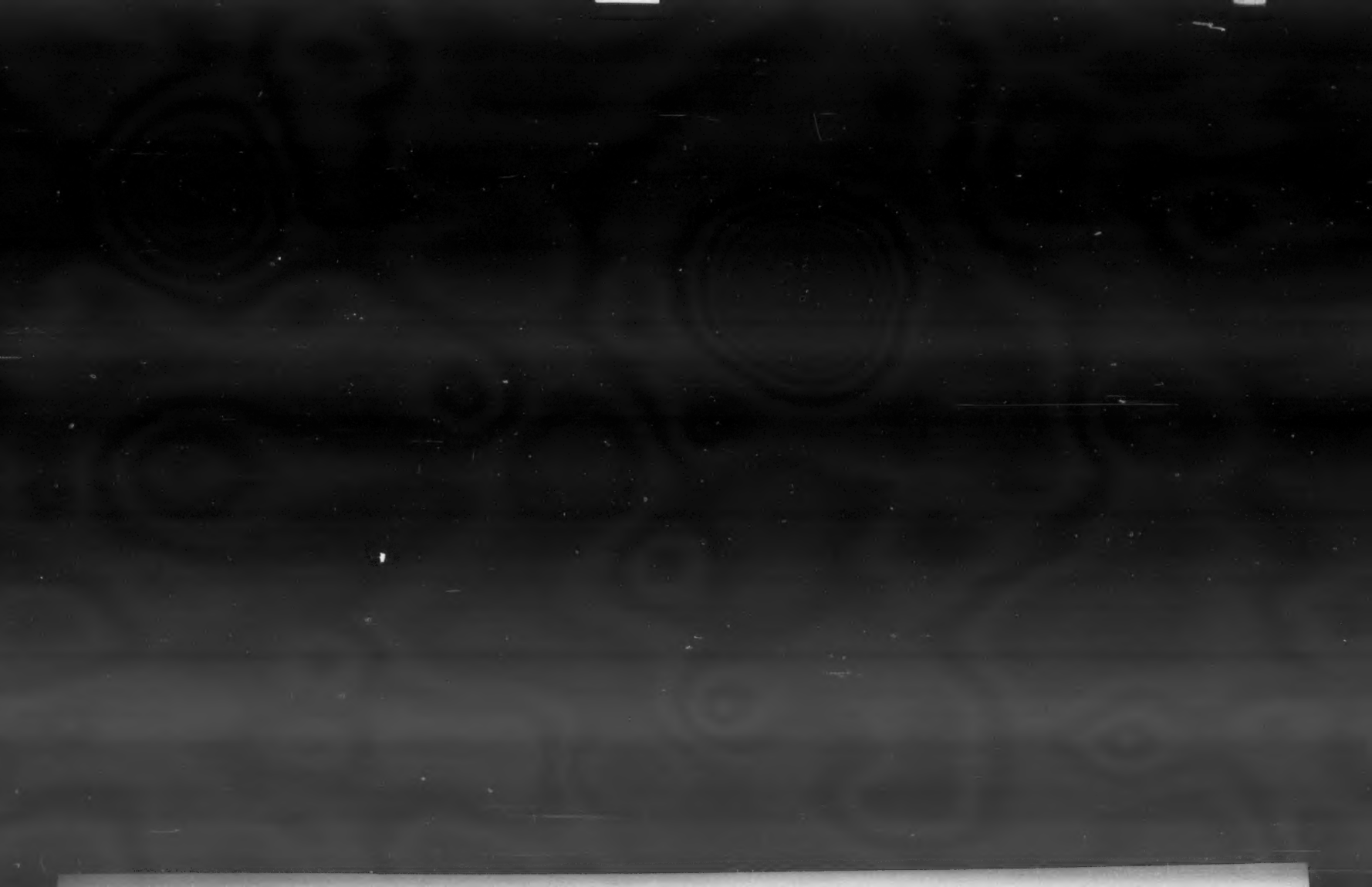

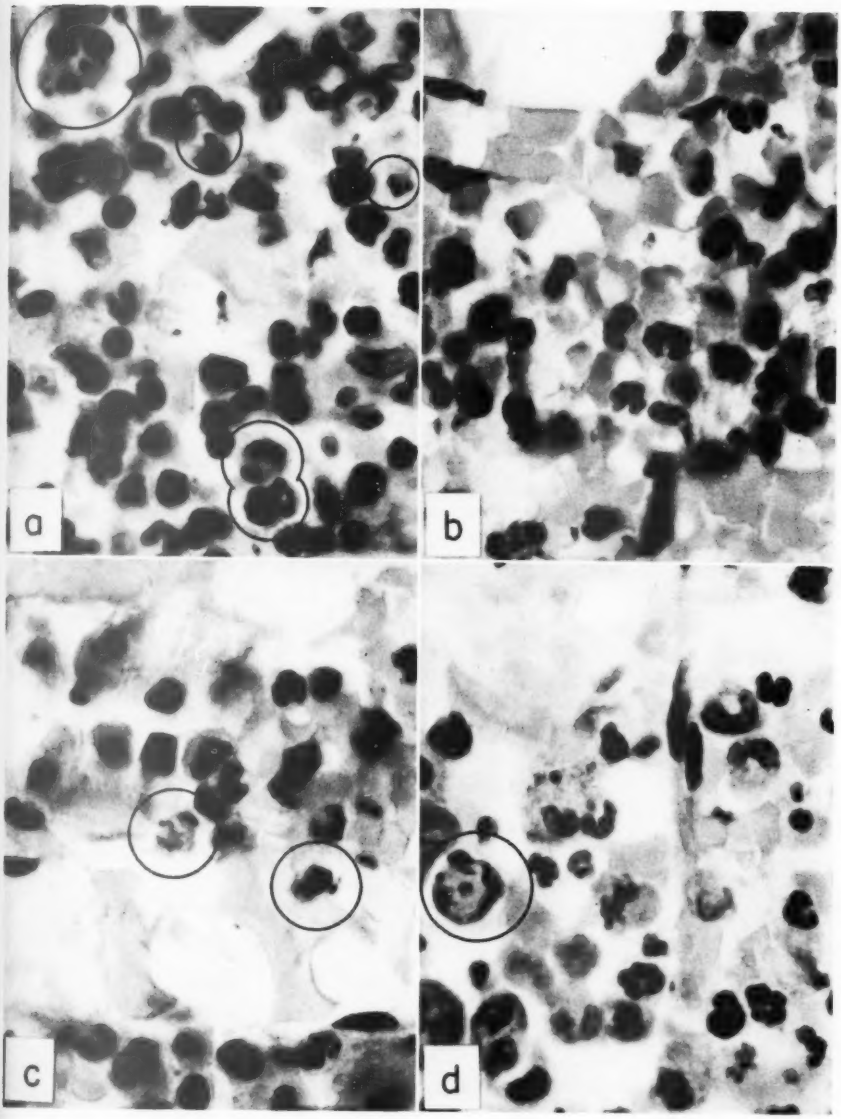

4

FIG. 5. Bone marrow of rats after 1,000 r x-irradiation. (a and b) Smears 18 hours after radiation and 30 minutes after the intravenous injection of H^3-thymidine: atypical mitosis, heavily labeled early myeloid cell, bizarre "giant" myelocytes, 2 of which are binucleated; (c) heavily labeled promyelocyte and myelocyte 12 hours after radiation; (d) abnormal mitosis 24 hours after radiation; note chromosomal fragments in the cytoplasm; (e) focal myelocytic regeneration at central sinusoid 5 days after radiation, 30 minutes after the intravenous injection of H^3-thymidine: note the high proportion of heavily labeled cells and mitotic figures; (f) regeneration 8 days after radiation, 30 minutes after the intravenous injection of H^3-thymidine: heavy labeling of cells is evident throughout the marrow. A and b, × 320; c and d, × 800; e and f, × 200.

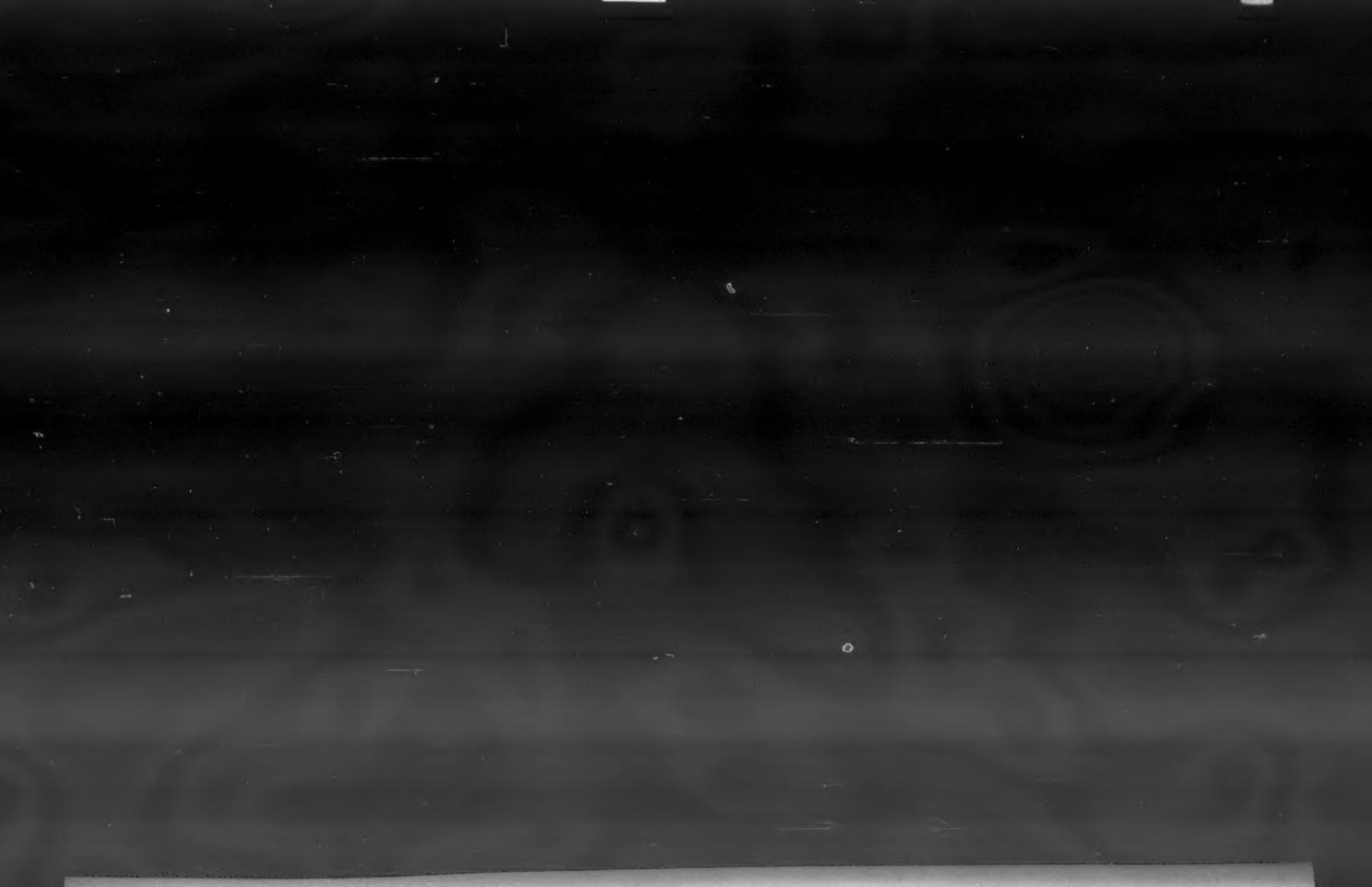

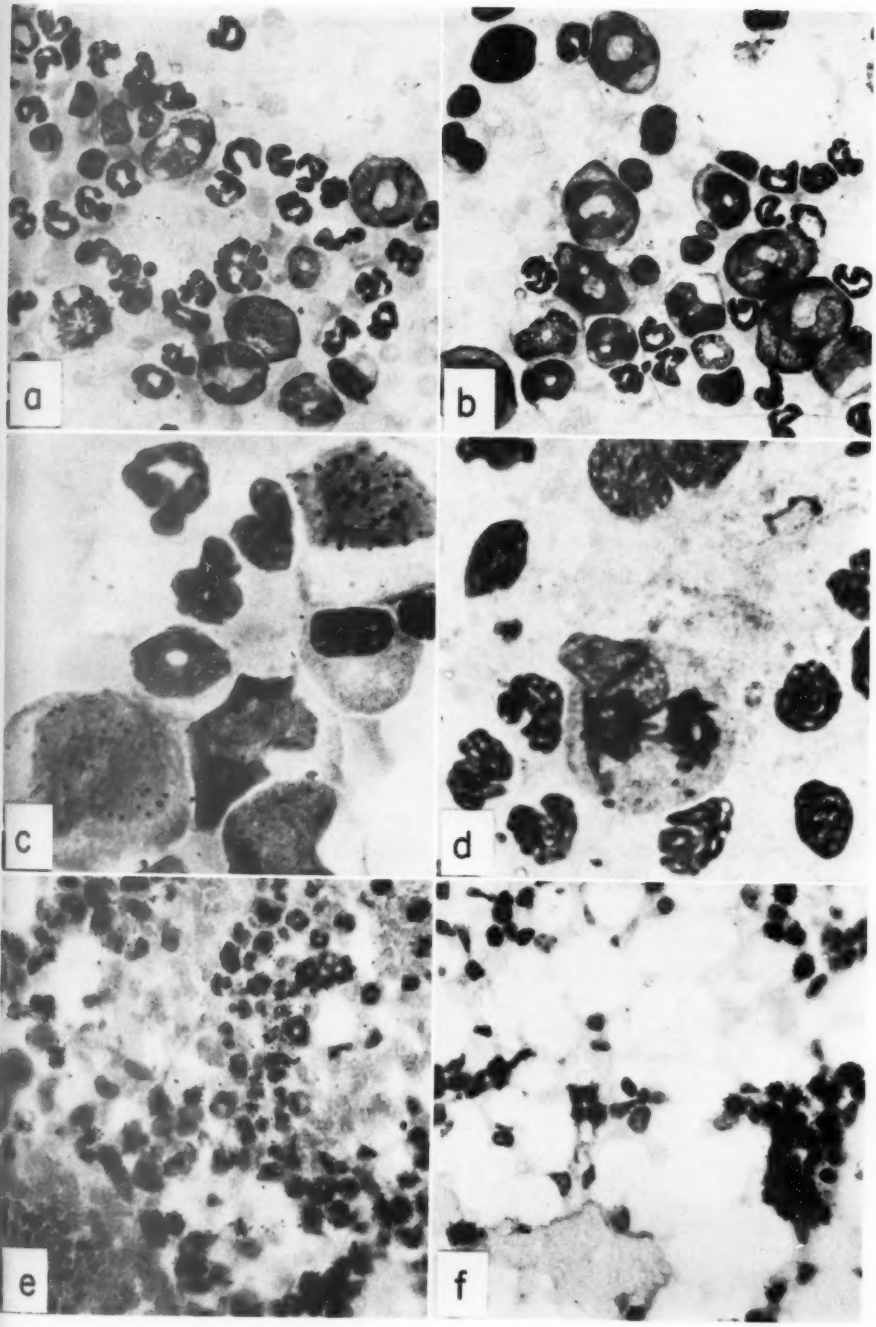

5

EXPERIMENTAL ANTHRAX IN THE RAT

II. The Relative Lack of Natural Resistance in Germ-Free (Lobund) Hosts

Martha J. Taylor, A.B.; James R. Rooney, D.V.M.,* and George P. Blundell, M.D.†

From the U.S. Army Chemical Corps Biological Laboratories, Fort Detrick, Frederick, Md.

The preceding report in this series[1] described an age-correlated increase in the natural resistance of conventionally reared albino rats to lethal infection with spores of *Bacillus anthracis*. The average rate at which a high degree of resistance developed was calculated for the Fischer 344 strain of rat, revealing that for every 1-day increase in injection age from the sixth through the 31st postnatal day, the spore dose corresponding to 50 per cent survival increased at a rate of 1.5-fold daily—from 10^4 to 10^9 spores. The LD_{100} for 1-day-old Fischer rats was less than 10^4 spores, while rats more than 5 weeks old at injection usually survived 10^9 spores.

The various factors affecting this level of resistance in the conventionally reared rat are not understood and are difficult to define. There is a need to analyze the morphologic and physiologic aspects of maturation of the host defense mechanisms and a variety of factors in the environment. The problems involved in designing adequately controlled experiments to investigate the development of nonspecific resistance to infection in laboratory animals are numerous. A controlled environment is one obvious essential. Experiments have now been performed with germ-free albino rats reared under conditions that eliminated exposure of the animals to micro-organisms present in the normal (conventional) rat colony maintained here. The results permit comparisons between germ-free and conventional rats, at age 5 weeks, with respect to (a) their level of resistance to lethal infection with *B. anthracis* spores, and (b) electrophoretically determined protein patterns in serums of noninfected animals. The level of resistance was investigated further by analyzing gross and microscopic features of the rats at death.

Presented in part before the 60th Annual Meeting of the Society of American Bacteriologists, May 4, 1960, Philadelphia.

Accepted for publication, December 30, 1960.

* Present address: Department of Animal Pathology, University of Kentucky, Lexington, Ky.

† Present address: Oscar B. Hunter Memorial Laboratory, 915 Nineteenth Street, N.W., Washington 6, D.C.

The results indicate that nonspecific factors in a conventional environment play a role in producing the naturally acquired resistance of the adult albino rat to lethal infection with *B. anthracis* spores.

Material and Methods

Breeding and Care of Rats

The germ-free rats, descendants of inbred Wistar stock, now bred at the Lobund Institute, were in the fourth to ninth generations of germ-free life, and conformed to Lobund standards for germ-free animals.[2] Five closely related litters were brought to and maintained at Fort Detrick in a Trexler flexible plastic isolator unit (Trexler,[3] Fig. 1), ventilated only with filtered air. Litter mates, and later the experimental groups of 3 to 7 rats, were housed in lucite cages equipped with the necessary bedding, lids, food, and bottles of water. They were fed Lobund diet L-356,[4] which is similar to the Purina Chow fed the Fischer rats with respect to analysis of protein, fat, and ash, but contains additional salts and minerals.

All equipment taken into the unit was autoclaved at 121° C. for at least 30 minutes, and then held for 30 minutes in an air lock attached to the unit and filled with peracetic acid vapor. The only cultural tests made at Fort Detrick were for bacteria that would grow aerobically on the surface of blood agar (made by adding 7 ml. of fresh, defibrinated, whole rabbit blood to each 100 ml. of Difco blood agar base). Tests for bacteria in the rats' environment were made by culture of swabs from cages, and of feces, on plates of blood agar. These samples were taken immediately prior to (a) sacrifice of the controls, (b) inoculation of the other animals with *B. anthracis* spores, and at intervals thereafter. The consistent failure to find colonies, other than those of *B. anthracis,* was considered adequate confirmation of the continuing, successful exclusion of air-borne bacterial contaminants.

Our colony of the genetically homogeneous Fischer 344 strain of rats has been described.[1]

Experimental Rats

In the first experiment, one litter of 7 Lobund rats was challenged with 10^7 spores. In the second experiment, 3 of 4 litters which came from the Lobund Institute 8 months later were challenged. These rats were identified with toe or ear markings on the day of arrival, and distributed to cages for 6 dose groups (Table II).

Control Rats

The first shipment of Lobund rats consisted of the litter of 7 mentioned above, and 1 extra male of unknown age. He was held in the unit, caged alone, as a non-inoculated control. On the day the injected litter died of anthrax, this rat was killed. His spleen and feces were cultured on blood agar. As additional controls, a 38-day-old litter (2 males and 1 female) in the second shipment of Lobund rats was removed from the unit on the day after arrival. These rats equaled Fischer rats of the same age and sex in weight and sexual development. Heart's blood was drawn from each to provide serums for electrophoretic analysis and for control on tests for antibody. The rats were weighed, killed, and necropsied. Samples of liver and feces were cultured aerobically on blood agar. Tissues of these 4 Lobund rats were prepared for comparative histologic study with similar tissues of the experimental animals.

Serums from conventionally reared Fischer rats, some the same age as the Lobund rats, and some older (Table V), were obtained to run concurrently with the Lobund serums in the electrophoretic analyses of serum proteins.

Gross necropsy records and histologic sections of normal and *B. anthracis*-infected tissues of Fischer rats, of nearly the same age at sacrifice or death as the Lobund rats, were available from earlier experiments for comparative studies.

Pathogen, Dose and Injection Route

The spores constituting the inoculums for these experiments were from the same suspension of spores of the virulent 1B sib-progeny of the Vollum strain of *B. anthracis* previously described.[1] The number of viable spores was counted repeatedly during 18 months of use and consistently found to be between 7×10^9 and 9×10^9 per ml. The suspension was heat-shocked at 60° C. for 30 minutes in May, 1957, and again in October, 1958. Storage was always in the refrigerator. This stock suspension was diluted in distilled water to the concentration intended for each inoculum. The calculated concentration was confirmed by plate counts for viable spores made within 24 hours of use. In the first experiment each rat received a dose of 10^7 spores in a volume of 0.1 ml. In the second experiment, each member of the designated groups of rats received 10^1, 10^2, 10^3, 10^4, 10^5, or 10^6 spores. Each dose was in 0.1 ml. of water (Table II).

On the day of injection, fur was snipped from a 1.5 $cm.^2$ area on the left flank, where each rat was then dosed with 0.1 ml. of spore suspension intradermally as superficially as a 27-gauge hypodermic needle could be introduced without leakage of inoculum. This raised a clearly visible bleb. Identical injection techniques had been used to challenge conventional Fischer rats with 10^6 and 10^9 spores.[1] In those experiments the 10^7 dose was delivered subcutaneously over the abdomen.

Time Between Inoculation and Death

Surveys for dead rats were made several times a day during the first 96 hours after injection and daily thereafter. Time to death was estimated to the nearest 6-hour interval.

Diagnostic Procedures

Dead animals were first weighed and then opened and necropsied aseptically. Tissue was taken for culture, impression smears were made, and the condition of inoculation site, lymph nodes, and viscera noted. The viscera were stripped from the carcass, the brain case opened, and everything placed in buffered 10 per cent formalin for fixation. Selected tissues from each animal were prepared for histologic study.

For culture, the cut surface of the tissue to be studied, or a fecal pellet was touched several times to the surface of blood agar plates. Part of the touched surface was loop-streaked to insure isolated colonies for observation of structure. Plates were read at 24 and 48 hours. The typical Vollum colony (on this agar, at 24 hours: 2 to 4 mm., abruptly raised, finely granular surface, with comma- or tail-like peripheral processes; at 48 hours: much larger, thick and cream colored), with no contaminants present, was accepted as evidence that a pure culture of *B. anthracis* had been recovered.

Impression smears were made from all livers, and from certain other organs in 1 case. Smears were air-dried, fixed in buffered formalin for 30 minutes to overnight, washed in running water, drained dry in the 37° C. incubator, and stained with Jenner-Giemsa.

For histologic study, all tissue sections were stained by a modified Lillie-Giemsa method. Comparisons were made as follows: (1) Unchallenged *versus* fatally infected Lobund rats 33 to 51 days old. (2) Unchallenged *versus* fatally infected Fischer rats 28 to 38 days old. (3) Lobund rats, fatally infected at age 33 to 37 days with 10^7 spores *versus* Fischer rats, fatally infected at age 27 to 32 days with 10^7, 10^6, or 10^5 spores (Table I). (4) Among groups of Lobund rats, fatally infected at age 33 to 37 days, with spore doses of 10^1 through 10^7 separated by 1-log intervals.

Analysis of Serums

Paper electrophoretic determinations were made on 0.01 ml. of serum in a hanging strip cell in 0.075Γ/2 veronal at pH 8.6. Eight strips of Whatman 3 MM paper were

run simultaneously in 1 cell for 16 hours at room temperature under constant current conditions of 8 ma. per cell. The strips were stained in bromphenol blue and evaluated by transmission densitometry with the Analytrol under the conditions recommended by the manufacturer.

TABLE I

CONVENTIONAL FISCHER 344 RATS DEAD WITH ANTHRAX * THAT WERE SELECTED FOR HISTOLOGIC COMPARISON WITH ANTHRAX IN THE GERM-FREE LOBUND RATS

Log of spore dose	Age at injection (days)	Sex	Weight at injection (gm.)	Time to death (hr.)	Edema at injection site
7†	28	F	52	27	±
7†	29	M	72	20	2+
7†	30	F	60	60	1+
8‡	32	M	85	32	1+
9‡	27	M	55	44	1+
9‡	27	M	51	37	2+

*Diagnosis confirmed by culture and Jenner-Giemsa-stained impression smears, both of liver. Individuals were selected on a basis of injection age and dose of spores most nearly comparable with the germ-free experiment.

† Injection was subcutaneous.

‡ Injection was intradermal.

RESULTS

Successful Control of Bacterial Environment

Pre-inoculation cultures from cages and feces, and cultures at necropsy of the 4 uninoculated Lobund rats' feces and tissues were entirely negative. Periodic postinoculation cultures from cages, feces, and various inside surfaces of the plastic unit always revealed the presence of *B. anthracis* and no other bacteria. The unit was still in this state of monocontamination when the 1 surviving rat was sacrificed 3 months after challenge.

Death and Survival

The hours between inoculation and death of each rat are listed in Table II. The smaller doses tended to prolong the time to death, although the animal that died a week later than any others received 10^6 spores. The 1 survivor received 10 spores. These 2 animals were litter mates.

Gross Necropsy and Diagnosis

Certain necropsy findings for the infected Lobund rats are included in Table II. The following statements are based upon a review of the full necropsy records for these rats, and for the many Fischer rats of comparable age dead of anthrax in previous experiments. Instead of the localized, necrotic, slightly edematous and hyperemic injection-site reaction observed in the conventional Fischer rats, the majority of the

Lobund site lesions were characterized by a thickened, dull-red area 1 to 3 cm. in diameter immediately under the point of needle entry. The lesion was surrounded by an extensive zone of gelatinous edema and hyperemia. This closely resembled the site lesions customarily seen in fatally infected mice, guinea pigs, and other species for which the LD_{50} of *B. anthracis* is approximately 10 spores injected intradermally or

TABLE II

SUMMARY DATA FOR GERM-FREE LOBUND RATS TESTED INTRADERMALLY WITH SPORES OF *B. anthracis*

Log of spore dose	Age at injection (days)*	Sex	Weight at death (gm.)	Time to death (hr.)	Edema at site of injection	Fluid in chest
1	34	M	Survived †			
	36	M	121	132	0	0
	36	F	96	54	0	0
	37	F	109	138	0 ‡	0
2	34	M	101	72	0 §	Present
	36	M	80	48	2+	0
	36	F	84	48	+	0
	37	F	89	66	3+	0
3	34	F	96	54	3+	0
	36	M	110	144	4+	0
	37	M	99	48	4+	0
	37	F	99	54	2+	0
4	34	M	113	54	2+	0
	36	F	100	30	±	0
	37	M	118	60	4+	0
5	34	M	98	30	3+	0
	36	F	85	42	4+	0
	37	M	106	54	4+	0
6	34	F	129	390	0	0
	36	M	89	30	4+	0
	37	M	98	30	4+	0
7	33	F	69	36	4+	0
	33	F	72	30	4+	0
	33	F	74	30	4+	0
	33	F	72	24	4+	0
	33	F	75	24	4+	0
	33	F	74	30	4+	0
	33	F	71	30	4+	0

* Rats the same age are litter mates. The first experiment (33-day-old litter) was inoculated in February, 1958. The second experiment (other 3 litters) was inoculated in October, 1958.

† Killed for special study 3 months after challenge.

‡ None at injection site, but considerable amount centered around the left eye. See text.

§ Small necrotic lesion in subcutaneous tissue; this resembled the conventional Fischer rat reaction.

subcutaneously. The site lesion was notably smaller in the Lobund rats dosed with 100 spores than with larger numbers of spores, and absent from those rats given 10 spores and from the one that died on the 17th post challenge day. One of the rats with no injection-site lesion had subcutaneous edema around the left eye. All conventional rats that died consistently exhibited copious, clear pleural fluid (hydrothorax); only 1 Lobund rat (a litter mate of the survivor) had pleural fluid. The Lobund rat spleens were generally dark red and plump—not notably different from those of conventional rats and other rodents with anthrax. The lymph node (left axillary) receiving drainage from the injection site was usually enlarged; all others appeared relatively nonreactive.

Jenner-Giemsa-stained impression smears of liver from each rat, and of several additional tissues from the rat dead at 17 days, revealed the omnipresence of characteristic bacilli.

Of the 59 cultures (27 liver, 21 fecal, 3 lung, 3 spleen, 2 lymph node, 3 tail-blood) of necropsy material from 27 animals, 58 gave pure *B. anthracis*. One (of an extremely autolyzed liver) was negative, but stained smears confirmed the presence of morphologically characteristic bacilli, and other tissues cultured from this rat gave *B. anthracis* colonies. No other bacterial species was recovered.

Histologic Features

The typical histologic findings in tissues of 6 Fischer (Table I) and 22 Lobund rats* dead following injection with *B. anthracis* spores are listed in Table III, and illustrated in Figures 1 to 5. The table shows that the Fischer rats reacted with the development of a localized skin lesion that included necrosis of the epidermis. Focal lesions also occurred in the regional lymph node, liver, and spleen. The Lobund rats reacted with (a) a larger, more diffuse skin lesion without necrosis, (b) diffuse necrosis of the regional lymph node and other lymph nodes, and (c) massive diffuse necrosis of the spleen. Reactions were also present in the adrenal and thymus of the Lobund rats that were not noted in the Fischer rats. The degree of "sequestration" of mononuclear cells and bacilli within the pulmonary vessels of the Fischer rats was greater than in the Lobund rats. The intra-alveolar edema and fluid within the pleural cavity were features of the Fischer rats only. The bacilli were seen in greater numbers in the blood vessels and diseased organs of the Lobund than in the Fischer rats. The renal lesions were similar in both rat types.

The 34-day-old litter of 6 Lobund rats, with 1 representative in each of the second experiment's dose groups, was atypical in its resistance

* The 34-day-old litter of 6 was atypical in certain respects, and is discussed separately below.

level and in its histologic pattern. The rat given 10 spores survived, although there was serologic and histologic evidence of infection and recovery. The lesions in the 4 rats receiving 10^5 through 10^2 spores showed a consistently definite trend toward the reaction pattern observed in conventionally reared Fischer rats—intra-alveolar edema and "sequestration" were increased in severity with decreasing spore dose, as was epidermal necrosis at the inoculation site. The adrenal hemor-

TABLE III

HISTOLOGIC FINDINGS IN TISSUES OF CONVENTIONAL FISCHER 344 AND GERM-FREE LOBUND RATS OF COMPARABLE AGES, DEAD FOLLOWING INJECTION OF *B. anthracis* SPORES

Tissues	Fischer *	Lobund †
Site of injection	Acute cellulitis Epidermal necrosis Few bacilli	Acute cellulitis No epidermal necrosis Masses of bacilli
Regional lymph node	Focal, subcapsular necrosis Mononuclear cell accumulation	Liquefaction necrosis Hemorrhage Many bacilli
Other lymph nodes	Normal	Variably affected by lymphoid necrosis, hemorrhage, and bacilli
Liver	Kupffer cell hypertrophy Phagocytosis of bacilli Intralobular mononuclear cell foci, frequently undergoing necrosis	Little or no Kupffer cell response Masses of bacilli pack the sinusoids
Spleen	Demarcated mononuclear cell foci, with necrosis Moderate hyperemia Few bacilli	Massive, diffuse necrosis Severe hyperemia Many bacilli
Kidney	Same picture in both sets of rats: Acute glomerulitis—necrosis, thrombosis, bacilli Acute segmental necrosis of the cortical convoluted tubules	
Adrenal	Normal	Marked cortical hemorrhages
Thymus	Normal	Hyperemia Necrosis of thymocytes
Lung	Striking "sequestration" of mononuclear cells and of bacilli in the pulmonary arteries Hyperemia Intra-alveolar edema	Minimal "sequestration" Marked hyperemia No alveolar edema Large numbers of bacilli in blood vessels

* Three rats, 28, 29, 30 days old, dosed subcutaneously with 10^7 spores. Three rats, 27, 27, 32 days old, dosed intradermally with 10^6, 10^5 and 10^4 spores respectively; 4 experiments represented.

† Twenty-two rats, 33, 36, 37 days old, dosed intradermally with 10^1 through 10^7 spores at 1-log intervals. See text for discussion of 1 atypical 34-day-old litter.

rhages and thymic involution, however, which had not been observed in the Fischer rats but which were typical of the Lobund rats, were observed even at the 10^2 spore dose level. The rat given 10^6 spores died on the 17th postinjection day. The cellular response in this rat more closely resembled that of the conventional Fischer than of the Lobund rats, the long course of the disease having allowed a definite chronic

TABLE IV

EVIDENCE FOR THE PRODUCTION OF ANTIBODY * TO THE PROTECTIVE ANTIGEN OF *Bacillus anthracis* BY GERM-FREE LOBUND RATS FOLLOWING INJECTION OF SPORES

Rat				
Strain	Treatment	Age (days)	Number of days after injection	Antibody titer †
Fischer	None	38		Nil
Lobund	None	38		Nil
Fischer	None	141		Nil
Lobund	10^6 spores	50	16	1/8
Lobund	10^3 spores	50	16	1/4
Lobund	10^3 spores	127	93	1/16

* Serums were tested by the agar-diffusion method of Thorne and Belton.[5]

† Highest dilution of serum neutralizing the reaction of standard amounts of protective antigen with standard antiserum.

reaction to develop. Again, though, the necrosis of cells in the thymus was like that of the other Lobund rats.

Antibody Production

Neutralizing antibody to the *B. anthracis* protective antigen was demonstrated in the serums of 2 Lobund rats that lived to supply blood samples on the 16th postinjection day, and in the serum of the one of these that was tested again 2½ months later (Table IV). This finding is reported as evidence that at age 34 to 50 days rats reared germ-free responded effectively (produced antibody promptly) to antigenic stimulation.

Gamma Globulin

The electrophoretic patterns obtained for serum proteins of the 38-day-old noninoculated germ-free Lobund and the 36 and 38-day-old noninoculated conventional Fischer rats were indistinguishable from each other and corresponded to those figured by Gustafsson and Laurell[6] for 50- to 150-day-old germ-free rats, notably regarding the faintness of the gamma globulin bands. This band was more intense in the serums of our 128- and 333-day-old Fischer rats, appearing about as it does in

serums of Gustafsson and Laurell's 50- to 150-day-old conventional rats. The values obtained for gamma globulin relative to total serum protein are shown in Table V. Other serum protein fractions in our samples of Lobund and young Fischer rats exhibited no obvious deviations from those present in the older Fischer rats. Serums from additional animals would have to be analyzed to determine whether smaller, but possibly significant, differences exist.

Discussion

The small numbers of germ-free rats tested do not permit calculation of a spore LD_{50}, but the results place the LD_{100} at less than 100 spores. This is 1/10,000,000th the LD_{50} for a 31-day-old and 1/100th the LD_{50}

Table V

GAMMA GLOBULIN IN SERUM PROTEIN OF NONINOCULATED GERM-FREE LOBUND AND CONVENTIONAL FISCHER 344 RATS

Rats	Age (days)	Sex	Weight (gm.)	Gamma globulin (%)* Individual	Gamma globulin (%)* Average	Measure of resistance to *B. anthracis*
Germ-free	38	M	107	5.4	4.8	LD_{100}† = less than 100 spores
	38	M	98	3.8		
	38	F‡	91	5.1		
Conventional	38	F‡	87	4.7	5.6	98 to 100% survive 10^8 spores
	38	F‡	98	6.0		
	38	F§	83	5.3		
	36	F‡	85	5.1		
	36	F‡	86	6.8		
Conventional	128	F	194	9.7	8.9	Not tested
	128	F	181	9.0		
	128	F	173	8.1		
Conventional	333	M	415	10.8	10.0	Not tested
	333	F	262	9.4		
	333	F	297	9.8		

* Values obtained by transmission densitometry for gamma globulin divided by the value for total serum protein, times 100.

† Dose per rat required to kill 100 per cent of the animals tested, in this case by the intradermal route.

‡ Vagina open.

§ Vagina closed.

for 6-day-old conventional Fischer rats. Unpublished results from a limited number of experiments indicate the LD_{100} for 2- to 5-day-old Fischer rats to be betwen 10^2 and 10^3 spores. Thus, the 33- to 37-day-old Lobund rats resist fewer spores than 2- to 5-day-old conventional rats. The 35- to 40-day-old Fischer rats, which were entirely comparable in weight and sexual development with the Lobund rats, usually survived

10^9 spores. Although genetic differences must exist between the Lobund and Fischer rat, there is no reason to suppose that they are responsible for the tremendous difference observed in resistance levels. The bacteria in the conventional environment are likely candidates for a causal role in the production of this naturally acquired resistance of the adult white rat to infection with *B. anthracis* spores. Since adults of several other rodent species do not develop such resistance, in spite of exposure to similar environmental factors, more attention must be directed toward learning how this is accomplished by the rat.

The mechanisms by which gamma globulins promote resistance remain unknown. Gustafsson and Laurell provided evidence that strongly suggested that "the normal flora of microorganisms is an important stimulant for the gamma globulin-producing cells."[6] If their observed values for gamma globulin, which were reported as gm. per hundred ml. of serum, are converted to per cent of total serum protein, the mean value for this component in germ-free serums is 3.8 and in the conventional serums 8 per cent. Wostmann and Gordon's data,[2] similarly recalculated, show 3 and 8 per cent gamma globulin in germ-free and conventional Lobund rats. These values serve to substantiate ours, which were obtained from small numbers of individuals. Our results suggest that there is no correlation between electrophoretically measured serum gamma globulin levels and the degree of resistance in the rat to the spores of *B. anthracis*—a high level of resistance to anthrax exists in the Fischer rat at an age when its serum gamma globulin is still as low, within the limits of the reliability of the method, as that of the highly susceptible Lobund rats. If environmental bacteria enhance natural resistance to *B. anthracis* through stimulating production of nonspecific antibody gamma globulin, the product cannot be detected by paper electrophoresis.

Histologic examination revealed that anthrax bacilli produced focal lesions in specific tissues in the Fischer rats. Corresponding tissues in the Lobund rats showed diffuse involvement, and additional organs evidenced a reaction. It thus appears that the conventional Fischer rat possesses greater ability to localize and contain the destructive action of the bacilli.

The "sequestration" of mononuclear cells and bacilli within many of the pulmonary blood vessels was greater in the Fischer than in the Lobund rats. This condition takes on added significance as a major contributing cause of death when one considers the gross finding of excess fluid in the pleural cavity and the microscopic feature of intra-alveolar edema in the Fischer rat. Although "sequestration" was occasionally observed in Lobund rats, hydrothorax and intra-alveolar edema were

absent. The more severe cutaneous edema in the Lobund rat may have prevented the occurrence of the intra-alveolar edema and pleural effusion found in the Fischer rats. It has been suggested that death of guinea pigs with anthrax may be due to secondary shock.[7] This is acceptable for the Lobund rat. The more resistant Fischer rat dies with pulmonary edema associated with pulmonary vascular sequestration and shows no evidence of shock.

Summary

Albino rats, reared germ-free at the Lobund Institute, were transported in an isolator unit to our laboratory and tested at the age of 5 weeks for their susceptibility to intradermally injected spores of *Bacillus anthracis*. The LD_{100} for these rats was found to be less than 100 spores, which is 1/10,000,000th the LD_{50} for 31-day-old and 1/100th the LD_{50} for 6-day-old conventionally reared Fischer rats. This places the level of the 5-week-old germ-free rat's resistance at least as low as that of conventional rats less than 1 week old, and suggests that the rat maturing in a conventional environment may improve its resistance to *B. anthracis* spores through contact with this environment.

The presence of antibody to the *B. anthracis* protective antigen in serums of 2 rats alive on the 16th day after challenge demonstrated that these rats were capable of producing antibody in response to antigenic stimulation.

Gamma globulin levels, determined electrophoretically, were equally low in serums of 5-week-old germ-free and conventional rats compared with the higher level found in 4- and 11-month-old conventional rats. This means that the development of high resistance to *B. anthracis* in the conventional rat precedes the detected rise in serum gamma globulins.

As a result of histologic studies, it is suggested that death may result from different causes in the germ-free and in the conventional rat.

References

1. Taylor, M. J.; Kennedy, G. H., and Blundell, G. P. Experimental anthrax in the rat. I. The rapid increase of natural resistance observed in young hosts. *Am. J. Path.*, 1961, **38**, 469–480.
2. Wostmann, B. S., and Gordon, H. A. Electrophoretic studies on the serum protein pattern of the germfree rat and its changes upon exposure to a conventional bacterial flora. *J. Immunol.*, 1960, **84**, 27–31.
3. Trexler, P. C. The use of plastics in the design of isolator systems. *Ann. New York Acad. Sc.*, 1959, **78**, 29–36.
4. Larner, J., and Gillespie, R. E. Gastrointestinal digestion of starch. III. Intestinal carbohydrase activities in germ-free and non-germ-free animals. *J. Biol. Chem.*, 1957, **225**, 279–285.

5. THORNE, C. B., and BELTON, F. C. An agar-diffusion method for titrating *Bacillus anthracis* immunizing antigen and its application to a study of antigen production. *J. Gen. Microbiol.*, 1957, **17**, 505–516.

6. GUSTAFSSON, B. E., and LAURELL, C.-B. Gamma globulins in germ-free rats. *J. Exper. Med.*, 1958, **108**, 251–258.

7. SMITH, H.; KEPPIE, J.; STANLEY, J. L., and HARRIS-SMITH, P. W. The chemical basis of the virulence of *Bacillus anthracis*. IV. Secondary shock as the major factor in death of guinea-pigs from anthrax. *Brit. J. Exper. Path.*, 1955, **36**, 323–335.

We are indebted to Professor P. C. Trexler for the Lobund rats; to Mr. Elliott Purlson whose active cooperation made it possible for us to control their bacterial environment after arrival; to Dr. Leonard Spero who made and interpreted the electrophoretic analyses; to Dr. Martha K. Ward who made the agar diffusion tests for antibody; and to the Armed Forces Institute of Pathology, Washington, D.C., for making the photomicrographs of our sectioned tissues.

LEGENDS FOR FIGURES

The interval between inoculation with *B. anthracis* spores and death is enclosed in parentheses. All sections were stained by a modified Lillie-Giemsa method.

FIG. 1. AFIP 18–1R. Skin of a Lobund rat at the injection site. Large numbers of bacilli and moderate cellulitis are evident. (25 hr.) × 115.

FIG. 2. AFIP 18–3R. Liver of a Fischer rat with marked Kupffer cell hyperplasia and few bacilli. (27 hr.) × 500.

FIG. 3. AFIP 18–2R. Liver of a Lobund rat in which the sinusoids are filled with bacilli and the Kupffer cell reaction is slight. (25 hr.) × 500.

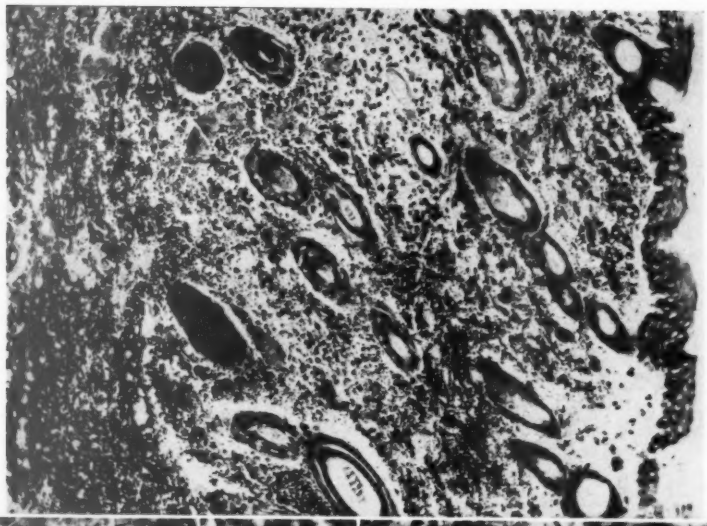

1

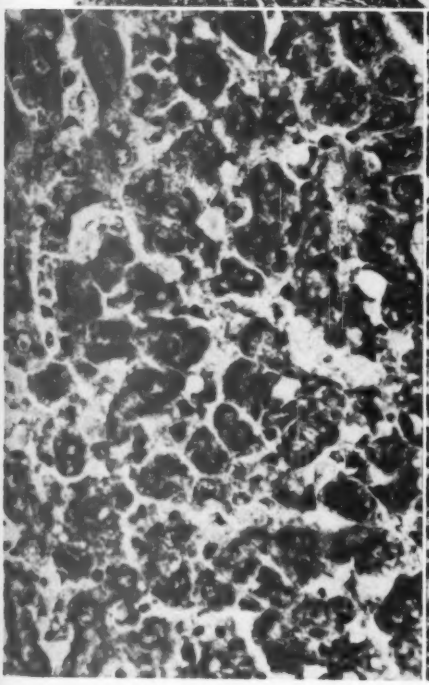

2

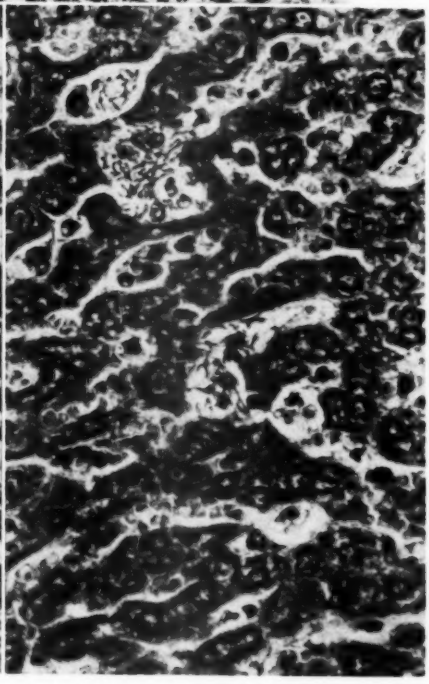

3

4

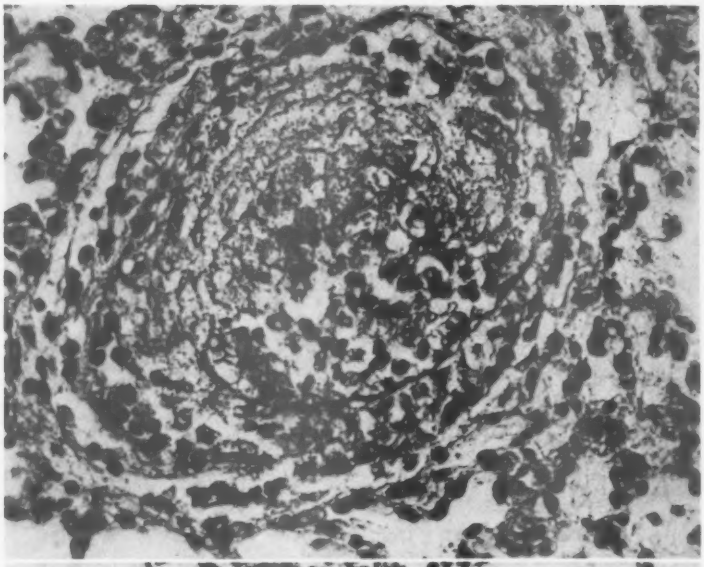

5

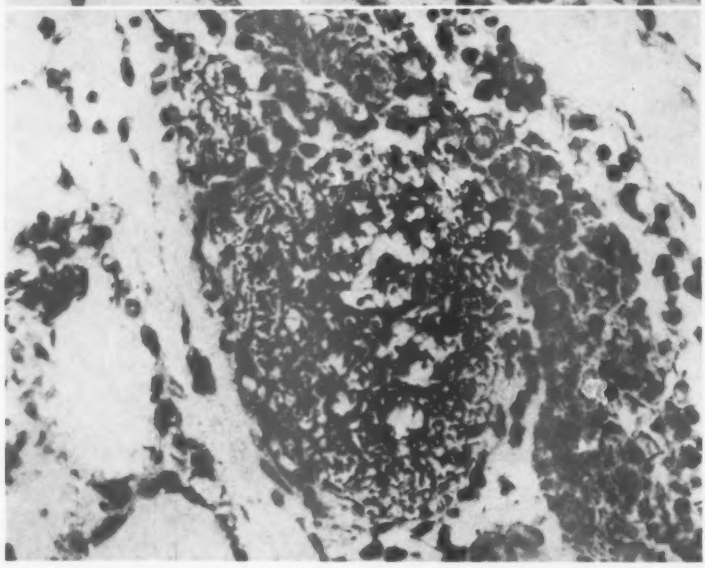

FIG. 4. AFIP 18–4R. Lung of a Fischer rat in which a small pulmonary artery is partially occluded by a thrombus and an aggregate of mononuclear cells. Bacilli are scarce. (20 hr.) × 500.

FIG. 5. AFIP 18–5R. Lung of a Lobund rat in which a small pulmonary artery is filled with bacilli. Note the absence of the mononuclear reaction and thrombus formation seen in the Fischer rat (Fig. 4). (25 hr.) × 500.